2011

# "CLICKED" BIVALENT MULTIFUNCTIONAL LIGANDS IN ALZHEIMER'S DISEASE.

RONAK GANDHI
*Virginia Commonwealth University*

Virginia Commonwealth University

This is to certify that the thesis prepared by Ronak Prakashchandra Gandhi entitled "Clicked" bivalent multifunctional ligands in Alzheimer's disease has been approved by his committee as satisfactory completion of the thesis or dissertation requirement for the degree of Mater of Science.

Director: Dr. SHIJUN ZHANG, Ph.D.

ASSISTANT PROFESSOR, DEPARTMENT OF MEDICINAL CHEMISTRY,

VIRGINIA COMMONWEALTH UNIVERSITY

Dr. UMESH R. DESAI, Ph.D.

PROFESSOR, DEPARTMENT OF MEDICINAL CHEMISTRY, VIRGINIA

COMMONWEALTH UNIVERSITY

Dr. DARLENE H. BRUNZELL, Ph.D.

ASSISTANT PROFESSOR, DEPARTMENT OF PHARMACOLOGY AND TOXICOLOGY, VIRGINIA COMMONWEALTH UNIVERSITY

Dr. RICHARD A. GLENNON, Ph.D.

DEPARTMENT CHAIR, VIRGINIA COMMONWEALTH UNIVERSITY

Dr. VICTOR A. YANCHICK, Ph.D.

DEAN, SCHOOL OF PHARMACY, VIRGINIA COMMONWEALTH UNIVERSITY

Dr. DOUGLAS F. BOUDINOT, Ph.D.

DEAN, SCHOOL OF GRADUATE STUDIES, VIRGINIA COMMONWEALTH UNIVERSITY

05/12/2011

**“CLICKED” BIVALENT MULTIFUNCTIONAL LIGANDS IN ALZHEIMER’S DISEASE.**

A thesis submitted in partial fulfillment of the requirements for the degree of Master’s of Science at Virginia Commonwealth University.

By

RONAK P. GANDHI

BACHELOR OF PHARMACY, THE MAHARAJA SAYAJIRAO UNIVERSITY, INDIA, 2008

Director: Dr. SHIJUN ZHANG, Ph.D.

ASSISTANT PROFESSOR, DEPARTMENT OF MEDICINAL CHEMISTRY

Virginia Commonwealth University

Richmond, Virginia

May 2011

**Acknowledgements**

I would like to thank Dr. Shijun Zhang for his guidance and unceasing support with my project. I am indeed very grateful to him for giving me a very long rope with my project and for being very inspiring, which motivated me to work with diligence and assertiveness. I would also like to thank Dr. Li and Dr. Liu, from the bottom of my heart for nurturing a chemist in me and for their constant help from time to time with executing my project at Zhang lab. I ought to mention my family and friends for their undying love and affection which always made me feel indefatigable and work with single-minded determination.

Table of Contents

List of Figures

Page

List of Synthetic Schemes:

Page

## Abstract

**"CLICKED" BIVALENT MULTIFUNCTIONAL LIGANDS IN ALZHEIMER'S DISEASE.**

**By RONAK PRAKASHCHANDRA GANDHI, MS**

A thesis submitted in partial fulfillment of the requirements for the degree of masters of Science at Virginia Commonwealth University.

Virginia Commonwealth University, 2011

Major Director: Dr. SHIJUN ZHANG

ASSISTANT PROFESSOR, DEPARTMENT OF MEDICINAL CHEMISTRY

Alzheimer's disease (AD) is a neurodegenerative disorder characterized by beta-amyloid (Aβ) aggregation/oligomerization, biometal dyshomeostasis, oxidative stress, and neuroinflammation. The multifactorial nature of AD may indicate the therapeutic potential of multifunctional ligands that tackle various risk factors simultaneously as effective AD-modifying agents. This notion is further supported by the fact that while numerous AD-modifying agents targeting one single risk factor have been developed and

a number of them entered clinical trials, none of them has been successfully approved by the FDA. Furthermore, neuronal cell membrane/lipid rafts (CM/LR) have been demonstrated to associate with all the indicated risk factors, indicating that this relationship can be exploited therapeutically to design strategically distinct multifunctional ligands by incorporating CM/LR anchorage into molecular design. With the long-term goal of developing multifunctional ligands to slow or stop the progression of AD, recently we have embarked on the development of bivalent multifunctional Aβ oligomerization inhibitors (BMOIs) as potential AD-modifying agents. These BMAOIs contain curcumin as the multifunctional moiety and cholesterol as the CM/LR anchorage moiety linked by a spacer to co-target AβOs, CM/LR, and oxidative stress. The *hypothesis of the BMAOI strategy* is that BMAOIs will anchor/target the multifunctional AβO inhibitor moiety inside, or in the vicinity of, CM/LR in which Aβ oligomerization, Aβ/biometal interaction and oxidative stress occur to efficiently interfere with these processes. In support of this hypothesis, proof-of-concept of the BMAOIs strategy has been reached through our preliminary studies. Our results demonstrated that: 1) BMAOIs containing curcumin as the multifunctional AβO inhibitor and cholesterol as CM/LR anchor primarily localize to CM/LR while curcumin does not; 2) BMAOIs with optimal spacer length efficiently inhibit the production of intracellular AβOs and protect MC65 cells from AβO-induced cell death ($EC_{50}$~3 μM) while curcumin exhibits no significant activity; 3) these active BMAOIs retain curcumin's antioxidant and metal complexation properties. Our preliminary studies also demonstrated the critical roles of spacer length and connectivity in the molecular design of BMAOIs and one lead compound was

identified for further structural modification and optimization. Furthermore, this lead compound was shown to cross the blood-brain barrier (BBB) in a preliminary in vivo study as well as bind to Aβ plaques. Taken together, these results clearly reach the proof-of-concept of BMAOIs and confirm the rationale of designing BMAOIs to develop potential AD-modifying agents.

In this thesis, we continued the exploration and validation of the BMAOI strategy by designing and biological characterizing a series of BMAOIs containing cholesterylamine as the CM/LR anchorage moiety and curcumin as the multifunctional moiety. Ten BMAOIs with the spacer length of 15, 17, 19, 21, and 23 atoms were designed and synthesized. Initially, these BMAOIs were tested for the neuroprotective activity against the AβO-induced cytotoxicity in human neuroblastoma MC65 cells. Then, Western blot analysis was performed for active BMAOIs to confirm the association of neuroprotection and suppression of AβOs. Furthermore, active BMAOIs were examined for antioxidant and metal complexation properties. Finally, Aβ plaque binding was examined using transgenic AD mice brain sections. Our results demonstrated that the same spacer length but different connectivity are preferred in this new series of BMAOIs for neuroprotective activity as that of the lead compound from cholesterol series. Moreover, the neuroprotection activity is closely associated with the inhibition of AβOs as demonstrated by Western blot analysis. In addition, the active BMAOIs retain the antioxidant and biometal binding properties of curcumin. More importantly, the binding affinity to the Aβ plaques was again confirmed for the new BMAOIs containing cholesterylamine. In summary, the design and characterization of the new series BMAOIs further confirmed

the rationale of BMAOI strategy and their potential to lead to a new direction in development of effective AD-modifying and treatment agents.

# Chapter 1 Introduction

## 1.1 Alzheimer's disease

Alzheimer's disease (AD) is a fatal neurodegenerative disorder characterized by a progressive and global deterioration of mental function, most notably in cognitive performance. The manifestation of AD begins with a mild cognitive impairment that progressively develops over the next few years into a severe dementia and mental disability. At the late stage of AD, patients are unable to respond to their environment and to carry on with normal social interactions. More often patients become unable to control their own movement and to perform basic daily activities including eating or using the toilet.

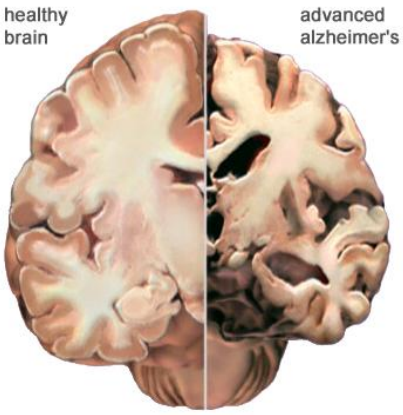


**Figure 1. A crosswise "slice" through middle of the brain between the ears. In Alzheimer's brain cortex shrivels up. Hippocampus shrinks severely and ventricles grow longer.[1]**

Currently, there is no treatment or prevention available for AD; the only available drugs approved by the FDA are for the short term symptomatic treatment of dementia, which with disease progression lose their efficacy leaving the patients and their families totally hopeless.[1]

### 1.2 History of AD research

AD was first described in 1906 by a German physician named Alois Alzheimer. Alzheimer described changes in the brain of a 56-year-old woman, Auguste D., who died of progressive dementia in post-mortem tissue analysis.


**Figure 2. Pictures of Dr. Alois Alzheimer and Mrs. Auguste D.[1]**

He demonstrated the presence of two specific features, neurofibrillary tangles and senile plaques, in the brain tissue associated with a severe neuronal loss. It wasn't until the introduction of electron microscopy that the neurofibrillary tangles were characterized as paired helical filaments and later were characterized to be filaments of hyperphosphorylated tau protein. As for the senile plaques, it wasn't until 1984 that the primary proteinaceous constituent of the plaques was discovered; it was found to be a 4-KDa protein, and by amino acid sequencing it was found to be a novel 42 amino acids long protein, now called amyloid beta (Aβ).[1, 2]

Certain similarities between AD and Down's syndrome helped in determining the nature and origin of the senile plaques. In addition to the mental disability observed in the two diseases and the high risk of developing Alzheimer's like-dementia among Down's syndrome patients living beyond age 40, histopathological examination of the brain of patients with Down's syndrome revealed the formation of similar histopathological features as in the brain of patients with AD including the senile plaques.[3] It was later found that these plaques are populated with the same 4-KDa amyloid protein.

**1.3 Epidemiology**

AD is the most common cause of dementia within the elderly population.[4] In 2009 there were an estimated 5.3 million Americans affected by AD; without a cure or a means to prevent the disease and with the population growing older and an aging baby boom generation, it is estimated that this number will triple by 2050.[5] The biggest risk factor for dementia is age; the prevalence of dementia with increasing age follows an exponential growth pattern, doubling approximately every 5 years of increase in age starting from the age of 65. It is estimated that 0.8% of 65 years old people, 1.6% of 70 year old, 3.3% of 75 year old, 6.5% of 80 year old, 12.8% of 85 year old, and 30.1% of >85 year old suffer from dementia in north America.

AD patients have a shorter life expectancy compared to the same age non-demented population, and according to the Center for Disease Control and Prevention, AD is the 6$^{th}$ leading cause of death among the general population, and the 5$^{th}$ leading cause of death among the elderly in the United States. The mechanism by which AD leads to death is

ambiguous, while impairment of correct judgment leading to fatal accidents is a common cause, it has widely been reported that bronchopneumonia is the main cause of death. There is no direct link between AD and pneumonia, however severe AD frequently causes complications such as immobility, swallowing disorders or malnutrition, which could be the reason for the increased risk of patients to develop pneumonia.

**1.4 Symptoms and Stages of AD**

AD symptoms vary among different individuals but in general patients, follow a certain pattern of disease progression. Different methods have been developed for staging the disease progression, but most commonly the disease has been divided into three main stages: mild, moderate and severe.[6]

In mild AD, patients experience occasional loss of recently acquired memory (short term memory), confusion, disorganized thinking, impaired judgment, and disorientation to time, space and location, which may lead to unsafe wandering and socially inappropriate behavior. With disease progression, these symptoms become more frequent and patient's memory further deteriorate. For example many patients find difficulties remembering familiar faces and start to mix peoples identity like a brother for a friend. Further in advanced stages of AD, patient's memory is severely affected, that they might completely forget close family members, and the patients might start to find difficulty in walking, speaking, and eating. At this stage, patients needs total assistance for daily living activities.

More recently, a period of very subtle changes in memory performance that prelude the frank dementia of AD was described, this phase was called MCI (mild cognitive impairment). Majority of patients with MCI progress to AD, so it is believed to be an important stage, which if detected early and with accurate means, could be the proper timing to begin with the treatment of AD, before further damage to the brain occurs.[7, 8]

**1.5 Histopathological features**

Since the description of the two histopathological features of AD by Alois Alzheimer, the senile plaques and the neurofibrillary tangles are considered the two classical hallmarks of AD, however, more recently gliosis, neuroinflammation, and oxidative stress have been recognized to be as important as the classical hallmarks of AD.[9]

**Neurofibrillary tangles**

Neurofibrillary tangles are intracellular deposits that are formed of a paired helical filament of aggregated hyperphosphorylated tau protein. Under physiological conditions tau protein is essential for normal neuronal functions and survival; it binds microtubules and promotes normal axonal transport and integrity.[10] Phosphorylation state of tau determines its binding affinity to microtubules. In AD, Tau proteins become hyperphosphorylated, which triggers their detachment from microtubules, which consequently leads to their disintegration and to an interruption of axonal transport and neuronal death. The hyperphosphorylated tau proteins misfold and aggregate forming the neurofibrillary tangles.

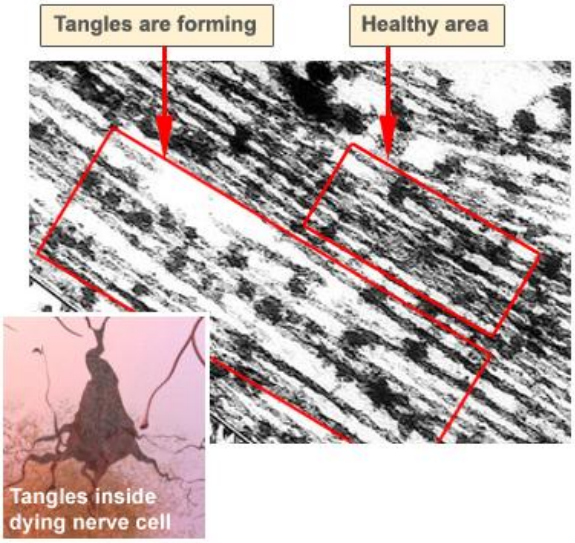


**Figure3. Electron microscope picture of healthy brain area versus brain with tangles. In healthy area, transport system which transports food material, cell part and other key material is organized like railway track. Tau protein keeps the track straight. In Alzheimer's disease tau collapses and forms tangles. Tracks fall apart and no longer stay available for transport.[1]**

The exact mechanism that leads to this hyperphosphorylation is not known, but evidence suggests that there's an imbalance between phosphorylation and dephosphorylation; tau kinases are responsible for tau phosphorylation while tau phosphatases are responsible for its dephosphorylation. The kinases that are found to be upregulated in AD include glycogen synthase kinase 3 (GSK3), cyclin-dependent protein kinase 5 (CDK5), calcium/calmodulin-dependent protein kinase II (CaMK2), phospho70S6 (p70S6) kinase, c-Jun N terminal kinase (JNK), and p38 kinase. The tau phosphatases that are found to be down regulated in AD are protein phosphatases PP1, PP2A, and PP2B.[10]

The filaments that compose NFTs have a characteristic ultra structure, consisting of two ribbon-like strands, twisted around each other to form paired helical filaments (PHFs). The diameter of each PHF alternates between 20 nm and 8 nm with a regular periodicity of 80 nm.[11] NFTs are frequently found in the brain of non-demented elderly individuals, but not in the isocortex: It has been shown previously that the neurofibrillary pathology in the brain accumulates in a hierarchical topographic fashion, with the trans entorhinal cortex affected first (stages I and II), followed by the entorhinal cortex and hippocampus (stages III and IV), and finally the isocortex (stages V and VI). Most patients with dementia are found to have stage V or VI pathology, while those at lower stages usually show no signs of dementia. In general, NFTs tend to fill much of the cell body and apical dendrite, giving a characteristic 'flame' shape. In neurons with a more rounded contour, the NFTs are more globular. In certain brain regions, such as the hippocampus, extracellular (ghost) tangles may persist in the extracellular space after the neuron dies.[12]

**Senile plaques**

Senile plaques (SPs) are extracellular spherical lesions, measuring up to 200 µm in diameter, they consist of a central deposit of Aβ protein, associated with various localized cellular changes.[13, 14, 15] Most of the Aβ that accumulates in senile plaques is the longer $A\beta_{42}$ species. In addition to Aβ, a variety of other molecules may be present in the extracellular component of SPs, including immune system proteins (such as complement and cytokines), growth factors, adhesion molecules, ApoE, and proteoglycans.

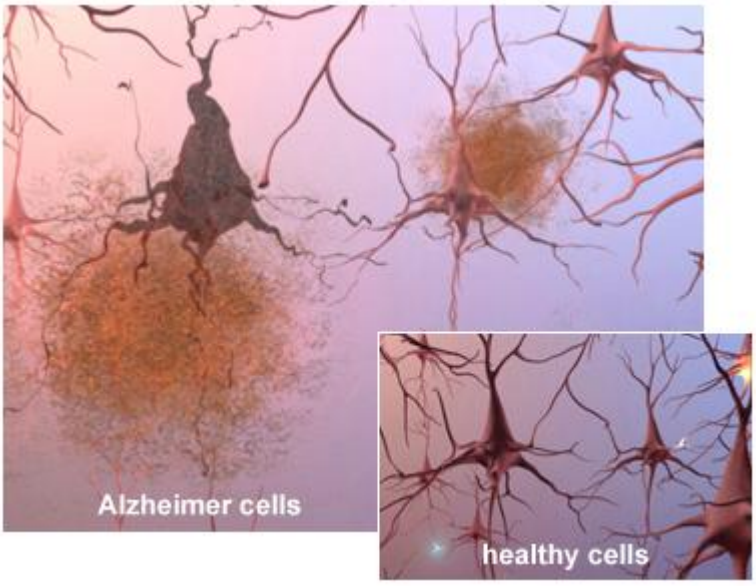


**Figure 4. Healthy versus Alzheimer brain tissue under microscope. Healthy brain tissue has more neurons and synapses compare to Alzheimer tissue.[1]**

Aβ is a 4-KDa protein consisting of 37 to 42 amino acids, it is generated by a sequential cleavage of the transmembrane protein amyloid precursor protein (APP), by two proteases: β secretase cleaves APP at the N-terminal and produces a 99 amino acid long transmembrane fragment called "C99", and γ secretase cleaves at the C-terminal of C99 to release Aβ[16]. The β secretase cleavage site is considered to be invariable at position 1 of Aβ, however, γ secretase cleavage is found to be variable; cleaving C99 at position 40 of Aβ, and less frequently at positions 37, 38, 39, and 42.[17]

SPs can be classified into four different morphological types: diffuse plaques, primitive neuritic plaques, classical neuritic plaques, and compact plaques.[15] Despite previous evidence suggesting that these different types are formed independently, it has been proposed that they evolve from one type into another.[15] The primitive and classical

neuritic senile plaques contain a cluster of radially oriented degenerated neuronal processes. These 'dystrophic neurites' are terminal dendrites and axons with dense bodies and vesicular structures. In classical neuritic SPs, the dystrophic neurites surround a central dense amyloid core, with less compact amyloid fibrils deposited between the neurites. Primitive neuritic SPs lack a well-defined central core of amyloid. Compact plaques have only a dense amyloid core, in the absence of any cellular component. Diffuse SPs are formed by an amorphous deposition of non-fibrillar Aβ that is not associated with any alteration in the cellular environment. Compact and diffuse senile plaques do not contain dystrophic neurons, therefore they don't fit within the classification of "neuritic" senile plaques. Neuritic senile plaques are the senile plaques associated with AD, while the brain of non-demented elderly people shows almost exclusively the diffuse type.[18]

Although neurofibrillary tangles and senile plaques are considered the 2 classical hallmark of AD, it is still debated whether they are a cause or consequence of AD pathogenesis and whether there's a relationship between the two lesions, in which one of them induces the formation of the other. But many evidence support a central role for Aβ rather than NFT in AD pathogenesis including direct evidence of neurotoxicity as shown in cell cultures and in animal studies, [19, 20] and the fact that all genetic mutations that were shown to cause AD affect the production of Aβ while none of the mutation causing AD are associated with tau protein or the enzymes responsible for its phosphorylation.[21] Mutations in the tau gene on chromosome 17 have been associated with the frontotemporal dementias with Parkinsonism (FTDP-17). These pathologies are

characterized with aggregations of tau in neurons and glia without the presence of amyloid deposits, and they produce a clinical phenotype of frontotemporal dementia (FTD) which is clinically distinguishable from AD.[20]

The normal physiological function of Aβ or its precursor protein is still not clear. To understand their physiological functions, APP knockout mice have been generated and these mice were found to be viable and fertile, however they were found to be 15-20% underweight compared with age-matched controls, exhibit reduced grip strength and locomotor activity, and show signs of reactive astrocytes and activated microglia.[22] This shows that APP and/or Aβ are important molecules for normal neuronal functions. It was suggested previously that APP can serve as a cell surface receptor, a heparin binding site, a precursor to a growth-factor-like agent, and as a regulator of neuronal copper homeostasis, but further studies are needed to confirm the normal physiological functions of APP.[23, 24]

In 1990, synthetic Aβ peptides were reported for the first time to be cytotoxic towards primary neuronal cultures; while low concentration were found to induce a neurotrophic effect to undifferentiated hippocampal neurons, higher concentration were found to be highly toxic, and the region between amino acids 25 and 35 of Aβ was found to be essential for inducing such neurotoxicity.[25] This toxicity was later shown to be dependent on the aggregation state of Aβ and reversal of Aβ aggregation resulted in the loss of such toxicity; in addition to its importance in neurotoxicity, the region 25-35 of Aβ was found to be also essential for aggregation, supporting an important role for aggregation in inducing the toxicity of Aβ.[26, 27] The important role of aggregation was later confirmed in

animal studies; microinjection of aggregated form, but not soluble form, of Aβ in the cerebral cortex resulted in extensive neuronal loss, tau hyperphosphorylation, and microglial activation in the brain of aged rhesus monkeys. Interestingly, the same level of aggregated Aβ was not toxic to young rhesus monkeys and mice. Higher levels of Aβ were found to be neurotoxic in mice, however this neurotoxicity is not associated with the formation of neurofibrillary tangles. This dissociation between Aβ toxicity and presence of neurofibrillary tangle questioned the validity of the amyloid hypothesis. However more recently it was found that iNOS knockout mice overproducing Aβ develop AD like neuropathological features including neurofibrillary tangles, neuronal loss, and behavioral changes, which suggests that low levels of nitric oxide in aged brain could be the factor that increases the susceptibility towards Aβ.[28, 29]

In addition to region 25-35 of Aβ, the last two amino acids of $A\beta_{42}$, were found to increase dramatically the aggregation potential and toxicity of $A\beta_{42}$ compared to $A\beta_{40}$.[20] This could explain the reason why $A\beta_{42}$ is the main constituent of the senile plaques despite the fact that the most abundant product of APP cleavage is $A\beta_{40}$.[20] Further support for an important role of $A\beta_{42}$ in neurotoxicity compared to $A\beta_{40}$ was obtained using mice selectively producing $A\beta_{40}$ or $A\beta_{42}$ independently of APP production. Mice expressing high levels of $A\beta_{40}$ did not develop overt amyloid pathology. In contrast, mice expressing lower levels of $A\beta_{42}$ accumulate insoluble $A\beta_{42}$ and developed compact amyloid plaques and diffusible Aβ deposits. When mice expressing $A\beta_{42}$ were crossed with mutant APP transgenic mice (Tg2576), there was also a massive increase in amyloid deposition.[30]

Aβ aggregation starts with the formation of dimers and trimers followed by the formation of low molecular weight oligomers, protofibrils and finally mature fibrils.[19] While fibrils were found to be more toxic than monomers, low molecular weight oligomers were the most toxic[31] and the presence of plaques was found not to be essential for Aβ to induce neuro and synaptotoxicity.[32] Soluble and highly toxic forms of amyloid aggregates were called Aβ-derived diffusible ligands (ADDLs) and they were found to be formed mainly of 12 unit of Aβ.[33, 34] ADDLs were first produced in vitro, however they were later discovered in vivo, and in comparing AD brain tissues to non demented controls, ADDLs were found to be 12 times more abundant in AD patients.[35]

Many attempts to use the level of Aβ in the cerebrospinal fluid (CSF) as a marker for AD have failed, in fact the brain of many non demented elderly people show high levels of Aβ and abundant senile plaques formation. However careful examination of the type of plaques revealed that while AD patient develop all 4 types of plaques, non demented individuals develop only the diffuse senile plaques, with rare neuritic senile plaques. Accordingly it was suggested that a pathological process is responsible for the conversion of diffuse plaques into neuritic senile plaques. One of these processes that might play an important role and that gained much attention recently is neuroinflammation, especially since an important difference between diffuse senile plaques and neurotic senile plaques is the presence of localized gliosis: activated microglia are often present within the plaque boundary and reactive astrocytes are found on the periphery. This suggests that the presence of Aβ is not sufficient to develop AD; however it is important to trigger an inflammatory reaction which is responsible for the neurotoxicity.[9, 14, 15]

**Neuroinflammation**

In addition to the two classical hallmarks of AD, recent evidence has shown that neuroinflammation plays an important role in the pathology of AD, in fact when Alois Alzheimer described the brain pathology of AD, he used the term "Gliosis" to describe the changes he observed in glial cells.[9]

Not a long time ago, the brain was considered to be an immune incompetent organ and until recently neuroinflammation was ignored in the field of AD research, but the epidemiological studies that showed a decreased risk of developing AD with a history of NSAIDs consumption,[36, 37, 38, 39] combined with the demonstration of an increased level of inflammatory markers in AD brain tissue, fueled the research in that field and lots of evidence have drawn a direct link between neuroinflammation and AD[9].

In physiological conditions, neuroinflammation is part of the innate immune system that protects the brain from harmful stimuli. Acute local inflammatory reactions are more often safe with limited and reversible damage; however chronic inflammatory reactions, in the CNS as well as in any other organ, will more often lead to tissue damage and scaring.[9] Brains of patients with AD display many signs of neuroinflammation including high level of cytokines and chemokines, [9] activation of classical and non-classical complement pathways, microglial activation, and astrocyte reactivity.[40]

The etiology of the inflammatory reaction observed in AD is still debated, but lots of evidence point to the Aβ peptide as the inflammatory triggering agent,[40, 41] either directly by activating microglia and astrocytes, or indirectly by inducing neurodegeneration which will then start an inflammatory reaction. In cell cultures, both mechanisms were

observed; Aβ can induce neuronal death, and it was also shown that Aβ can directly induce inflammatory responses by activating macrophages and microglia.[42, 43]

**Oxidative stress:**

An oxidative imbalance occurs, when production of oxidant species exceeds the endogenous antioxidant ability to destroy them. This leads to cellular oxidative stress, molecular oxidative damage, altered cellular functions and finally cell death. The CNS is highly populated with polyunsaturated fatty acids (PUFAs) which has high metabolic oxidative rate and high levels of potent pro-oxidants like transition metals and ascorbate. Therefore, CNS is at high risk for oxidative imbalance. Altered mitochondrial function, the Aβ peptides themselves and the presence of unbound transition metals are the sources of oxidant species in the CNS. In early stages of AD, Aβ enters mitochondria, increases generation of ROS and induces oxidative stress. In mitochondrial membranes Aβ and APP can block transport of protein and disrupt the electron transport chain followed by irreversible cell damage at the end. Oxidative stress is characterized by protein, DNA, RNA oxidation or lipid peroxidation. AD brain has all these signature markers of oxidative stress and this concept was originally used to support the 'oxidative stress hypothesis' of AD.[44-47]

### 1.6 Genetics of AD

Gamma secretase is a multi-subunit transmembrane protease complex; it is formed of 4 different subunit : presenilin 1 (PSEN1) or presenelin 2 (PSEN2), nicastrin, APH-1 (anterior pharynx-defective 1), and PEN-2 (presenilin enhancer 2). The presenilins are

the catalytic subunit of gamma secretase.[48] It was found that certain mutations in PSEN1 (on chromosomes 14) and PSEN2 (on chromosomes 1) and other mutations in APP (on chromosome 21) are linked with autosomal dominant AD inheritance, and further studies on these mutations revealed that they are associated with either a total increase of Aβ production or with an increase in the production ratio of $A\beta_{42}/A\beta_{40}$. As AD caused by any of these mutations is genetic and follows an autosomal dominant inheritance it is referred to as familial Alzheimer's disease (FAD); FAD is usually characterized by an early disease onset (before 65 years old). By 2008, it was found that 32 different mutations in the APP gene account for 18% of FAD, 165 different mutations in the PS1 gene account for 78% of FAD, and 12 different mutations in PS2 gene account for 4% of FAD.[48] Despite the numerous mutations associated with AD, FAD accounts for less than 5% of all AD cases. In the rest of AD cases, also called sporadic AD or late onset AD, there is no genetic link associated with the development of AD, but apolipoprotein E gene polymorphism has been associated with an increase risk of developing AD. The E4 allele of ApoE is considered to be the only established genetic risk factor for the late onset AD.[49, 50, 51]

ApoE is a 299 amino acid protein that mediates the binding of lipoproteins to the low-density lipoprotein (LDL) receptor and the LDL receptor-related protein (LRP), it is the major apolipoprotein expressed in the brain and it is thought to be important for mobilizing lipids during normal development of the nervous system and during regeneration of peripheral nerves after injury.[52, 53] It exists in three major isoforms: ApoE2, ApoE3 and ApoE4 which arise from different alleles (e2, e3, and e4) of a gene

on chromosome 19. The e3 allele is the most common form among the general population, accounting for about 75% of all alleles, whereas e2 and e4 account for 10% and 15%, respectively.[53]

The mechanism by which ApoE alleles affect the occurrence of AD is not clear. ApoE is one of the proteins found in the neuritic plaques, and apoE4 binds Aβ more readily than apoE3 does. AD patients who are homozygous for the e4 allele has larger and denser senile plaques than patients homozygous for the e3 allele.[54] Therefore apoE4 may facilitate plaque formation or reduce the clearance of Aβ from brain tissue. However, more recent evidence suggest that ApoE plays an important role in clearing Aβ from the brain, and that APOE4 is less effective than APOE3 or APOE2, which support other evidence suggesting that sporadic AD is caused by a decrease in Aβ degradation and clearance from the brain.[55-58]

**1.7 Diagnosis of AD**

Early detection of AD can be very challenging, while its identification later in its course is very often more obvious. At the moment, the diagnosis of AD is only made clinically and with a certain amount of uncertainty; there has not been any test or imaging technique that proved to be accurate enough for its application in the diagnosis of AD. In diagnosing patients with dementia, AD can only be suspected after other form of dementia has been ruled out, this include: vascular dementia, frontotemporal dementia, corticobasal degeneration, progressive supranuclear palsy, dementia with Lewy body, Parkinson disease dementia, hypothyroidism, syphilis, normal-pressure hydrocephalus,

nutritional deficiencies such as vitamin B12, folic acid, and thiamine deficiency, and prion diseases including Creutzfeld– Jacob Disease (CJD), Gerstmann–Straussler–Scheinker syndrome (GSS), fatal familial insomnia (FFI), Kuru and Alpers syndrome. The ultimate diagnosis of AD can only be made by histopathological analysis of postmortem brains from patients diagnosed clinically of having AD.[59]

### 1.8 Treatment strategies of AD

#### Acetylcholine esterase inhibitors

Direct analysis of neurotransmitter content in the cerebral cortex shows a reduction of many neurotransmitters that parallel neuronal loss; impairment in the cholinergic neurotransmission is found to be the most consistent finding in AD brains and the degree of damage to cholinergic system correlates closely with the severity of AD;[60] so it was hypothesized that the lack of acetylcholine is responsible for the dementia, especially that central cholinergic antagonists such as scopolamine can induce a confusional state that resembles the dementia of AD;[61] for these reasons the "cholinergic hypothesis" of AD emerged stating that dementia in AD is caused by a neurodegeneration affecting cholinergic neurons, and it was hypothesized that supporting the cholinergic deficiency by drugs that activate the cholinergic receptors or prevent the degradation of acetylcholine would be beneficial. In postmortem examination of AD brains, the most severe neurodegeneration is usually found in the hippocampus, temporal cortex, and nucleus basalis of Meynert.[62] It was suggested that the reduction of acetylcholine may be related in part to degeneration of the cholinergic neurons in the nucleus basalis of

Meynert that project to many areas of the cortex. According to the "amyloid hypothesis", Aβ is responsible for the neurodegeneration leading to the cholinergic deficiency.[60]

One approach to elevate the level of acetylcholine is to inhibit the enzyme responsible for its degradation: acetylcholine esterase. All drugs presently available in the market for the treatment of mild to moderate AD are acetylcholine esterase inhibitors. The main problem with this class of drugs is that they support the synaptic transmission of a progressively degenerating neuronal network, which with further degeneration the patients fail to respond to this drug family.[63, 64]

Four inhibitors of AChE are currently approved by the FDA for the treatment of AD: tacrine (COGNEX), donepezil (ARICEPT), rivastigmine (EXCELON), and galantamine (RAZADYNE).

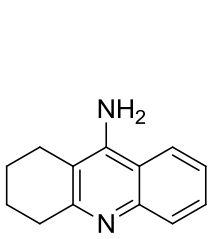


Tacrine

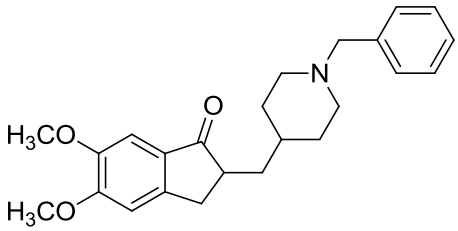


Donepezil

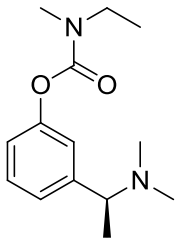


Rivastigmine

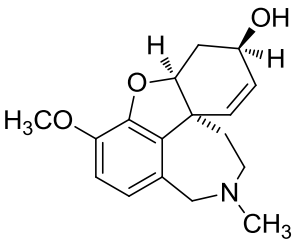


Galantamine

Tacrine is a potent centrally acting inhibitor of AChE.[63, 64] The side effects of tacrine often are significant and dose-limiting; abdominal cramping, anorexia, nausea, vomiting,

and diarrhea are observed in up to one-third of patients receiving therapeutic doses, and elevations of serum transaminases, marker of liver injury, are observed in up to 50% of those treated. Because of significant side effects, tacrine is not widely used clinically. Donepezil is a selective inhibitor of AChE in the CNS with little effect on AChE in peripheral tissues. It produces modest improvements in cognitive scores in AD patients and has a long half-life, allowing once-daily dosing. Rivastigmine and galantamine are dosed twice daily and produce a similar degree of cognitive improvement. Adverse effects associated with donepezil, rivastigmine, and galantamine are similar in character but generally less frequent and less severe than those observed with tacrine; they include nausea, diarrhea, vomiting, and insomnia. Donepezil, rivastigmine, and galantamine are not associated with the hepatotoxicity that limits the use of tacrine, but due to the longer half life of Donepezil, it is preferred over rivastigmine or galantamin.[63]

**NMDA receptor antagonist**

An alternative strategy for the treatment of AD is the use of the NMDA glutamate receptor antagonist memantine (NAMENDA). Memantine was approved in 2003 by the FDA for the treatment of mild to severe cases of AD; however the efficiency of memantine is surrounded with lots of controversies.

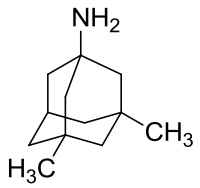


Memantine

Glutamate is the principle excitatory neurotransmitter in the cortical and hippocampal neurons. Neurochemical analysis of AD brain shows excess glutamate concentrations. While moderate activation of the glutamate receptor, NMDA, is essential for learning and memory, excessive activation increases the vulnerability of CNS neurons leading to neuronal degeneration.[65] Memantine blocks glutamate gated NMDA channels in an activation dependant manner, thereby blocking excessive and pathological activation without affecting the moderate and normal physiological activation.[66, 67, 68] In contrast to ACIs, which are approved for the early and intermediate stages of AD only, memantine is approved for treating the advanced stages of AD.[65] Data regarding memantine efficiency for AD treatment are controversial. A randomized clinical trial on 252 patients found that memantine significantly reduces deterioration of mental functions.[69] However this was not confirmed by a more recent double blind, placebo-controlled trial involving 350 patients. This trial showed no statistically significant treatment benefit at study end point on any primary or secondary outcomes measured after 24 weeks. A Cochrane systematic review reported only a small beneficial effect at 6 months in moderate to severe AD on cognition, Activities of Daily Living (ADLs), and behavior supported by clinical impression of change. There is evidence that combination therapy with donepezil may provide better outcomes with regards to cognition, ADLs, global outcome, and behavior as illustrated in a 24-week trial in 322 patients.[70]

**Aβ lowering strategies**

According to the amyloid hypothesis, Aβ plays a central role in the etiology of AD. This hypothesis initiated a wide spread research to find drugs that would lower the level of Aβ in the brain; this includes the inhibition of beta secretase, modulation or inhibition of gamma secretase, and immunization against Aβ.[65, 71] Drugs that lower the level of Aβ are believed to be disease modifying agents and would provide an advantage over the symptomatic treatment of acetylcholine esterase inhibitors.[72]

Active immunization against Aβ faced recently big challenges due to severe immunological reactions leading to encephalopathy and death observed among some patients participating in the clinical trial: following the success in the reduction of Aβ plaques in animals by active immunization against Aβ, [73] clinical trials were conducted on AD patients by Elan Pharmaceuticals/Wyeth. Phase IIa clinical trials were suspended when 6% of patients in the active treatment group developed meningoencephalitis characterized by subacute neurologic deterioration, lymphocytic pleocytosis, and white matter abnormalities on imaging, by the time the trial was halted five patients receiving the drug have died. Passive immunization, using monoclonal antibodies, is still under investigation, especially that this technique is considered to be a safer approach compared to active immunization.

Beta secretase (BACE1) inhibition is still a major target, as it has been reported previously that BACE1 knockout mice are healthy with no detectable pathological consequences.[74] The major challenges facing BACE inhibitors is their molecular weight which greatly affects their ability to cross the blood brain barrier,[75] this fact made it

difficult for any BACE inhibitor to reach clinical trials, however with recent progress, newer and smaller BACE inhibitors that crossed the BBB in animal models have emerged giving hope for this approach. As for gamma secretase inhibition, it was associated with severe side effects, including gastrointestinal toxicity and eosinophilia;[76-79] the reason for these side effects is due to the inhibition of notch cleavage: notch is a transmembrane protein that is cleaved by gamma secretase, the same enzyme that cleaves APP, to release an intracellular domain that is then translocated to the nucleus where it acts as a transcription factor; Notch is essential for the differentiation of different cell types including cells of the gut and the immune system, which explains the eosinophilia and gut toxicity that are associated with gamma secretase inhibition.[76-80] However it has been suggested recently that the gamma secretase enzyme can be modulated by a group of NSAIDs in order to cleave C99 less frequently at position 42 leading to a selective reduction of Aβ42 production without affecting notch cleavage.[64] The link between NSAIDs and Aβ42 production started when epidemiological studies suggested that chronic NSAIDs consumption reduced the risk, delayed the onset, and slowed the progression of AD. It was thought that this activity is due to the anti-inflammatory properties of NSAIDs, including the inhibition of microglial activation, however evidence has shown that a subset of NSAIDs, including flurbiprofen, sulindac sulfide, and indomethacin, are capable of lowering the levels of $A\beta_{42}$ and the ratio of $A\beta_{42}/A\beta_{40}$. The term selective amyloid lowering agents (SALA) was coined for this "new" drug class, represented by *R*-flurbiprofen (tarenflurbil), a drug that provided positive phase 2 clinical trial data in AD patients before failing in a phase 3 trial.[81, 82]

The failure of tarenflurbil raises concern about the validity of the "amyloid hypothesis" as a causal factor for AD. However, by thorough analysis of the in vivo pharmacological and pharmacokinetic studies and the setup of the clinical trial, many weak points can be discovered raising question if tarenfluril is a valid candidate to be used for judging the amyloid hypothesis and if the setup of the clinical trial as to the time of drug administration is a valid method: Tarenflurbil showed consistent evidence for activity in lowering Aβ in *ex vivo* experiments and in animal models of AD;[83-84] despite consistent activity in lowering Aβ, many problems were discovered including poor bioavailability and weak activity; only 1% of the drug crosses the blood brain barrier, and in cell culture the EC50 for lowering Aβ level is higher than 100 μM.[85] As for the setup of the clinical trial, the patients selected for the trial were patient that had already developed the symptoms of AD, however it was suggested previously that lowering Aβ levels in the brain as a treatment strategy should be initiated before the pathological manifestation of the disease. In fact some of the epidemiological studies revealed that a lag period of 2 years is important for the protective activity of NSAIDs against AD.[86] This requirement was demonstrated in vivo using a transgenic mouse model that genetically mimics the arrest of Aβ production with Aβ lowering agents; these mice, overexpressing mutant APP from a vector that can be regulated by doxycycline, produced high-level of APP and quickly induced amyloid plaques formation under normal conditions; Doxycycline administration inhibited transgenic APP expression by greater than 95% and reduced Aβ production. When doxycyclin was administered before plaques were formed it suppressed the amyloid pathology while long term doxycyclin administration after

plaques formation had little effect on amyloid pathology. The already formed amyloid plaques remained in the brain for more than a year, and the brain showed little sign of active amyloid clearance, and surprisingly, while Aβ production was inhibited as detected by the inhibition of APP expression, the levels of soluble Aβ remained relatively high, suggesting that the plaques dispersion requires longer than to assemble and that once these plaques are formed they act as an amyloid pool slowly shedding soluble Aβ. Many enzymes shown to degrade Aβ were shown to be ineffective in degrading aggregated forms of Aβ; this could be the explanation for the long-term presence of these amyloid plaques in doxycyclin treated mice. However due to the short life span of mice, the amyloid plaques were monitored up to one year, leaving a possibility that plaques might eventually disappear but not within one year.[87]

As discussed previously, amyloid plaques are formed mainly of Aβ fibrils which are not most toxic form of Aβ. It is the Aβ-derived diffusible ligands (ADDLs) that are the most toxic form, so constant presence of plaques after the administration of flurizan or the use of NSAIDs without a lag phase might not be a direct cause for the failure of these anti-AD therapies, but it's the constant shedding of soluble Aβ from these plaques, as described by jankowsky et al, that can be the cause. The prolonged lag period could be essential for giving the already formed senile plaques enough time to disintegrate and degenerate to a level that wouldn't be able to release enough Aβ to cause any damage. So Aβ lowering agents might be used for AD prevention rather than AD treatment and to be effective, the therapy might need to be initiated at the appropriate moment before the

onset of clinical symptoms. An effective biomarker or diagnostic tool might prove very efficient in the future for predicting this appropriate moment.[87]

If clinical symptoms of AD have already started and lowering Aβ level is a long term process, an additional approach would be to support the neurons using a neuroprotective or anti-inflammatory drugs until an adequate level of Aβ is reached.[89] It has been proposed previously, that if the onset of AD can be delayed by 5 years, the number of affected people in the United States will decrease by almost 50% by 2050, and even with a modest delay of one year, the prevalence will decrease by close to one million.[90]

# Chapter 2 Design, synthesis, and biological characterization of BMAOIs containing curcumin and cholesterol

## 2.1 Introduction

Alzheimer's disease (AD) is a devastating neurodegenerative disease and is the most common cause of dementia. The etiology of AD still remains elusive and multiple factors have been suggested to contribute to the development of AD, among which amyloid-β (Aβ) and oxidative stress have been well documented.[91,92] Emerging evidence indicates that small Aβ oligomers (AβOs), rather than insoluble Aβ fibrils, are responsible for disruption of neuronal synaptic plasticity and the resulting early cognitive impairment associated with AD.[93] Studies of brain samples from AD patients also confirmed the correlation of AβOs with the severity of dementia.[94-96] Despite the fact that multiple assemblies of AβOs and a variety of underlying mechanisms have been suggested in the literature,[97-101] one point of consensus remains clear: the requirement of AβOs. Collectively, these findings provide compelling support for developing Aβ oligomerization inhibitors as novel therapeutic agents for the treatment of AD. Increased oxidative damage by reactive oxygen species (ROS) and reactive nitrogen species is another feature consistently found in the brains of AD patients.[92, 102] Many factors have been demonstrated to cooperatively contribute to the production of ROS in the AD brain such as biometals, mitochondria dysfunction and Aβ.[103] Transgenic mouse studies have also showed a correlation of increased oxidative stress and Aβ accumulation.[104]

Recently, a wealth of data has implicated the roles of neuronal cell membrane/lipid rafts (CM/LR) in the oligomerization and toxicity of Aβ.[105,106] Once associated with the

membranes, Aβ exhibits an enhanced rate of aggregation that is dependent on pH, metal ion and ganglioside interactions.[107-109] Recently, evidence has also indicated that lipid rafts, a cell membrane microdomain enriched in cholesterol and sphingolipids, can accelerate the cell membrane binding of Aβ and AβOs formation.[105-106] On the other hand, destruction of lipid rafts affects Aβ membrane binding and protects cells from Aβ toxicity.[110] Furthermore, Aβ precursor protein (APP), APP cleavage enzymes (β- and γ-secretases), Aβ and AβOs have all been identified in lipid rafts, suggesting that lipid rafts may be a critical platform for Aβ production and oligomerization.[111] In addition, oxidative stress has been shown to up-regulate presenilin-1, the critical component of γ -secretase, in lipid rafts of neuronal cells to promote Aβ production.[112] Altogether, it is apparent that CM/LR are important regulators in AD development and this relationship can be exploited to design and develop novel AD therapies.

Numerous chemical ligands have been developed as potential AD treatments by targeting Aβ and oxidative stress.[113, 114] However, very few of them moved to clinical trials and none of them has been approved by FDA, which suggests that targeting a single risk factor is not an ideal strategy for developing treatments for this multifaceted disease. In contrast, new approaches that co-target multiple risk factors involved in AD are emerging as promising strategies for developing effective treatment agents for AD.[115-117] Herein, we hypothesized that a bivalent multifunctional Aβ oligomerization inhibitors (BMAOIs) strategy that targets AβOs, oxidative stress and CM/LR would be a novel approach to design strategically distinct ligands with the potential to overcome the limits posted by the traditional single-factor based approach. Conceptually, these BMAOIs

contain a multifunctional AβO-inhibitor pharmacophore that accommodates additional antioxidant properties as well as a CM/LR anchor pharmacophore linked by a spacer (Figure 5). The use of bivalent strategies to explore protein-protein interactions has been particularly successful in opioid receptor research field.[118] Recently, this concept has been extended to neurodegenerative diseases in developing acetylcholinesterase inhibitors and metal chelators.[115] We envisaged that such BMAOIs would chaperone the multifunctional AβO-inhibitor moiety in close proximity to CM/LR in which AβOs and oxidative stress are produced to increase its accessibility to interfere with these multiple processes, thus improving its clinical efficacy (Figure 5). In this report, we rationally designed, synthesized and biologically characterized a series of BMAOIs and one compound was identified as a new hit for further investigation.

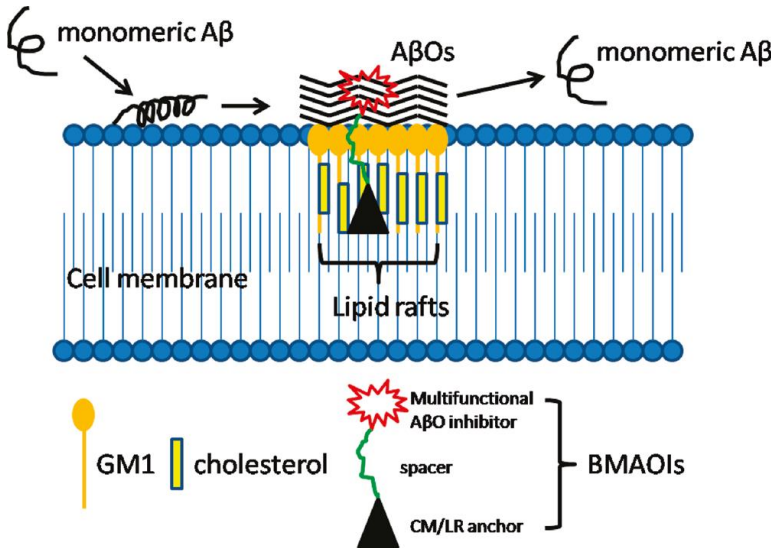


**Figure 5. BMAOIs strategy and design**

**2.2 Design and Chemistry:**

The desired BMAOIs must contain an AβO-inhibitor moiety with intrinsic antioxidant effects, as well as incorporate a residue able to efficiently interact with CM/LR, spanned by a stable linkage. Thus in our designed BMAOIs, curcumin (**1**) was selected as the multifunctional AβO-inhibitor pharmacophore and on the other end, connected by a spacer, cholesterol (**2**) was selected as the anchor pharmacophore to the CM/LR (Figure 6). The selections of **1** and **2** were based on the following reasons: 1) **1** is an important phytochemical that has long been known for its antioxidant, anti-inflammatory properties as well as recently discovered anti-Aβ properties;[119-122] 2) it has been demonstrated that **2** and other sterols linked with another moiety can anchor CM/LR in mammalian cells and function as a carrier to induce internalization via endocytosis.[123,124] The crucial consideration in designing BMAOIs is to determine the loci on the two pharmacophores for attaching the spacer and the nature and length of the spacer. Given the fact that alkylation of the 3-OH of **2**/sterol does not affect their binding affinities to CM/LR, [123-124] we selected this position as spacer attachment position. On the other end, one of the phenolic oxygens and the C-4 position (methylene carbon between the two carbonyl groups) of **1** were selected to design two series of BMAOIs to investigate the optimal attachment. Since it is not clear whether Aβ oligomerization occurs on the surface or inside of CM/LR and optimal spacer length range cannot be predicted from existing literature, we varied spacer length as a key parameter for investigation. Since the cell membrane thickness is frequently cited as 3 nm (although ranging from 2.5 to 10 nm), we have decided to initially vary the spacer length from 11 to 21 atoms (Figure 6). Two

monovalent ligands (**1** attached to spacer but not cholesterol) (**15** and **16**) were also designed to evaluate the influence of spacer attachment on **1**'s activity. Recently "click chemistry"[125] methodology has been successfully applied to connect **1** to peptides by Ouberai et al.[126] Therefore, to efficiently assemble the two pharmacophores together, we adopted this "click chemistry" methodology to include a 1,4-disubstituted triazole ring in the spacer.

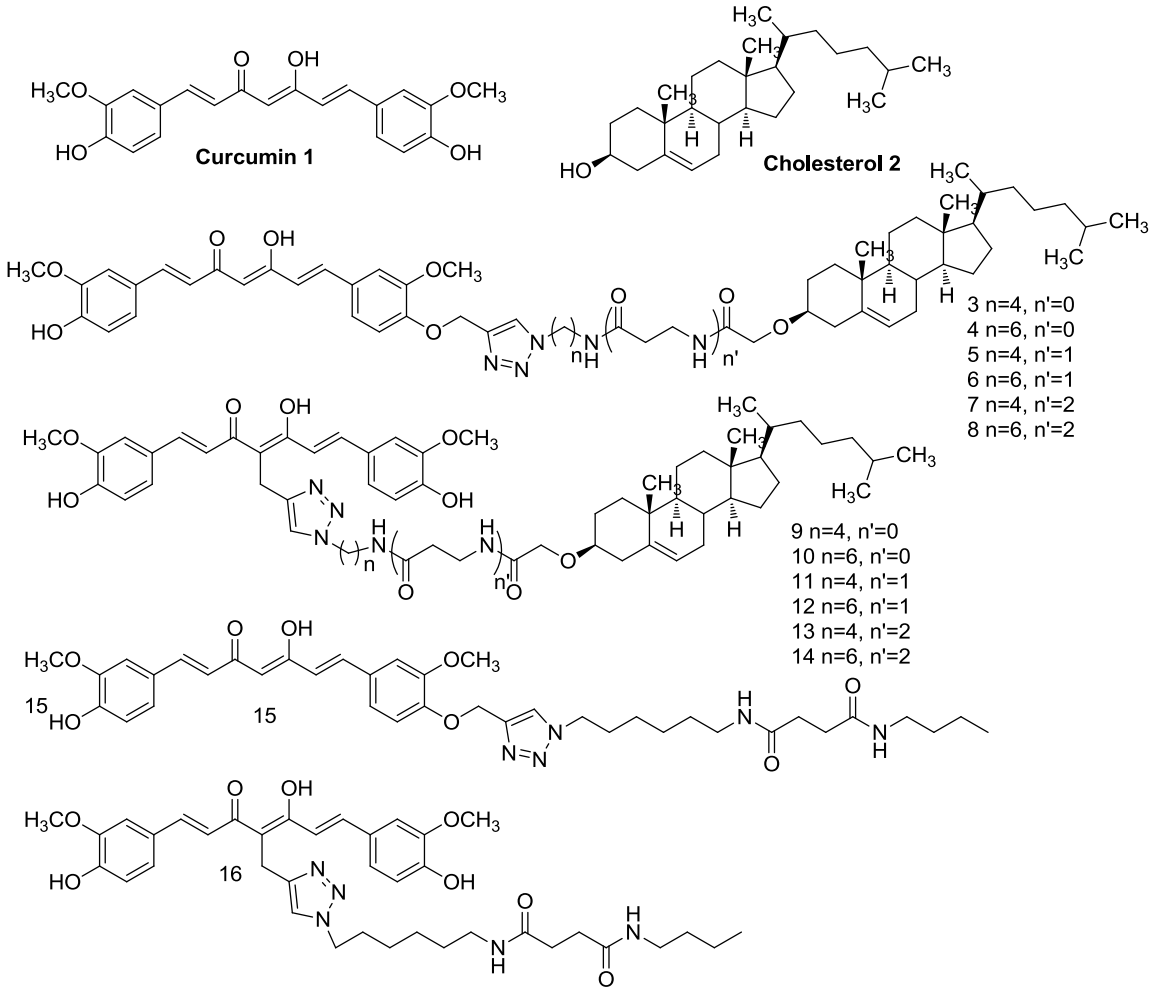


**Figure 6. Chemical structures of 1, 2, designed BMAOIs and monovalent ligands.**

The synthesis began with the preparation of alkyne intermediates **20** and **23** through well established Pabon reaction (Scheme 1).[127]

**Scheme 1. Synthesis of intermediates 20 and 23**[a]

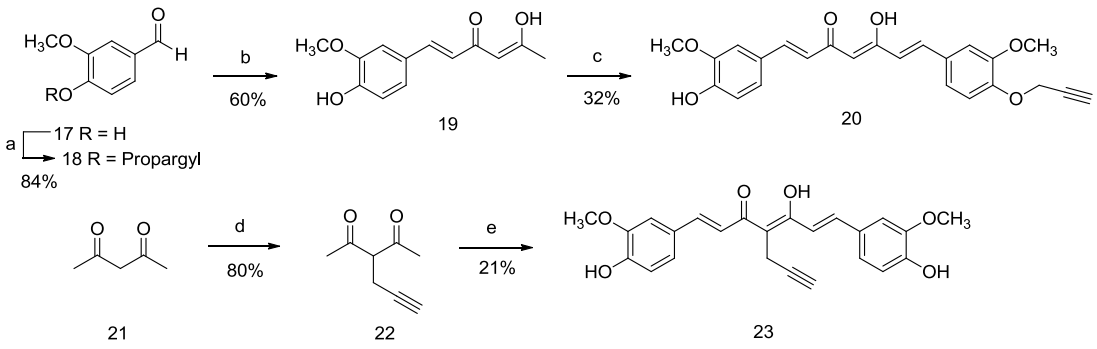


[a]Reagents and conditions: (a) propargyl bromide, $K_2CO_3$, DMF; (b) i. $B_2O_3$, acetylacetone; ii. $(BuO)_3B$, piperidine; iii. 1 N HCl; (c) i. 19,$B_2O_3$, ii. 18, $(BuO)_3B$, piperdine; iii. 1 N HCl; (d) propargyl bromide,$K_2CO_3$, benzene; (e) i. $B_2O_3$, 17, $(BuO)_3B$, n-$BuNH_2$; ii. 1N HCl.

Briefly, alkylation of vanillin **17** with propargyl bromide provided **18**. Aldol reaction of **17** with 2,4-pentane-dione followed by another Aldol reaction with **18** afforded intermediate **20**. Alkylation of 2,4-pentane-dione with propargyl bromide in the presence of 1,8-Diazabicycloundec-7-ene (DBU) in benzene yielded **22** which on Aldol reaction with **17** afforded intermediate **23**.

**Scheme2. Synthesis of Intermediates 32-37**[a]

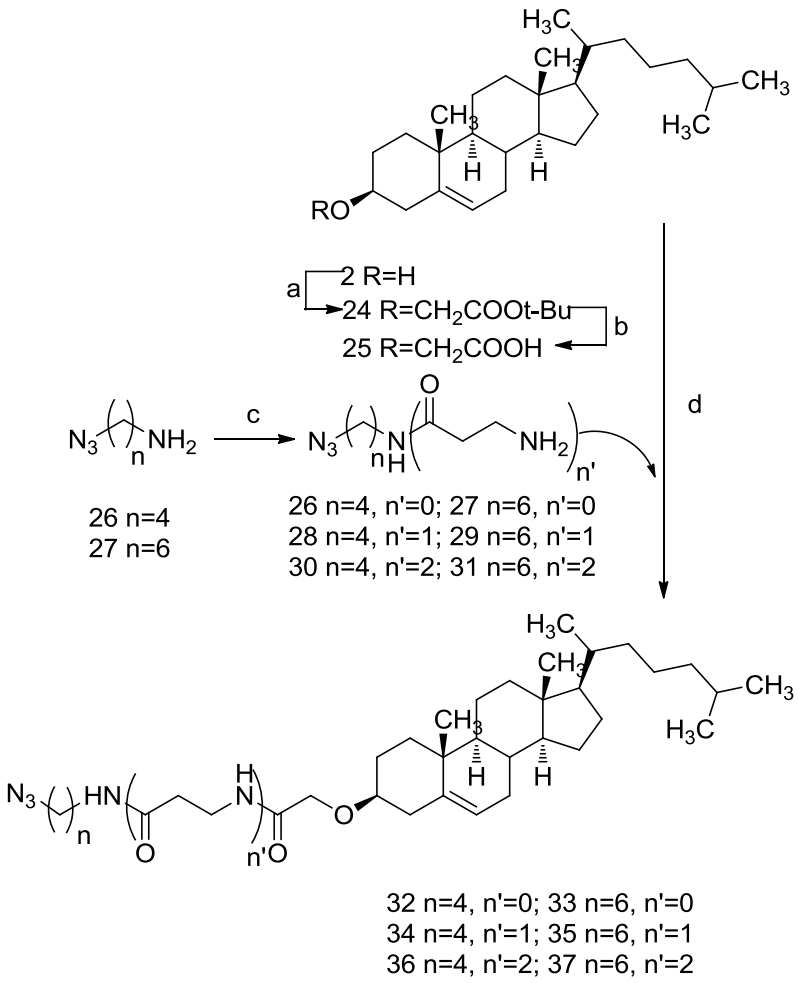


[a]Reagents and conditions: (a) tert-butyl-2-bromoacetate, NaH, THF; (b) formic acid/$Et_2O$; (c) i. Boc protected beta-alanine or Boc protected beta-alanylalanine, EDC, HOBt, $CH_2Cl_2$; ii. TFA/$CH_2Cl_2$; (d) EDC, HOBt, $CH_2Cl_2$.

As shown in Scheme 2, carboxylic acid **25** was synthesized following the reported procedure.[124] Then, coupling reactions of **25** with various azidoamines **26-31** which were synthesized through coupling reactions of azidoalkylamines **26** and **27** with Boc protected β-alanine followed by Boc deprotection afforded azido intermediates **32-37**.

**Scheme3. Synthesis of designed BMAOIs and Monovalent Ligands**[a]

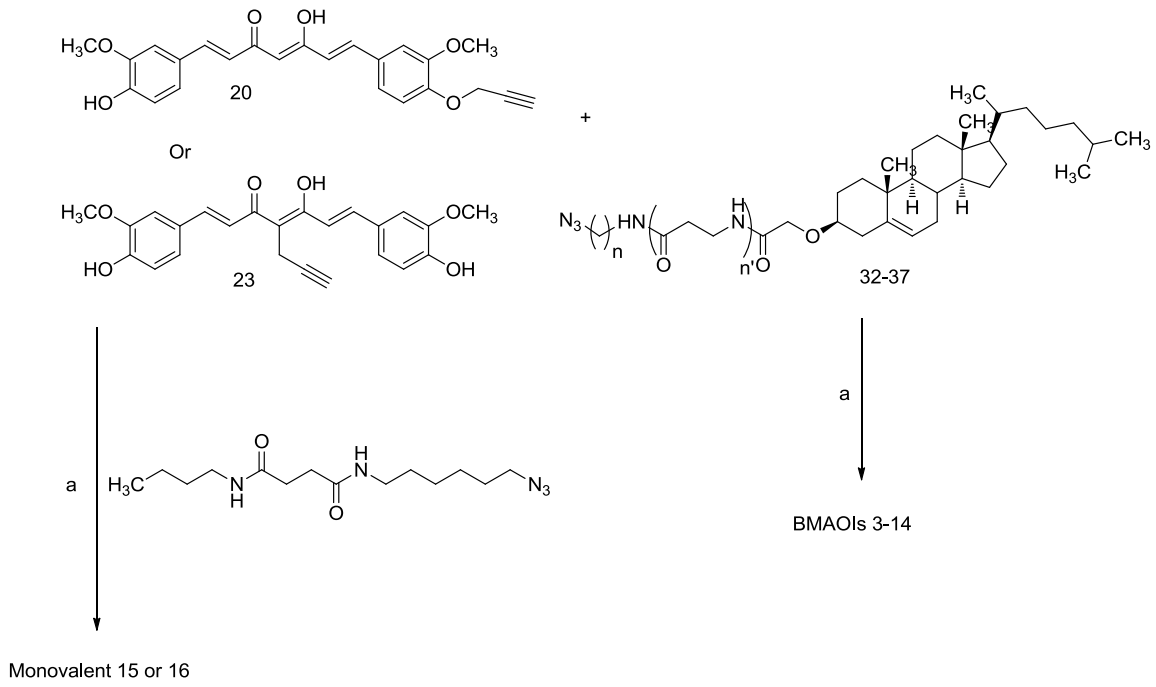


[a]Reagents and conditions: (a) CuSo4, sodium ascorbate, THF/H2O (1:1).

Once all the required intermediates were available, the click reactions of the alkynes **20** or **23** with **32-37** were applied under sodium ascorbate and $CuSO_4$ in THF/$H_2O$ conditions to obtain the designed BMAOIs **3-8** or **9-14**, respectively (Scheme 3). All the designed BMAOIs are in keto-enol forms in chloroform judged by $^{1}$HNMR and $^{13}$CNMR. The synthesis of the monovalent compounds **15** or **16** is similar to the synthesis of BMAOIs. Click reactions of **20** or **23** with azido intermediate **38** which was synthesized from the reaction of butylamine with succinic anhydride followed by amide coupling with 6-azidohexylamine achieved the synthesis of **15** or **16**, respectively.

## 2.3 Results and Discussion

### 2.3.1 Inhibition of AβOs Production by Designed BMAOIs.

The rational design of BMAOIs targeting CM/LR and AβOs as well as oxidative stress will require demonstration of anticipated effects in a biologically relevant system. The whole cell assay is a composite of not only Aβ oligomerization inhibition, but also permeability, stability, and other factors will validate the accessibility and function of our BMAOIs. MC65 is a human neuroblastoma cell line that conditionally expresses C99, the C-terminus fragment of APP using tetracycline (TC) as transgene suppressor.[128]Upon removal of TC, these cells can produce intracellular Aβ aggregates including small AβOs. Most importantly, the induced cytotoxicity in these cells by TC removal has been associated with the accumulation of AβOs.[129]Furthermore, oxidative stress has been indicated as one potential effector to impart neurotoxicity upon the accumulation of intracellular AβOs in this cells.[130] Therefore, MC65 cells were initially employed to validate and test our BMAOIs using Western blot analysis. All BMAOIs were first evaluated at a single concentration of 10 μM. Candidate compounds with inhibitory activities at this concentration were further evaluated in a dose-dependent manner in the following assays.

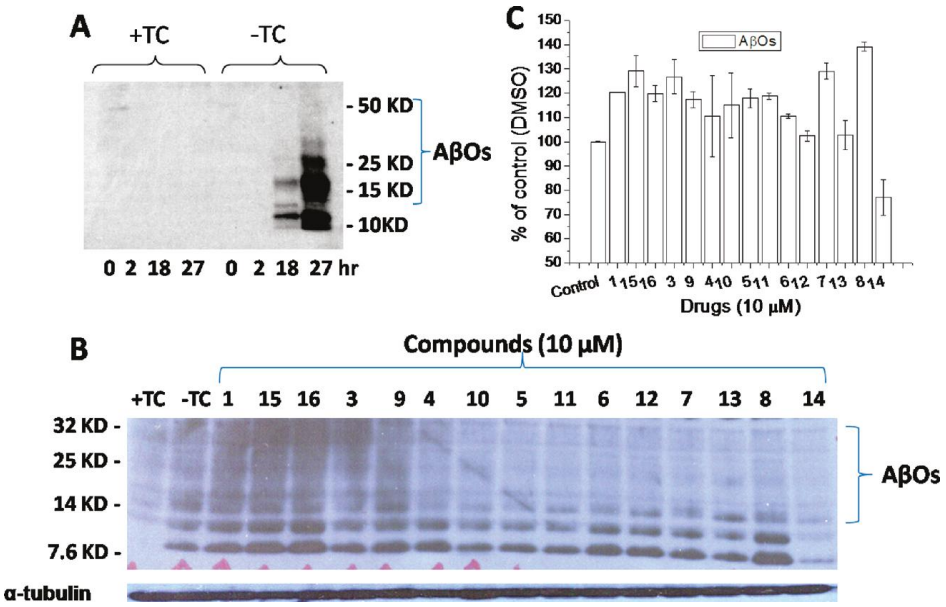


**Figure 7. Inhibition of AβOs formation by 14 in MC65 cells and ML60 cells. (A) MC65 cells were cultured under +TC or-TC conditions for varying intervals (0, 2, 18, 27 h), and then cell lysates were analyzed by Western blot using 6E10 antibody. (B) MC65 cells were treated with indicated compounds (10 μM) for 24 h immediately after the removal of TC. Lysates from cultures were analyzed by Western blotting using 6E10 antibody. The image represents the results from one of three independent experiments. (C) ML60 cells were treated with test compounds (10 μM) for 24 h and extracellular AβOs in conditioned medium were analyzed by ELISA. Data were expressed as mean percentage of AβOs (n = 4) with parallel DMSO cultures set at 100%. Errorbars represent standard error of mean (SEM).**

As shown in Figure 7A, withdrawal of TC induced the production of AβOs consistent with reported results.[129] 1 did not exhibit inhibition on the formation of AβOs (Figure 7B). Spacer attachment at both positions (15 and 16) did not change the activity of 1.

BMAOIs 3, 4 and 9, 10 (spacer length ranging from 11 to 13 atoms) showed no inhibition on the formation of small AβOs. BMAOIs 5-7 and 11-13 (spacer length ranging from 15 to 19 atoms) slightly inhibited the formation of AβOs with specific suppression of the 24-kDa bands. Notably, among the BMAOIs tested, 14 (with 21 atoms in the spacer) significantly inhibited AβOs production. Thismay indicate that spacer length is an important structural determinant for their inhibition on AβOs formation in MC65 cells with a 21-atom-spacer best supporting the design of BMAOIs tested here. Most importantly, it is notable that 8, with the same spacer length (21 atoms) as 14 but different spacer attaching position on 1, did not show inhibitory effects on AβOs formation, which suggests the importance of attachment position on 1 as well. Next, another cell line, ML60, was employed to evaluate the inhibition of AβOs production. ML60 cell line is a line of Chinese hamster ovary (CHO) cells stably expressing wild type APP and mutant presenilin 1 (M146L missense mutation) and can specifically produce high levels of extracellular AβOs.[131] As shown in Figure 7C, only 14 inhibited the production of extracellular AβOs in ML60 cells, and surprisingly all the other compounds increased the production of AβOs at a tested concentration (10 μM). It has been demonstrated that AβOs are formed intracellularly and then excreted outside the cells.[132] The results from ML60 cells may further reflect 14's ability to reduce intracellular AβOs, which is consistent with the results from MC65 cells. Altogether, these results suggest that spacer length and attachment position on 1 are important structural determinants for inhibitory activities on the formation of AβOs and BMAOIs with optimal spacer length can improve their potencies. In order to further confirm the

inhibition of smallAβOs by 14 in MC65 cells, an AβO-specific antibody A1143 combined with Alexa Fluor 568 conjugated secondary antibodies was employed to detect the expression of AβOs in MC65 cells using immunocytochemistry techniques.

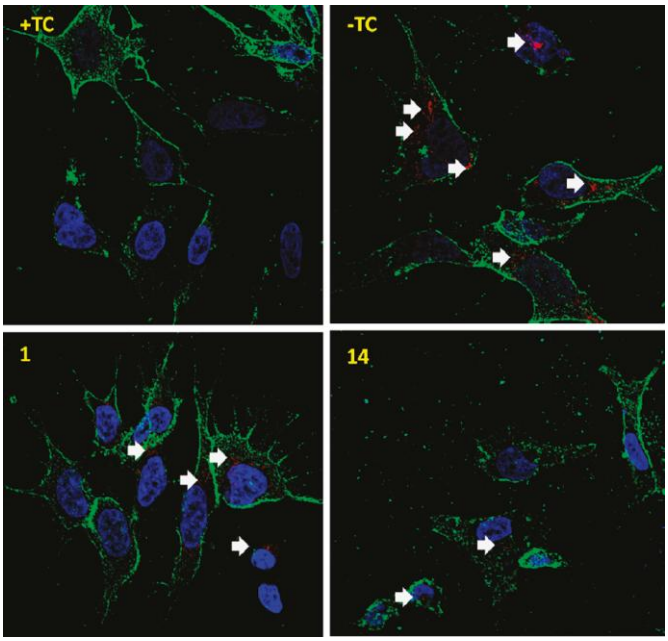


**Figure 8. Immunocytochemistry of 1 and 14 in MC65 cells. MC65 cells were treated with the indicated compounds (10 μM) immediately after the removal of TC. After 24 h, the cells were fixed and immunofluorescently stained for AβOs (red), CM/LR (green), and nucleus (blue) and imaged with Leica TCS-SP2 AOBS confocal laser scanning microscope. White arrows indicate the red puncta of AβOs. The image represents one of five areas examined.**

As shown in Figure 8, removal ofTCinduced rapid intracellular accumulation of AβOs (red fluorescence puncta). Consistent with Western blot results, 14 significantly inhibited the formation of AβOs in MC65 cells upon the removal of TC. Surprisingly, 1 slightly

suppressed the formation of AβOs in this assay while it exhibited no inhibitory effects on the formation of AβOs in Western blot analysis. This might be due to the different antibodies used for detection in these two assays with A11 antibody more specific to AβOs. In addition to confirming Western blot data, these results also indicate that both 14 and 1 can cross the cell membrane of MC65 cells.

**2.3.2 Interactions of 14 with AβOs and Cell Membrane of MC65 Cells.**

In order to confirm 14 can bind toAβOs, the inhibition of Aβ42 oligomerization was performed and assessed using Western blot analysis as described in the literature.[119]

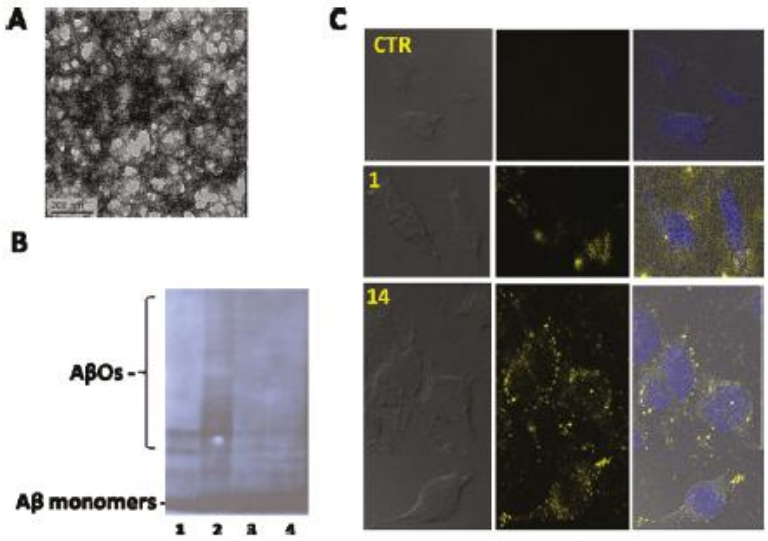


**Figure 9. Binding interactions of 14 with Aβ42 and the CM/LR of MC65 cells. (A) TEM image of AβOs. (B) Aβ42 (5 μM) was incubated with or without compounds (20 μM), and then samples were analyzed by Western blot using 6E10 antibody. Lane 1 - Aβ42 without incubation; Lane 2 - Aβ42 with incubation; Lane 3 - Aβ42 with 1; Lane 4 - Aβ42 with 14. (C) MC65 cells were treated and imaged as in Figure 4. Left panel - differential interference contrast (DIC) images ofMC65 cells; central**

**panel - fluorescence of 14 and 1; right panel - overlay of left and central panels plus DAPI staining of nucleus.**

As shown in Figure 9A, Aβ42 formed oligomers under the reported protocol as demonstrated by transmission electron microscopy (TEM) analysis. After incubation in Ham's F-12medium for 4 h at 37 $^{0}$C, higher order species of AβOs were formed (Figure 5B, lane 2). Notably, both 1 and 14 inhibited the oligomerization of Aβ42 (Figure 9B, lanes 3 and 4), which demonstrates their direct binding to Aβ42. This further confirms that the addition of spacer in 14 does not affect its binding interactions with Aβ42. Next, immunocytochemistry studies were conducted to confirm the interactions of 14 with the CM/LR taking advantage of the intrinsic fluorescence of 14. As shown in Figure 9C, 14 was detected primarily on the cell membrane of MC65 cells (yellow puncta) and inside of MC65 cells as well (bottom panel). 1 was detected inside of MC65 cells but not on the cell membrane (middle panel). The results demonstrate that 14 can directly interact with CM/LR of MC65 cells and anchor the ligand primarily to the CM/LR. Given the fact that Aβ aggregates on the cell surface,17-19 the anchorage of 14 to CM/LR may increase its target accessibility and consequently increase its potency. Collectively, these results support our design rationale of using BMAOIs to cotarget AβOs and CM/LR.

**Protective Effects of 14 on AβOs-Induced Cytotoxicity in MC65 Cells and Differentiated Human Neuroblastoma SH-SY5Y Cells.**

The production of intracellular AβOs has been suggested to be the major factor leading to cytotoxicity in MC65 cells.[129] Therefore, to test whether the suppression of AβOs

formation by 14 correlate with functional activities, 14 was further evaluated for its protective effects on MC65 cell viability upon removal of TC.

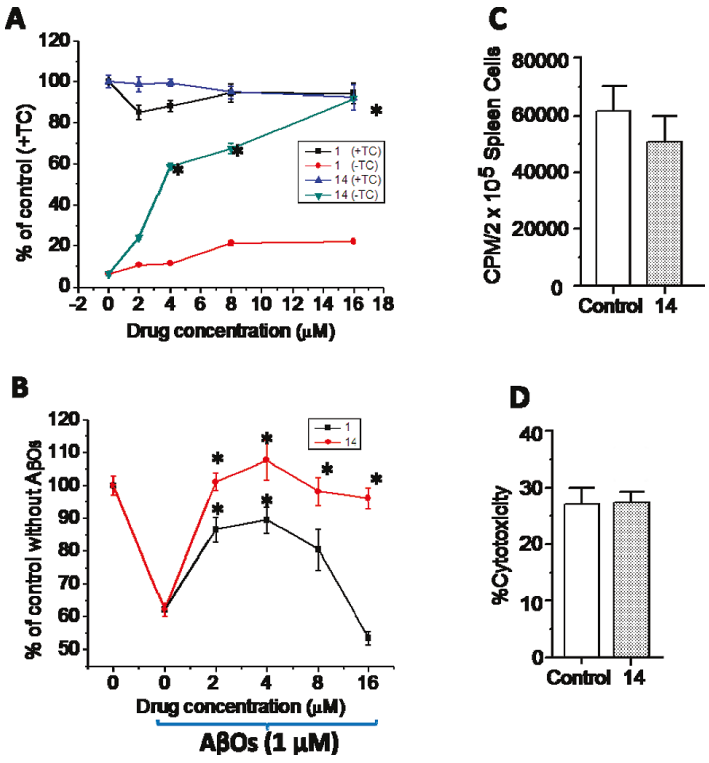


**Figure10. Protective effects of 14. (A) MC65 cells were treated with 1 or 14 at indicated concentrations under +TC or -TC conditions for 72 h. Cell viability was assayed by MTS assay. Data were expressed as mean percentage viability (n = 6) with parallel +TC cultures set at 100% viability. Error bars represent SEM. (B) Alltrans- retinoic acid differentiated SH-SY5Y cells were treated with AβOs (1 μM) in the presence or absence of test compounds at indicated concentrations for 48 h. Cell viability was assayed byMTS assay. Data were expressed as mean percentage viability (n = 6) with cultures without AβOs set at 100% viability. Error bars**

**represent SEM. (C) Effects of 14 (10 μM) on anti-CD3 antibody mediated splenocyte proliferation. (D) Effects of 14 (10 μM) on IL-2 augmented NK cell activity in vitro. The experiments were performed as described in the Experimental Section. Data were presented as mean (n = 4) ( SEM. *P < 0.05 indicates significant differences from control group (without TC inA and withoutAβOs in B) analyzed by one way ANOVA.**

As shown in Figure 10A, 1 and 14 exhibited no toxic effects at tested concentrations in the presence of TC. Upon removal of TC, MC65 cell viability was significantly decreased and 14 protected MC65 cell survival in a dose-dependent manner with nearly full rescue at 16 μM. 1 only exhibited minimal protective effects on MC65 cell viability consistent with reported results.[129] 8 and 12 exhibited no protective effects under these conditions (data not shown) which further suggests the importance of spacer length and attachment position on their activities. Together with the results from Western blot and immunocytochemistry assays, these data suggest that the localization of 14 to theCM/LRmay increase 14's target accessibility and produce a more profound inhibition of the formation of AβOs and elevate the survival of MC65 cells. To further verify whether 14 can protect cells from extracellular AβOsinduced cytotoxicity, all trans-retinoic acid differentiated human SH-SY5Y cells were employed. As shown in Figure 10B, freshly prepared AβOs (1 μM) from Aβ42 significantly decreased SH-SY5Y cell viability (~40% decrease). Notably, 14 completely restored the cell viability at all of the tested concentrations. On the other hand, 1 only exhibited moderate protective activities at 2, 4, and 8 μM concentrations but not at 16 μM. This may be due to its toxic effect on

SHSY5Y cells at this concentration since 1 has been reported to have cytotoxicity on SH-SY5Y cells at higher concentrations. [134] These results suggest that 14 can protect cells from both intracellular and extracellular AβOs-induced cytotoxicity, while 1 only exhibits protective activity toward extracellular AβOs-induced cytotoxicity even though it cancross the cell membrane under these experimental conditions. This may further indicate that while both 1 and 14 can bind to AβOs, CM/LR anchorage of 14 can increase its accessibility to intracellular target AβOs. Since CM/LR are crucial for many aspects of cell signaling and functions, 14 was further evaluated for its potential cytotoxicity in mouse spleen and natural killer (NK) cells. 14 showed minimal cytotoxic effects in mouse spleen (Figure 10C) and no cytotoxic effects in NK cells (Figure 10D). This suggests that localization of BMAOIs to the CM/LR will not affect the normal cellular functions. Taken together, it is clear that 14 is more active than 1 in inhibiting the production of AβOs and in protecting cells from the in situ AβOs-induced cytotoxicity.

**2.3.3 Antioxidant Activity of 14**

One of the BMAOIs design goals is to reduce oxidative stress that potentially contributes to the development of AD. Furthermore, oxidative stress has been indicated as one potential effector to impart neurotoxicity upon the accumulation of intracellular AβOs in MC65 cells.[130] Therefore, we decided to further evaluate the antioxidant activity of 14 in MC65 cells. Despite the availability of several chemical antioxidation assays, the ability to predict and correlate these chemical assays with in vivo activity is questionable. In contrast, a cellular antioxidation assay may provide a more biologically relevant system that best addresses the permeability, distribution, and metabolism issues to evaluate

potential antioxidant properties. Recently, a dichlorofluorescein diacetate (DCFH-DA) based cellular antioxidant assay has been established and widely used for this purpose.[135] We therefore adopted this DCFH-DA assay in MC65 cells to evaluate the antioxidant effects of 14 and 1.

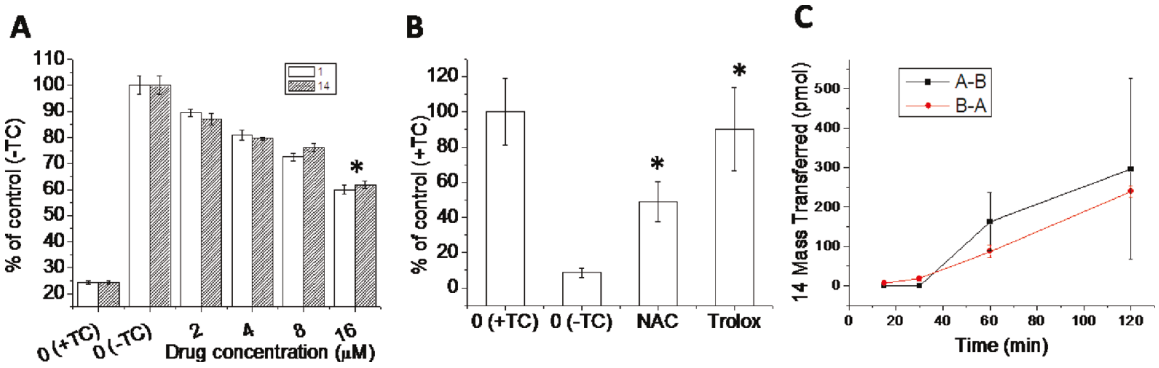


**Figure 11. Antioxidant effects and Caco-2 permeability of 14. (A) MC65 cells were treated with 1 or 14 at indicated concentrations under +TC or -TC conditions for 24 h, and then DCFH-DA (25 μM) was loaded and fluorescence intensity was analyzed at 485 nm (excitation) and 530nm (emission). Data were presented as mean percentage of fluorescence intensity (n=5) with parallel TCcultures set at 100%. Error bars represent SEM. (B) MC65 protection was performed as described in Figure 6A with NAC (8 mM) or trolox (32 μM) (n=5). (C) Caco-2 cells were plated on transwell filters. Test compounds (10 μM) were added to either the apical or basolateral side, and then samples were analyzed by HPLC to determine flux (A-B: apical-to-basolateral; B-A: basolateral-to-apical) at indicated time points. Data were presented as mean (n=3) ±SEM. *P<0.05 indicates significant differences from control group (-TC) analyzed by one-way ANOVA.**

As shown in Figure 11A, upon TC removal, intracellular oxidative stress, as measured by fluorescence intensity, is significantly increased compared to normal growing MC65 cells in the presence of TC. Notably, both 14 and 1 suppressed the intracellular oxidative stress in a dose-depndent manner. These results may indicate that the curcumin moiety in 14 is responsible for its antioxidant activities. Although 1 exhibited antioxidant activities in this cellular model, it did not protect MC65 cell survival (Figure 10A). To compare whether other antioxidants can protect MC65 cells from AβOs-induced cytotoxicity, N-acetylcysteine (NAC) and trolox (6-hydroxy-2,5,7,8-tetramethyl chroman-2-carboxylic acid), an analogue of vitamin E, were tested in MC65 cells. As shown in Figure 11B, trolox (32 μM) completely rescued MC65 cells from AβOs-induced cytotoxicity, while NAC (8 mM) rescued MC65 cells by 48% consistent with reported results.[130] Given the fact that NAC is mainly a hydrogen peroxide scavenger while trolox, a chain-breaking antioxidant, is particularly effective against lipid peroxidation within the cell membrane,[136] these results may indicate lipid peroxidation within the cell membrane as a major contributor underlying the mechanism of AβOs-induced cytotoxicity in MC65 cells, which is consistent with the results from Woltjer et al.[137] The discrepancy of 1 and the other two antioxidants in MC65 cell-protection may suggest that 1 either cannot reach the targets or only partially suppress lipid peroxidation in MC65 cells. Together with the results from Western blot analysis, immunocytochemistry, and cell protection, the results of antioxidation assay further suggest that 14 can retain the antioxidant property of 1 while exhibiting superior capability to reach intracellular AβOs by interacting with the CM/LR, thus efficiently reducing the formation of AβOs and ultimately exhibiting better

overall protective activities in these cells when compared to 1. This further supports the idea that our BMAOIs strategy has the potential to provide clinically efficient multifunctional agents for treatment of AD.

**2.3.4 Assessment of Permeability and P-Glycoprotein Using Caco-2 Cell Model**

Because of the adverse effects of AD in the central nervous system, effective drug candidates need to cross the blood-brain barrier (BBB). To test whether 14 has the potential to reach the brain, we determined its permeability and transport directionality using the Caco-2 model.[138] Although the Caco-2 cell monolayer model is derived from the colon rather than the brain, this model expresses efflux transporters such as P-glycoprotein which are also expressed at the BBB. The Caco-2 model does not predict BBB penetration as well as other models, such as PAMPA-BLM, ECV/C6, or hCMEC/D3;[139-141] however, this model can provide early screening regarding the transcellular diffusional permeability and directional efflux transport across the BBB.52 As shown in Figure 11C, the apical-to-basolateral and basolateral-to-apical permeabilities of 14 were 7.1 (4.6×10-6 and 4.7 (0.5±10-6 cm/s, respectively. Thus, 14 exhibits good bidirectional permeability in Caco-2 cells. In contrast, we were unable to detect transport of 1, likely due to its extensive metabolism by glutathione-S-transferase enzymes. [143] This further indicates that CM/LR anchorage of 14can improve its metabolic stability compared to 1. The permeability directional ratio (efflux ratio) for 14 is 0.63, so it does not appear to be a substrate for BBB efflux transporters such as P-glycoprotein, since the efflux ratio is <2.54. These data further support the potential of 14 as a new lead

to develop effective AD treatment agents. Furthermore, in vivo studies have demonstrated the ability of 1 to cross the BBB, [119, 145, 146] so 14 is anticipated to be able to cross the BBB and the results from Caco-2 assay also supports this notion. Future in vivo studies will assess the BBB permeability more directly, and studies are being undertaken in our laboratory to evaluate 14's BBB permeability in mice.

**2.3.5 14 crosses the blood-brain barrier (BBB) in B6C3F1 mouse and stains Aβ plaques in TgCRND8 mouse brain section.**

Though assays using caco-2 cell model has demonstrated the ability of 14 to cross BBB, we believe in vivo animal studies will provide more meaningful and ultimate evidence for BBB penetration. Therefore, we further determined the ability of 14 to cross the BBB and reach the brain using B6C3F1 mice.

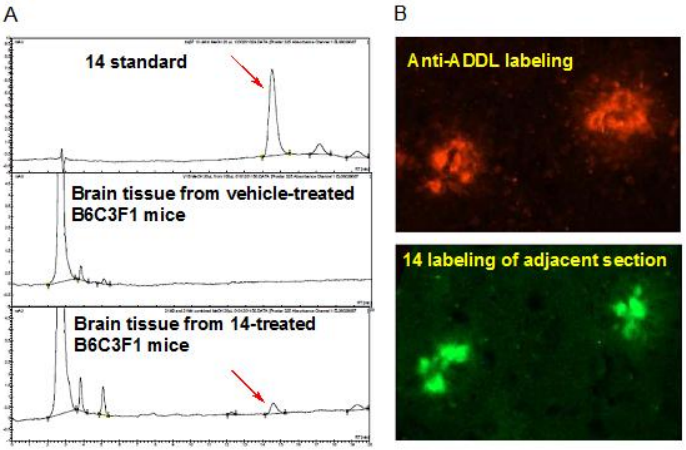


**Figure 12. 14 crosses the blood-brain barrier (BBB) in B6C3F1 mouse and stains Aβ plaques in TgCRND8 mouse brain section.**

As shown in Figure 12A, **14** was detected by HPLC (high-performance liquid chromatography) using reverse phase C18 column in the brain tissues of B6C3F1 mice

(n=4) 60 min after intravenous (i.v.) injection of **14** (10 mg/kg), which clearly indicates the ability of **14** to cross BBB. In order to further confirm **14** can bind to Aβ plaques, the cortex sections from transgenic TgCRND8 mice, a transgenic mouse model widely used for AD research, were used next to study the Aβ plaque binding capacity of **14** by taking advantage of the intrinsic fluorescence of **14**. As shown in Figure 12B, plaques in the cortex section of TgCRND8 mice were brightly labeled by **14**, consistent with the identified Aβ plaques by anti-ADDL antibody labeling in an adjacent section. This clearly indicates that **14** can bind to Aβ plaques nicely. Collectively, these results strongly suggest **14**'s potential as multifunctional ligand for further *in vivo* studies.

**2.4 Conclusion:**

In summary, a series of BMAOIs containing 1 and 2 were designed and synthesized to cotarget AβOs, oxidative stress, and CM/LR. Biological characterization from in vitro assays established that spacer length and the spacer attachment position on 1 are important structural determinants determinants for their biological activities. Among the designed BMAOIs, 14 with a 21-atom-spacer was identified to localize to the CM/LR of MC65 cells, to efficiently inhibit the production of intracellular AβOs inMC65 cells, and to protectMC65 cells and differentiated SH-SY5Y cells from the cytotoxicity of AβOs. Furthermore, 14 exhibited antioxidant properties and demonstrated potential to cross the BBB using a Caco-2 model. These results strongly encourage further optimization of 14 as a new hit to develop more potent BMAOIs. These results may also help validate BMAOIs strategy as a novel design strategy to provide effective multifunctional ligands as potential AD treatment agents.

## Chapter 3 Design, synthesis and biological characterization of BMAOIs containing cholesterylamine and curcumin:

### 3.1 Design and objectives:

In Chapter 2, a series of BMAOIs containing curcumin and cholesterol was designed, chemically synthesized and biologically assayed to reach the proof-of-concept of our BMAOI strategy. The results demonstrated that BMAOIs with optimal spacer length and connectivity localize to the CM/LR, efficiently suppress the production of intracellular AβOs, protect MC65 cells as well as retain the antioxidant and metal complexation activities. Furthermore, the lead BMAOI can cross the BBB and bind to the Aβ plaques. In order to further validate the BMAOI strategy and develop new and more potent BMAOIs as lead structures, a new series of BMAOIs containing cholesterylamine as the CM/LR anchorage moiety and curcumin as the multifunctional moiety were designed, synthesized and characterized in this chapter. The reason we chose cholesterylamine to replace the cholesterol is as the following: 1) It has been reported that N-alkyl derivatives of cholesterylamine can also effectively anchor CM/LR in mammalian cells and function as carrier via endocytosis with improved activity than cholesterol.[142-145] This might be due to the H-bond interactions with CM/LR components through the –NH- moiety of cholesterylamine. 2) Replacement of cholesterol with cholesterylamine may reduce the concern of introducing additional cholesterol into the body as higher cholestrerol level has been suggested to facilitate the development of AD even though the roles of cholesterol are still under debate.

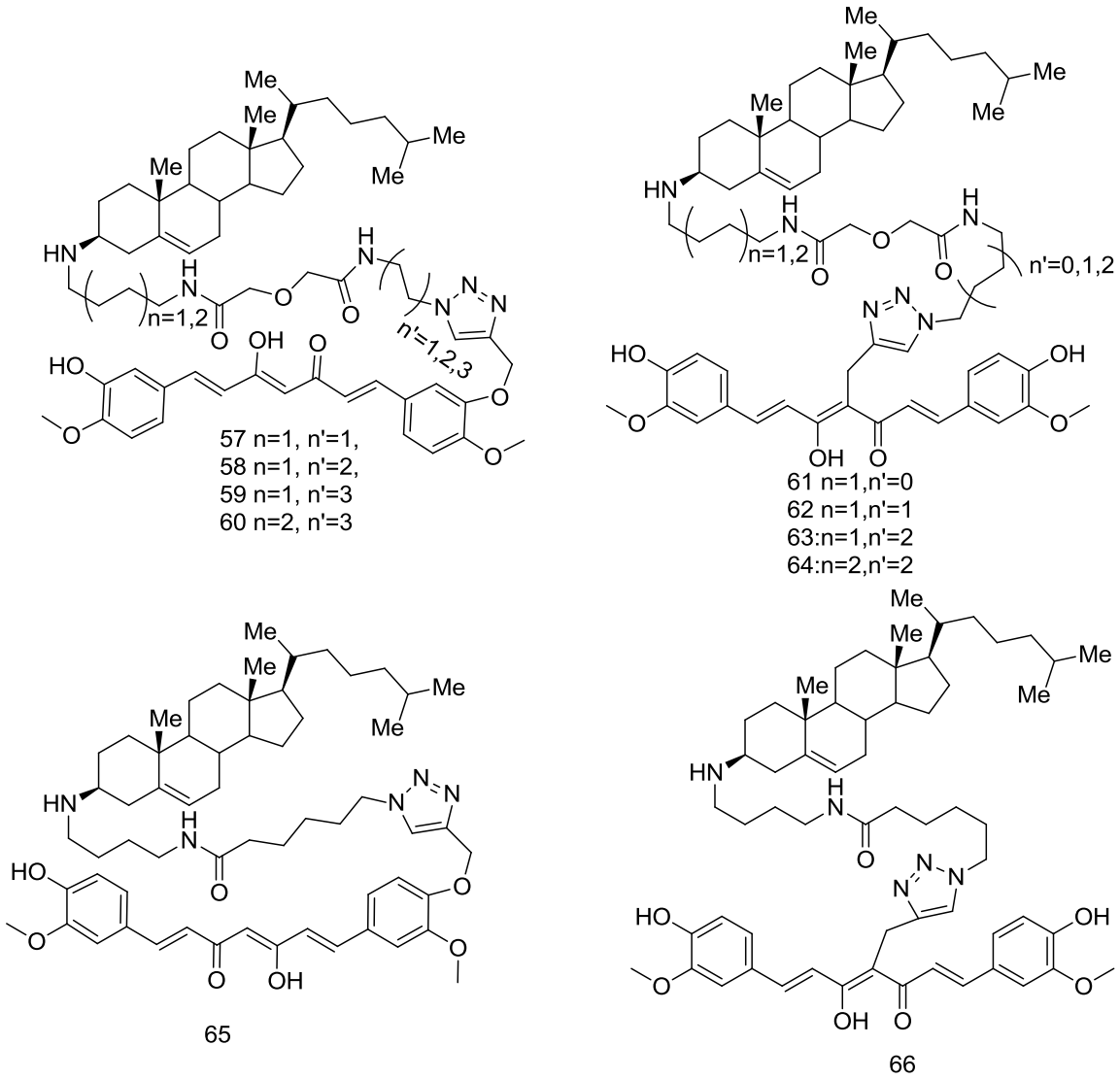


**Figure 13. Nitrogen series BMAOIs.**

As shown in Figure 13, a new series of BMAOIs with the spacer length varying from 15 to 23 atoms were designed to further validate the BMAOI strategy. The objectives of desiging this series of BMAOIs are to investigate 1) whether NH is preferred over O in the interaction with CM/LR; 2) whether spacer connectivity on **1** are still critical in this

series of BMAOIs; and 3) whether the optimal spacer length to produce desired activity will still be within similar range as our first generation BMAOIs.

**3.2 Chemistry:**

Synthesis of nitrogen series started with synthesis of curcumin analogs 20 and 23 as described previously. Azido intermediates were synthesized starting from cholesterol. Cholesterol was esterified using methane sulfonyl chloride to intermediate 39, which was converted to 3β-Azido-5-cholestene 40. 40 was reduced to 3β-Amino 5-cholestene 41 using lithium aluminum anhydride. 42 or 43 was synthesized from 41 using N-bromoalkyl-phthalimide and boc anhydride. 42/43 was deprotected using hydrazine to afford 44/45. 44/45 was coupled with diglycolic anhydride to get 46/47. Azido intermediates 52-55 were synthesized through coupling of 46/47 and azido amines 48-50. BMAOIs 57-64 with spacer length 17-23 were obtained through click chemistry reaction between alkyne intermediates 20/23 and azido intermediates 52-55 followed by Boc deprotection reaction. To synthesize BMAOIs with 15 spacer length, 44 was coupled with 6-azido hexanoic acid (51) to get azido intermediate 56 which was clicked with alkyne intermediate 20 and 23 followed by Boc deprotection to afford 65, 66 respectively.

**Scheme4. Synthesis of intermediates 52-56**[a]

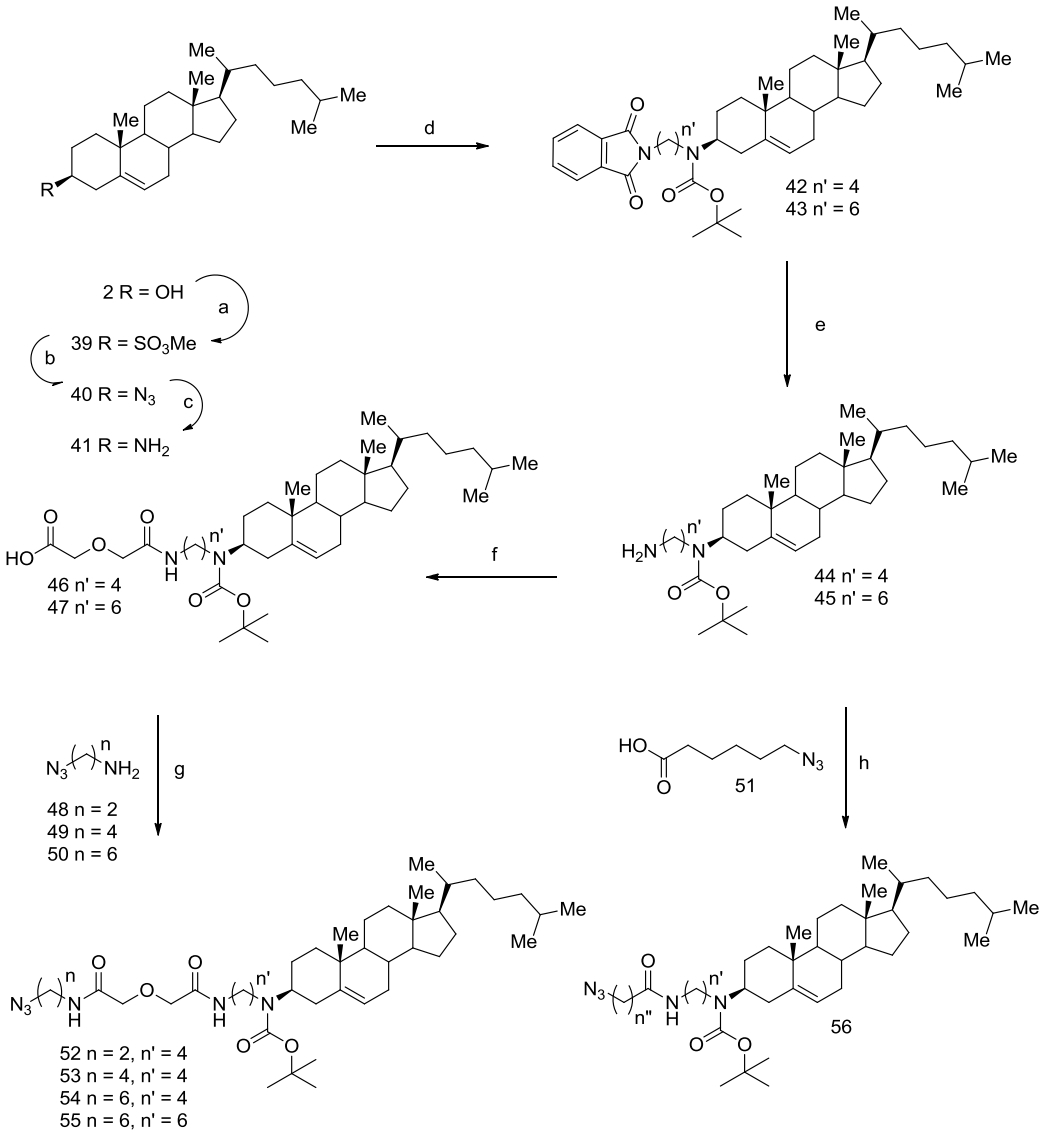


[a]Reagents and conditions: (a) Mesyl chloride, $Et_3N$, DCM (b) $TMSN_3$, $BF_3.OEt_2$, DCM (c) $LiAlH_4$, Diethyl ether
(d) (i) N-(bromoalkyl)-phthalimide, $K_2CO_3$, DMF (ii) Boc, DIEA, DCM (e) Hydrazine, Ethanol (f) Diglycolic anhydride, TEA, DCM
(g) EDCI, DIPA, DCM (h) EDCI, TEA, DCM.

**Scheme5. Synthesis of BMAOs 57-64**[a]

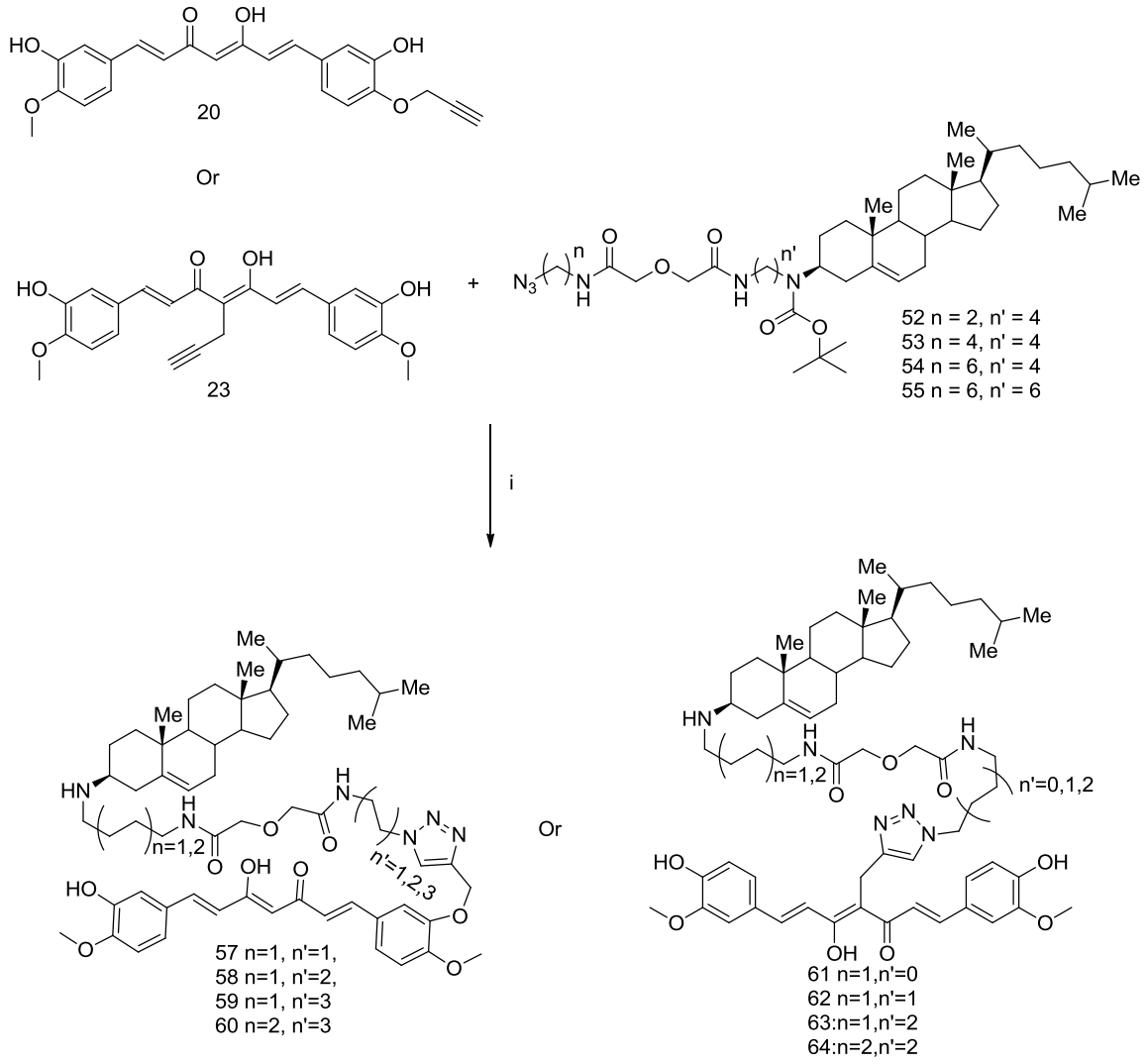


[a](i) (1) Sodium ascorbate, Copper sulphate, THF/Water (1:1), (2) TFA, DCM

**Scheme 6. Synthesis of BMAOIs 65-66**[a]

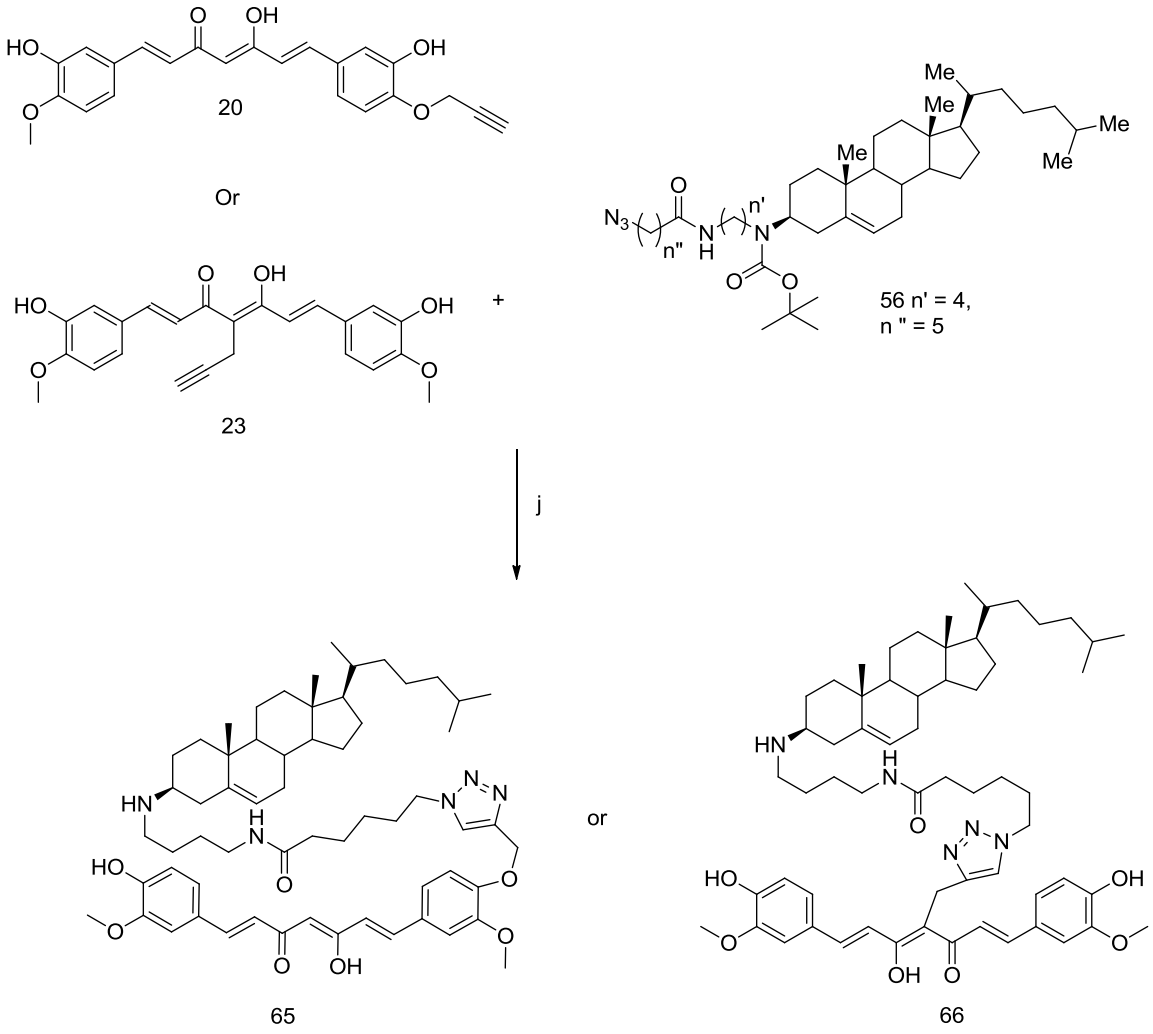


a(j) (1) Sodium ascorbate, Copper sulphate, THF/Water (1:1), (2) TFA, DCM

**3.3 Results and discussion:**

**3.3.1 Neuroprotection by nitrogen series BMAOIs.**

As discussed earlier, MC65 is a human neuroblastoma cell line that conditionally expresses C99, the C-terminus fragment of APP using tetracycline (TC) as transgene suppressor[128]. In absence of TC these cells produce intracellular Aβ aggregates. It has been proved that TC removal can be cytotoxic because of intracellular accumulation of AβOs[129]. In addition, intracellular AβOs can cause oxidative stress which leads to neurotoxicity. Therefore, for nitrogen series BMAOIs again MC65 cells were employed for their validation and testing. This time we started our biological characterization using cell viability assay. To check functional activities of nitrogen series BMAOIs, they were evaluated for its protective effects on MC65 cell viability upon removal of TC. MC65 cells were treated with BMAOIs at indicated concentrations using opti MEM as media. For positive control, Cells grown in regular growing media containing TC were selected as positive control. Opti MEM without TC was used as media to have a negative control. Cells were incubated for 72 h. Cell viability was measured by MTT assay. Data were expressed as mean percentage viability (n=6) with parallel +TC cultures set at 100% viability. As shown in figure 14, when MC65 cells were grown in Opti MEM without TC, it showed significant amount of toxicity and cell viability was significantly decreased. However, when cells were treated with nitrogen series BMAOIs using Opti MEM as media, they showed significant amount of cell survival compare to curcumin. Among BMAOIs, extent of neuroprotection by compounds 17M, 17P, 19M, 19P, and 23M was quite similar. Compounds 21M and 23P exhibited more neuroprotection

compare to other compounds. Compound 21P was found to be the most potent neuroprotective compound in nitrogen series BMAOIs. From this result we came to conclusion that for both series of BMAOIs most active comound is one with 21 atom linker. However, they differ in position of linker attachment at curcumin analong. These data suggest effectiveness of nitrogen series BMAOIs, particularly ligand 21P, on inhibition of the formation of AβOs and elevation of the survival of MC65 cells.

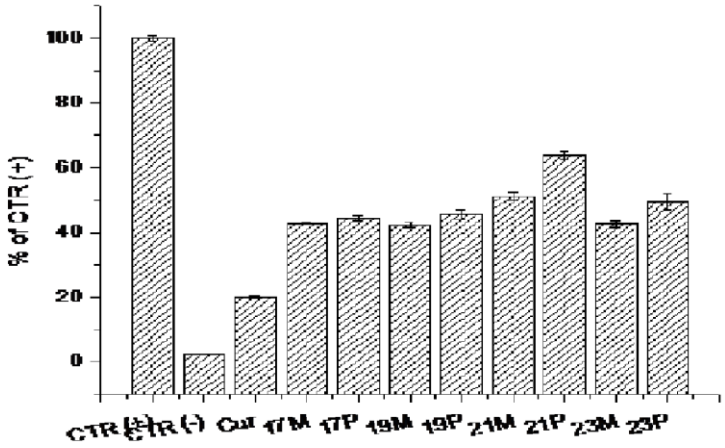


**Figure 14. Protective effect of nitrogen series BMAOIs. MC65 cells were treated with indicated compounds (10 uM) under +TC or -TC conditions for 72 h. Cell viability was assayed by MTT assay. Data were expressed as mean percentage viability (n = 6) with parallel +TC cultures set at 100% viability. Error bars represent SEM.**

### 3.3.2 Inhibition of AβOs Production by Designed BMAOI

Compound 59 (21P) was found to be most potent compound from cell viability assay on MC65 human neuroblastoma cell line. After getting most potent compound, we further tested it for Aβ oligomerization inhibition. We carried out western blot analysis on MC65

cell lines to check for Aβ oligomerization inhibition. 21P was evaluated on dose dependent manner. As shown in figure14, it was tested for indicated dose. 21P exhibited dose dependent inhibition on small AβOs. As shown in figure, at dose of 10 uM and 3 uM 21P singnificantly inhibits small AβOs (two bands between 7 KD and 15 KD). At same doses 21P totally inhibits band around 24 KD. However, figure clearly shows inhibiton of AβOs reduces at lower doses as shown by results for 21P at 1 uM and 0.3 uM. Thus, 21P at proper doses can inhibit Aβ oligomerization. These results further signifie importance of attachment position on curcumin and spacer length.

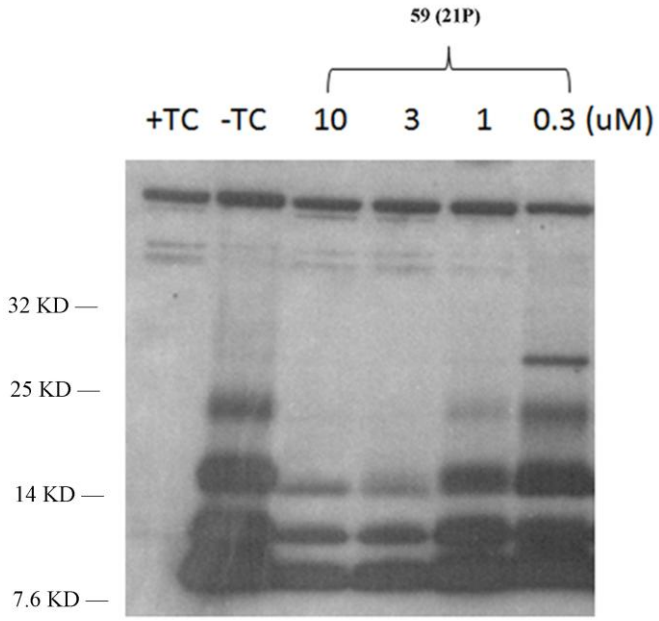


**Figure 15. Inhibition of AβOs formation by compound 59 (21P). MC65 cells were treated with 59(21P) (10 uM, 3 uM, 1 uM, 0.3 uM) for 24 h immediately after the removal of TC. Lysates from cultures were analyzed by Western blotting using 6E10 antibody.**

### 3.3.3 Antioxidant activity

As discussed earlier, one of the BMAOIs design goals is to reduce oxidative stress that potentially contributes to the development of AD. Furthermore, oxidative stress has been indicated as one potential effector to impart neurotoxicity upon the accumulation of intracellular AβOs in MC65 cells. Therefore, we decided to further evaluate the antioxidant activity of 21P in MC65 cells. Despite the availability of several chemical antioxidation assays, the ability to predict and correlate these chemical assays with in vivo activity is questionable. In contrast, a cellular antioxidation assay may provide a more biologically relevant system that best addresses the permeability, distribution, and metabolism issues to evaluate potential antioxidant properties. Again,

A dichlorofluorescein diacetate (DCFH-DA) based cellular antioxidant assay was chosen to evaluate the antioxidant effects of 21P in MC65 cells. As shown in figure 16, intracellular oxidative stress is significantly increased upon TC removal as shown by high fluorescence intensity signal. MC65 cells were treated with compounds at indicated concentrations using OPTI MEM as media for 24 h, and then DCFH-DA (25 uM) was loaded and fluorescence intensity was analyzed at 485 nm (excitation) and 530 nm (emission). Data were presented as mean percentage of fluorescence intensity (n=5) with parallel + TC cultures set at 100%. Regular growing media with TC was used as positive control and OPTI MEM with no TC was used as negative control. Figure 16 shows suppression of oxidative stress by curcumin in dose dependent manner. 59 (21P) did not show oxidative stress suppression in dose dependent manner. However, its antioxidant was quite similar with curcumin. Notably, both 21P and 1 suppressed the intracellular

oxidative stress. Again, from this result it is clear that the curcumin is responsible for antioxidant effect of 21P. Together with the results from neuroprotection assay, westerblot assay and antioxidant assay we can conclude that 21P can retain antioxidant effect of 1 while exhibiting superior capability to inhibit intracellular AβOs compare to curcumin.

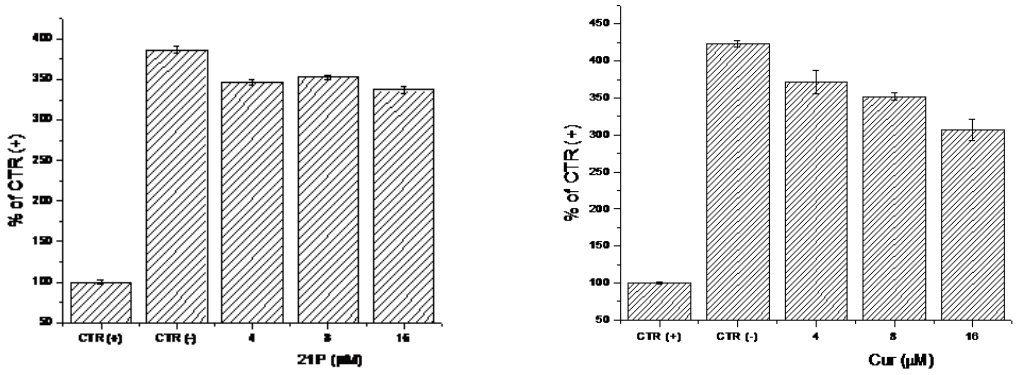


**Figure 16. Antioxidant effect of 59 (21P). MC65 cells were treated with 1 and 21P at indicated concentrations (4 uM, 8 uM and 16 uM) for 24 h, and then DCFH-DA (25 μM) was loaded and fluorescence intensity was analyzed at 485 nm (excitation) and 530nm (emission). Data were presented as mean percentage of fluorescence intensity (n=5) with parallel +TCcultures set at 100%. Error bars represent SEM.**

### 3.3.4 Biometal complexation

Metals such as copper, zinc and iron play very critical role in AD by inducing amyloid aggregation or oxidative neurotoxicity. AD brain has these metals in mM concentrations. These metals can bind to Aβ and induce its aggregation. They can also play a role in

generation of reactive oxygen species. Copper and iron can lead to neurotoxic redox reaction of Aβ and can induce oxidative cross-linking of the peptide into stable oligomers as well. Clioquinol and desferrioxamine are well known chelators. They chelate copper and zinc on Aβ and thus slow down Aβ aggregation by dissociation of Aβ –metal complex. Apart from dissolution of Aβ aggregates, clioquinol and desferrioxamine can also block cross-linked, covalently bonded Aβ oligomer formation and inhibits Aβ redox toxicity as well. Curcumin is a polyphenolic diketone which has anti-oxidant, anti-inflammatory, and metal chelation property. Like clioquinol and desferrioxamine, curcumin can easily chelate redox active metals like iron and copper on Aβ compare to redox inactive zinc. Thus, curcumin can also prevent Aβ aggregation and toxicity. Therefore, our BMAOIs with curcumin as one the pharmacophore can act as metal chelator and can prevent neurons against Aβ mediated toxicity.

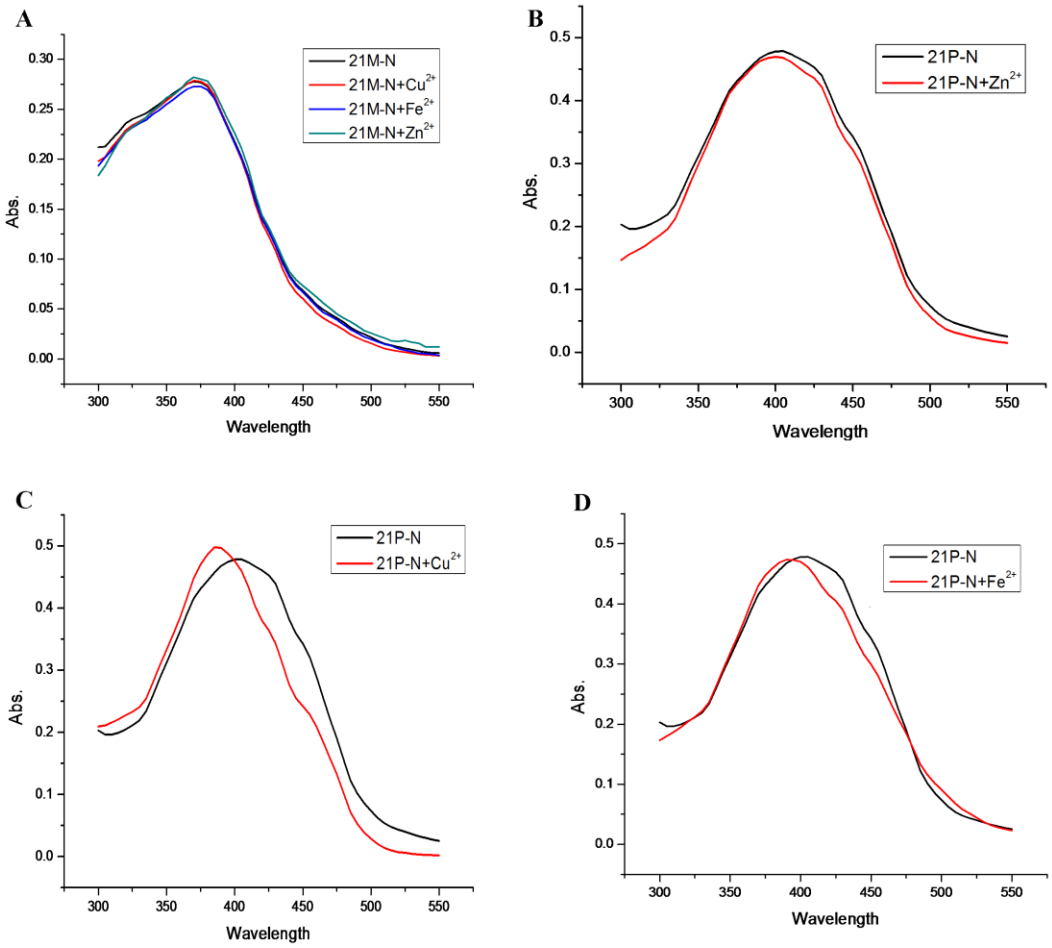


**Figure 17. Absorption spectra of 21P or 21M (50 uM) and 21P or 21M (50 uM) mixed with divalent metal cations (60 uM). In case of only drug 188uL of compound solution and 12uL of $H_2O$ were added while for compound and metal 188uL of compound solution and 12uL of metal working solution were mixed together. For metal control 188uL of $H_2O$ and 12uL of metal working solution were mixed.**

Curcumin can absorb light most strongly at ~430 nm. Binding of curcumin with metal ions shifts absorbance maximum[147]. Our BMAOIs contain curcumin as an active moiety. Therefore it should also show maximum absorbance ~430 nm. When metal ion binds to

our BMAOIs, then there should be also change in optical spectra. From figure 17A it is clear that there is no difference in absorption spectra of 21M only and 21M with metal ion. Therefore we can say that 21M does not chelate metal ions. 21P can bind itself to bivalent iron and copper as shown by difference in absorption maximum of compound and compound with added metal ion (figure 17 C and 17D). However, 21P did not show significant binding with zinc ion. No shift in absorption maximum when mixed with zinc ion. (figure 17B). All together, we can say that 21P retains metal chelation and thus Aβ oligomerization inhibiton property of curcumin. From this assay it is clear that spacer length as well as its positon of attachment on curcumin analog is important for its metal chelation property.

**3.4 Conclusions:**

Based on MC65 cell viability assay and westernblot assay, compound 21P with 21 atom linker and linker attachment at phenolic oxygen on curcumin, was found to be most potent inhibitor of AβOs compare to other BMAOIs as well as curcumin. Further, it retains antioxidant activity as well as metal chelation property of curcumin. Thus, results demonstrated that the same spacer length but different connectivity are preferred in this new series of BMAOIs for neuroprotective activity as that of the lead compound from cholesterol series. Putting all results together, the design and characterization of the new series BMAOIs further confirmed the rationale of BMAOI strategy and their potential to lead to a new direction in development of effective AD-modifying and treatment agents.

## Chapter 4Experimental section:

### 4.1 Chemistry

#### 4.1.1 3-methoxy-4-(prop-2-ynyloxy)benzaldehyde (18)

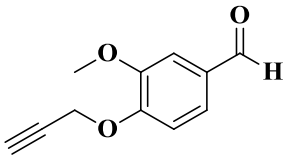

**Route 1:** Vanillin (760 mg, 4.9 mmol, 1 equivalent), potassium carbonate (960 mg, 6.9 mmol, 1.4 equivalent) and propargyl bromide (1.19 g, 9.9 mmol, 2 equivalent) were added to dimethyl formamide (30 mL). The mixture was refluxed for 1h at 80 $^{0}$C. Reaction was cooled to 0$^{0}$C in ice bath and filtered under vacuum using celite. Reaction was quenched with 1M HCL (10 mL) and extracted with ethyl acetate. Organic phase was washed with water and dried it over sodium sulfate. Solvent was removed under vacuum and crude was purified using silica gel column using hexane: ethyl acetate (8:2 v/v), which gave 3-methoxy-4-(prop (740 mg, 80%) as white solid.

**Route 2 (Mitsunobu reaction):** Vanillin (4 g, 26.3 mmol, 1 equivalent), propargyl alcohol (1.61 mL, 26.3 mmol, 1 equivalent) and tri-phenyl phosphine (7.59 g, 28.9 mmol, 1.1 equivalent) were dissolved in tetra hydro furan (50 mL). To that, added diethyl azodicarboxylate (DEAD) (5.04 g, 28.92 mmol, 1.1 equivalent) at 0$^{o}$C. Reaction was stirred over night at room temperature. After completion of reaction as evidence by TLC

crude was purified on silica gel column with hexane:ethyl aceate (8:2 v/v) solvent system as eluent to get 3-methoxy-4-(prop-2-ynyloxy)benzaldehyde (4.2 g, 84%) as white solid.

$^{1}$H NMR 400 mHz ($CDCl_3$) δ 2.57 (t,1H), 3.94 (s, 3H), 4.85-4.86 (d, J = 2.44 Hz, 2H), 7.13-7.15 (d, J = 8.16 Hz, 1H), 7.43-7.47 (m, 2H), 9.87 (s, 1H)

$^{13}$C NMR 100 mHz ($CDCl_3$) δ 56.06, 56.65, 109.58, 112.71, 126.21, 131.00, 150.11, 152.17, 190.85

**4.1.2(1*E*,4*Z*)-5-hydroxy-1-(4-hydroxy-3-methoxyphenyl)hexa-1,4-dien-3-one (19)**

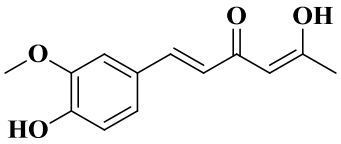


2,4-pentendione (820 mL, 8 mmol, 1 equivalent) and boron oxide (500 mg, 7.2 mmol, 0.9 equivalent) were dissolved in ethyl acetate (5 mL). The mixture was stirred at 80$^{o}$C for 30 min. Ethyl acetate (10 mL) solution of vanillin (555 mg, 3.6 mmol, 0.45 equivalent) and tributyl borate (0.97 mL, 3.6 mmol, 0.45 equivalent) was added to reaction mixture. After stirring for 30 min at 80$^{o}$C, n-butylamine (0.36 mL, 3.6 mmol, 0.45 equivalent) was added drop wise to the mixture, which was allowed to stir at 100$^{o}$C for 1h. Reaction was treated with 1N HCL (10 mL) at 50$^{o}$C for 30 min. Extraction was done with ethyl acetate followed by washing of organic layer with water which was dried over sodium sulfate. Purification of crude product was done with silica gel column using hexane:ethyl acetate (8:2 v/v) solvent system to obtain (1*E*,4*Z*)-5-hydroxy-1-(4-hydroxy-3-methoxyphenyl)hexa-1,4-dien-3-one (2) (505 mg, 60%) as yellow solid.

$^{1}$H NMR 400 mHz ($CDCl_3$) δ 2.14 (s,3H), 3.92 (s, 3H), 5.62 (s, 1H), 6.29-6.33 (d, J = 15.76 Hz, 1H), 6.90-6.92 (d, J = 8.2 Hz, 1H), 7.00 (s, 1H), 7.06-7.08 (d, J = 6.36 Hz, 1H), 7.50-7.54 (d, J = 15.4 Hz, 1H),

$^{13}$C NMR 100 mHz ($CDCl_3$) δ 26.78, 55.96, 56.50, 100.67, 109.59, 114.87, 120.35, 122.65, 127.68, 140.09, 146.86, 147.79, 178.05, 196.91

**4.1.3 (1E,4Z,6E)-5-hydroxy-7-(3-hydroxy-4(prop-2-ynyloxy)phenyl)-1-(3-hydroxy-4-methoxy phenyl)hepta-1,4,6-trien-3-one (20):**

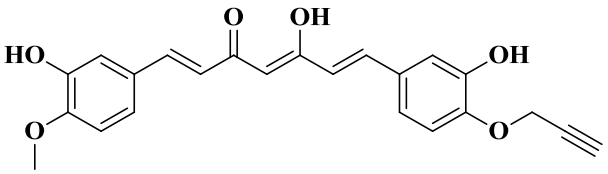


Compound 20 (410 mg, 1.7 mmol, 1 equivalent) and boron oxide (180 mg, 2.51 mmol, 1.48 equivalent) were dissolved in ethyl acetate (5mL) at 80$^{o}$C. To this, added ethyl acetate (5 mL) solution of compound 19 (195 mg, 1.03 mmol, 0.6 equivalent) and tri butyl borate (0.7 mL, 2.51 mmol, 1.48 equivalent). After Stirring reaction mixture for 30 min, it was treated with piperidine (0.07 mL, 0.60 mmol, 0.354 equivalent) at 80$^{o}$C for 30 min and then with 0.4 N HCL (5 mL) at 50$^{o}$C for another 30 min. Finally reaction mixture was extracted with ethyl acetate, washed with water, dried over sodium sulfate and concentrated in vacuo. Purification of crude was done with silica gel column using hexane:ethyl acetate (8.5:1.5 v/v) solvent system to afford (1E,4Z,6E)-5-hydroxy-7-(3-hydroxy-4(prop-2-ynyloxy)phenyl)-1-(3-hydroxy-4-methoxy phenyl)hepta-1,4,6-trien-3-one (3) (105 mg, 32%) as orange solid.

$^{1}$H NMR 400 mHz ($CDCl_3$) δ 2.53-2.54 (t, J = 4.84, 3H), 3.92-3.93 (d, J = 6.2 Hz, 6H), 4.79-4.80 ( d, J = 2.32 Hz, 2H), 5.81 (s, 1H), 6.45-6.51 (m, 2H), 6.91-6.93 (d, J = 8.2 Hz, 1H), 7.04 (s, 2H), 7.08-7.12 (m, 3H), 7.57-7.61 (d, J = 15.72 Hz, 2H),

$^{13}$C NMR 100 mHz ($CDCl_3$) δ 26.78, 55.97, 56.67, 60.41, 101.28, 109.70-129.31, 140.08-149.83, 182.83, 183.68

**4.1.4 3-(prop-2-ynyl)-pentane-2, 4-dione (22):**

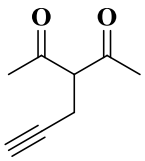

Propargyl bromide (320 mg, 2.7 mmol, 1 equivalent), potassium carbonate (225 mg, 16.2 mmol, 6 equivalent) and 2, 4-pentanedione (1.38 mL, 13.5 mmol, 5 equivalent) were mixed together in acetone (15 mL). The mixture was stirred for 24 hr at 60$^{o}$C. After completion of reaction, vacuum distillation was carried out to obtain pure 3-(prop-2-ynyl)-pentane-2, 4-dione (4) (300 mg, 80%) as colorless liquid.

$^{1}$H NMR 400 mHz ($CDCl_3$) δ 2.03-2.04 (t, J = 5.28 Hz, 1H), 2.22 (s, 3H), 2.25 (s, 3H), 2.68-2.71 (m, 2H), 3.84-3.87 (t, J = 15.08 Hz, 1H)

$^{13}$C NMR 100 mHz ($CDCl_3$) δ 14.45, 29.33, 29.41, 68.70, 70.79, 86.13, 202.18, 202.63

**4.1.5 (1*E*, 4*Z*, 6*E*)-5-hydroxy-1, 7-bis (3-hydroxy-4-methoxyphenyl)-4-(prop-2-ynyl) hepta-1, 4, 6-trien-3-one (23):**

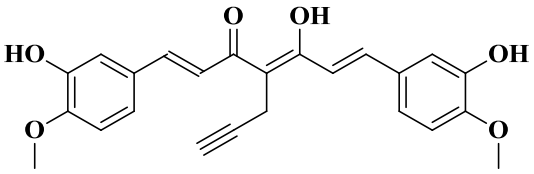


3-(prop-2-ynyl)-pentane-2, 4-dione (4) (810 mg, 5.9 mmol, 1 equivalent) and boron oxide (285 mg, 4.1 mmol, 0.7 equivalent) were dissolved in anhydrous ethyl acetate (10 mL). The resulting mixture was stirred for 30 min at $40^0$C. To this, added vanillin (180 mg, 11.8 mmol, 2 equivalent) and tri-butyl borate (6.3 mL, 23.6 mmol, 4 equivalent) followed by another 30 min stirring. N-butyl amine (0.85 mL, 8.8 mmol, 1.5 equivalent) was diluted with anhydrous ethyl acetate (10 mL) and added to reaction mixture over a period of 50 min. The mixture was heated to $40^o$C. After 24 hr 1 N HCL (10 mL) was added, heated to $65^o$C and stirred for 1 hr. The aqueous phase was extracted with ethyl acetate, dried it over sodium sulfate and concentrated in vacuo. The pure (1*E*, 4*Z*, 6*E*)-5-hydroxy-1, 7-bis (3-hydroxy-4-methoxyphenyl)-4-(prop-2-ynyl) hepta-1, 4, 6-trien-3-one (5) (500 mg, 21 %) was obtain as orange solid after running silica gel column using hexane:ethyl acetate (8.5:1.5 v/v) solvent system as eluent.

$^1$H NMR 400 mHz ($CDCl_3$) δ 2.14-2.16 (t, J = 5.08 Hz, 1H), 2.89-2.92 (m, 2H), 3.91 (s, 3H), 3.95 (s, 3H), 6.68-6.72 (d, J = 15.8 Hz, 1H), 6.90-7.26 (m, 8H), 7.56-7.74 (m, 2H)

$^{13}$C NMR 100 mHz ($CDCl_3$) δ 16.27, 56.03, 69.61, 70.57, 82.66, 106.24, 109.83-127.97, 142.43-148.87, 182.68, 193.34

**4.1.6(3S,10R,13R,17R)-10,13-dimethyl-17-((R)-6-methylheptan-2-yl)-2,3,4,7,8,9,10,11,12,13,14,15,16,17-tetradecahydro-1H-cyclopenta[a]phenanthren-3-yl methanesulfonate (39)**

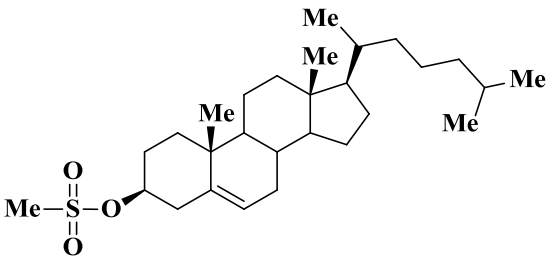


To a solution of cholesterol (20 g, 51.8 mmol, 1 equivalent) in anhydrous DCM (300 mL) at 4$^{o}$C was added triethylamine (10.8 mL, 77.6 mmol, 1.5 equivalent), followed by drop a drop wise addition of solution of methanesulfonyl chloride (4.26 mL, 54.4 mmol, 1.05 equivalent) in anhydrous DCM (20 mL). The reaction was stirred at 4$^{o}$C for 30 min, followed by 24 hr stirring at room temperature. After completion of reaction, it was concentrated in vacuo. The resulting residue was dissolved in DCM (20 mL) and the product was recrystallized by addition of methanol. Vacuum filtration afforded Cholest-5en-3β-ol, methanesulfonate (6) (22 g, 91%) as white solid.

$^{1}$H NMR 400 mHz ($CDCl_3$) δ 0.67 (s,3H), 0.85-0.87 (dd, 6H), 0.90-0.91 (d, 3H), 0.99-2.52 (31H), 3.0 (s, 3H), 4.47-4.55 (m, 3H), 5.41-5.42 (t, 1H)

$^{13}$C NMR 100 mHz ($CDCl_3$) δ 10.96-42.41 (21C), 54.88, 55.64, 55.80, 81.03, 122.80, 137.67

**4.1.7 (3*S*,10*R*,13*R*,17*R*)-3-azido-10,13-dimethyl-17-((*R*)-6-methylheptan-2-yl)-2,3,4,7,8,9,10,11,12,13,14,15,16,17tetradecahydro1*H*-cyclopenta[*a*]phenanthrene (40)**

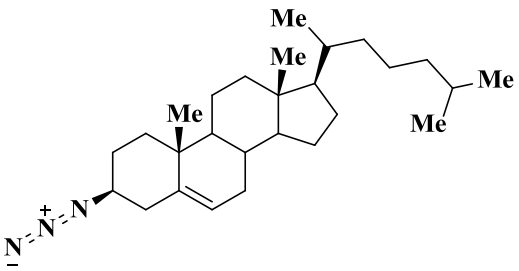


The flask was charged with cholest-5en-3β-ol, methanesulfonate (39) (11.77 g, 25.3 mmol, 1 equivalent), azidotrimethylsilane (3.71 mL, 27.7 mmol, 1.1 equivalent), boron trifluoride etherate (6.3 mL, 50.6 mmol, 2 equivalent) and anhydrous DCM (200 mL). The reaction mixture was stirred over night at room temperature. After completion of reaction as evidence by TLC (eluent:hexane) the reaction was slowly poured into aqueous NaOH (2.0 M, 100 mL) and stirred for 5 min. The aqueous layer was extracted with DCM. The organic layer was washed with brine, dried over sodium sulfate and concentrated in vacuo to obtain light yellow crude product. Silica gel column was run to get 3β-Azido-5-cholestene (7) (8.9 g, 85%) as white solid.

$^{1}$H NMR 400 mHz ($CDCl_3$) δ 0.67 (s,3H), 0.85-0.87 (dd, 6H), 0.90-0.91 (d, 3H), 0.99-2.03 (29H), 2.28-2.29 (d, 2H), 3.16-3.24 (m, 3H), 5.37-5.39 (t, 1H)

$^{13}$C NMR 100 mHz ($CDCl_3$) δ 11.85-42.32 (21C), 50.13, 56.18, 56.73, 61.18, 122.53, 139.86

**4.1.8 (3*S*,10*R*,13*R*,17*R*)-10,13-dimethyl-17-((*R*)-6-methylheptan-2-yl)-2,3,4,7,8,9,10,11,12,13,14,15,16,17-tetradecahydro-1*H*-cyclopenta[*a*]phenanthren-3-amine (41)**

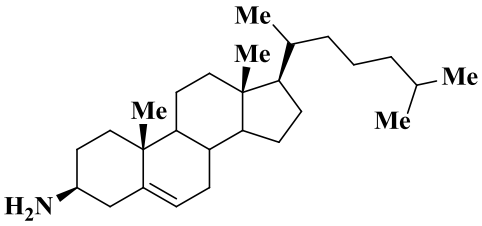


Solution of lithium aluminium hydride (1g, 26.3 mmol, 1.2 equivalent) in anhydrous diethyl ether (100 mL) was prepared and kept at 0°C. To this, solution of 3β-Azido-5-cholestene (7) (8.85g, 21.5 mmol, 1 equivalent) in anhydrous diethyl ether (100 mL) was added and stirred for 30 min at 4°C, followed by 2 h stirring at room temperature. After completion of reaction as evidence by TLC (eluent:hexane), the reaction was cooled to 4°C and very carefully quenched by 10% NaOH until evolution of hydrogen gas ceased. Reaction mixture was extracted with ethyl acetate, washed with brine, dried over sodium sulfate and concentrated in vacuo. The resulting solid was dissolved in chloroform and residual inorganic salts were removed by vacuum filtration. Concentration of filtrate gave 3β-Amino-5-cholestene (8) (7.1 g, 86%) as white solid.

$^{1}$H NMR 400 mHz ($CDCl_3$) δ 0.67 (s, 3H), 0.85-0.87 (dd, 6H), 0.90-0.92 (d, 3H), 0.99-2.17 (31H), 2.57-2.61 (m, 1H), 5.30 (t, 1H)

$^{13}$C NMR 100 mHz ($CDCl_3$) δ 11.86-43.37 (21C), 50.27, 52.01, 56.17, 56.82, 120.62, 141.87

**`4.1.9 2-(6-bromohexyl)phthalimide:**

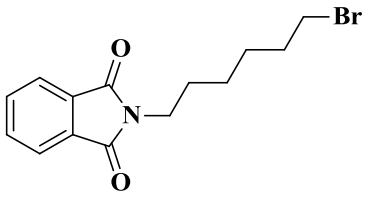


To a solution of 1,6-Dibromo hexane (5 g, 20.49 mmol, 1.5 equivalent) in DMF (30 mL) was added potassium carbonate ( 3.78 g, 27.32 mmol, 2 equivalent). The mixture was stirred for 10 min at room temperature. To this mixture, added solution of phthalimide (2 g, 13.66 mmol, 1 equivalent) in DMF (20 mL). The reaction was stirred for 90 min at room temperature. After completion of reaction cold water was added to reaction mixture and aqueous layer was extracted with DCM. The extract was concentrated in vacuo. Column chromatography with silica gel column using hexane:ethyl acetate (8.5:1.5 v/v) as eluent afforded 2-(6-bromo hexyl)isoindoline-1,3-dione (2.9 g, 68 %) as white solid.

**4.1.10 42, 43**

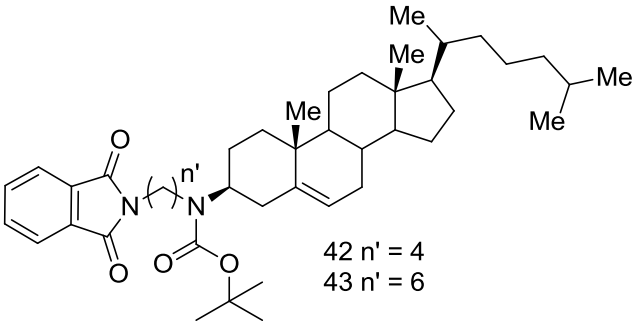


3β-Amino-5-cholestene (41) (1 equivalent), N-(4-bromobutyl)phthalimide/N-(6-bromohexyl)phthalimide (1.1 equivalent) and potassium carbonate (2 equivalent) were added to DMF. The reaction mixture was stirred for 24 h at 60$^{o}$C, cooled to room temperature and concentrated in vacuo. To the resulting solid was added DCM and insoluble residue was removed by vacuum filtration, followed by washing of residue with additional DCM. The combined filtrate and wash solution were rotavapored. The resulting residue, di-tert-butyl dicarbonate (1.5 equivalent) and diisopropyl ethyl amine (3 equivalent) were added to anhydrous DCM. The reaction mixture were stirred for 4 h at room temperature and concentrated in vacuo. The crude was purified by silicagel column using hexane:ethyl acetate (9:1 v/v) as eluent to afford 10,11 ( 60-65%) as white solid.

**42:** $^{1}$H NMR 400 mHz ($CDCl_3$) δ 0.67 (s, 3H), 0.85-0.87 (dd, 6H), 0.90-0.92 (d, 3H), 0.99-2.05 (35H), 2.43 (br, 1H), 3.06 (br, 2H), 3.66-3.69 (t, 2H), 5.31-5.32 (t, 1H), 7.69-7.71 (m, 2H), 7.83-7.85 (m, 2H)

**4.1.11 44, 45:**

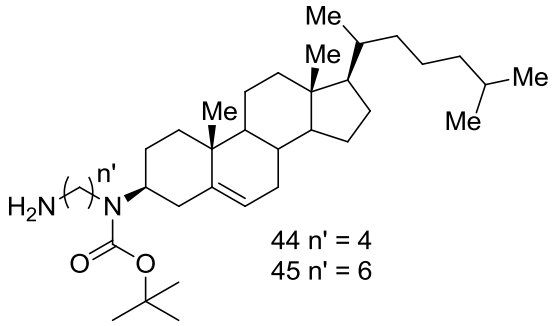


Anhydrous hydrazine (5.2 equivalent) was added to a solution of 42/43 (1 equivalent) in absolute ethanol. The resulting solution was stirred for 5 h at 50$^{o}$C. After completion of reaction as evidence by TLC (hexane/ethyl, acetate 8:2) it was cooled to room temperature. White precipitate was removed by filtration and filtrate was concentrated in vacuo. To the resulting solid was added chloroform and insoluble residue was removed by vacuum filtration. Concentration of filtrate resulted in phthalimide deprotected primary amine (85-90%).

**44:** $^{1}$H NMR 400 mHz ($CDCl_3$) δ 0.60 (s, 3H), 0.79-0.80 (dd, 6H), 0.85 (d, 3H), 0.93-1.91 (44H), 2.4 (br, 1H), 2.67 (t, 2H), 3.04 (br, 2H), 5.31-5.32 (t, 1H)

**45:** $^{1}$H NMR 400 mHz ($CDCl_3$) δ 0.67 (s, 3H), 0.85-0.87 (dd, 6H), 0.90-0.92 (d, 3H), 1.00-2.17 (48H), 2.49 (br, 1H), 2.68-2.72 (t, 2H), 3.08 (br, 2H), 5.32-5.33 (t, 1H)

**4.1.12 46, 47:**

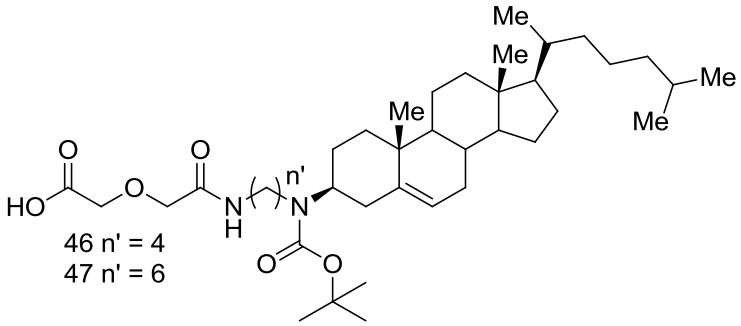


Flask was charged with 44, 45 (1 equivalent), diglycolic anhydride (2 equivalent), tri-ethyl amine (0.5 equivalent) and DCM. The reaction mixture was stirred at room temperature for 24 h and rotavapored. Silica gel column was run with DCM:methanol (9.2:0.8 v/v) solvent system to obtain 46/47 (70-75%) as white solid.

**xiv:** $^{1}$H NMR 400 mHz ($CDCl_3$) δ 0.68 (s, 3H), 0.85-0.87 (dd, 6H), 0.90-0.92 (d, 3H), 0.99-2.09 (44H), 2.50 (br, 1H), 3.14 (br, 2H), 3.33-3.36 (br, 3H), 4.13 (s, 2H), 4.19 (s, 2H), 5.29-5.33 (t, 1H)

**xv:** $^{1}$H NMR 400 mHz ($CDCl_3$) δ 0.68 (s, 3H), 0.85-0.87 (dd, 6H), 0.90-0.92 (d, 3H), 0.99-2.02 (48H), 2.54 (br, 1H), 3.14 (br, 2H), 3.30-3.34 (br, 3H), 4.19 (s, 2H), 4.23 (s, 2H), 5.32-5.33 (t, 1H)

**4.1.13 6-azidohexan-1-amine (50)/4-azidobutan-1-amine (49):**

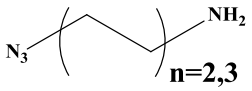


**49:n=2**
**50:n=3**

A solution of 4-amino-butan-1-ol/6-amino-hexan-1-ol (1 equivalent) and thionyl chloride (4.5 equivalent) in toluene was refluxed for 1 h. After 1 h solvent was evaporated to obtain intermediate 6-chloro-1-hexylamine/4-chloro-1-butylamine. The intermediate was added to a solution of sodium azide (3 equivalent) in water. The reaction mixture was heated to 90$^{o}$C and stirred for 2 h. After completion of reaction, it was basified to pH 12-14 with KOH (solid), extracted with DCM, dried over sodium sulfate and concentrated in vacuo to afford 4-azidobutan-1-amine (49)/6-azidohexan-1-amine (50) (65-70 %) as brown liquid.

**49:** $^{1}$H NMR 400 mHz ($CDCl_3$) δ 1.50-1.68 (m, 4H), 2.71-2.75 (t, 2H), 3.27-3.31 (t, 2H)

**50:** $^{1}$H NMR 400 mHz (DMSO) δ 1.29-1.54 (m, 6H), 2.49-2.52 (t, 2H), 3.29-3.33 (t, 2H)

$^{13}$C NMR 100 mHz (DMSO) δ 25.91, 26.06, 28.24, 33.26, 41.56, 50.56

**4.1. 14 2-azidoethanamine hydrochloride salt (48):**

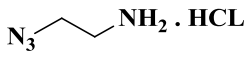

A solution of 2-Bromo-ethyl amine hydro bromide salt (3 g, 14.64 mmol, 1 equivalent) was prepared in water (30 mL) and sodium azide (2.86 g, 43.92 mmol, 3 equivalent) was added . The reaction was stirred for 24 h at 80$^{o}$C. After completion of reaction, solution was basified to pH 12-14 with solid KOH, extracted with ether, dried it over sodium sulfate and filtered. To the filtrate, added 4 M solution of HCL in dioxane (14 mL, 58.56 mmol, 4 equivalent) and concentrated in vacuo to afford 2-azidoethanamine hydrochloride salt (900 mg, 50 %) as colorless liquid.

**xviii:** $^{1}$H NMR 400 mHz (DMSO) δ 2.93-2.97 (m, 2H), 3.66-3.67 (t, 2H)

$^{13}$C NMR 100 mHz (DMSO) δ 37.85, 47.92

**4.1.15 52-55 :**

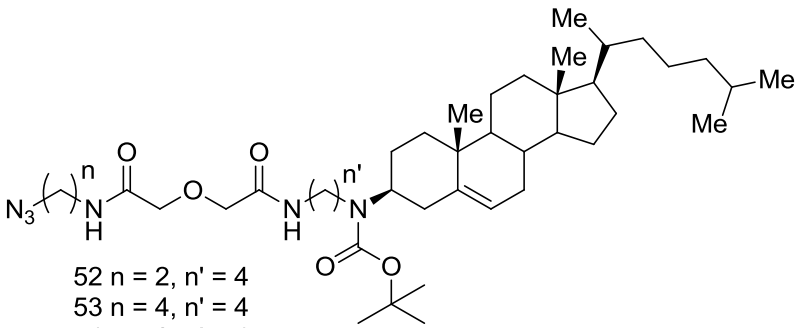


52 n = 2, n' = 4
53 n = 4, n' = 4
54 n = 6, n' = 4
55 n = 6, n' = 6

To a solution of 46/47 (1 equivalent) in DCM was added 4-azidobutan-1-amine (49)/6-azidohexan-1-amine (50) (2 equivalent) and EDCI (2 equivalent). The reaction mixture was stirred over night at room temperature. After completion of reaction, it was diluted with DCM, washed with water followed by washing with 0.5 N HCL and finally with

brine. Organic layer was dried over sodium sulfate and concentrated in vacuo. Silica gel column was run using DCM:methanol (9.6:0.4 v/v) solvent system as eluent to afford 52-55 (75-80 %) as brown dense liquid.

**52:** $^{1}$H NMR 400 mHz ($CDCl_3$) δ 0.67 (s, 3H), 0.85-0.87 (dd, 6H), 0.90-0.92 (d, 3H), 0.99-2.02 (50H), 2.49 (br, 1H), 3.15 (br, 2H), 3.32-3.35 (m, 5H), 4.04 (s, 2H), 4.05 (s, 2H), 5.32-5.33 (t, 1H)

$^{13}$C NMR 100 mHz ($CDCl_3$) δ 11.88-42.34 (30C), 50.16, 51.00, 51.02, 56.20, 56.77, 71.28, 121.40, 168.48

**53:** $^{1}$H NMR 400 mHz ($CDCl_3$) δ 0.68 (s, 3H), 0.85-0.87 (dd, 6H), 0.90-0.92 (d, 3H), 0.99-2.02 (54H), 2.49 (br, 1H), 3.15 (br, 2H), 3.25-3.32 (m, 5H), 4.04 (s, 4H), 5.32-5.33 (t, 1H)

$^{13}$C NMR 100 mHz ($CDCl_3$) δ 11.88-42.34 (32C), 50.16, 51.34, 56.20, 56.77, 71.30, 121.40, 168.37, 168.51

**54:** $^{1}$H NMR 400 mHz ($CDCl_3$) δ 0.68 (s, 3H), 0.85-0.87 (dd, 6H), 0.90-0.92 (d, 3H), 1.00-2.04 (58H), 2.49 (br, 1H), 3.15 (br, 2H), 3.21-3.34 (m, 5H), 4.04 (s, 4H), 5.32-5.33 (t, 1H)

$^{13}$C NMR 100 mHz ($CDCl_3$) δ 11.88-42.35 (34C), 50.20, 51.35, 56.21, 56.78, 71.25, 71.32, 168.30

$^{1}$H NMR 400 mHz ($CDCl_3$) δ 0.67 (s, 3H), 0.85-0.87 (dd, 6H), 0.90-0.92 (d, 3H), 0.99-1.99 (46H), 2.49 (br, 1H), 3.14 (br, 2H), 3.34-3.48 (m, 5H), 4.06 (s, 4H), 5.32-5.33 (t, 1H)

$^{13}$C NMR 100 mHz ($CDCl_3$) δ 11.88-42.34 (28C), 50.16, 50.61, 56.18, 56.76, 71.14, 71.22, 79.50, 121.38, 168.48

**4.1.16 56 :**

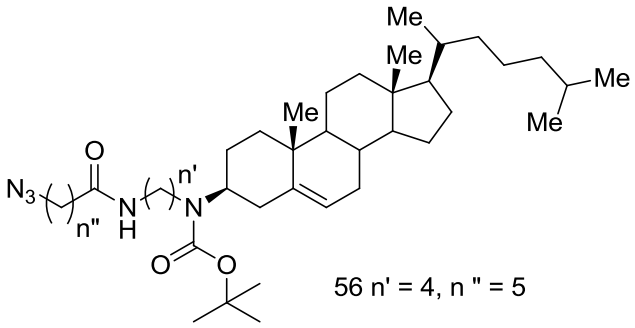


To a solution of 44 (400 mg, 0.6 mmol, 1 equivalent) in DCM was added 2-azidoethanamine hydrochloride salt (110 mg, 0.9 mmol, 1.5 equivalent), EDCI (170 mg, 0.9 mmol, 1.5 equivalent) and di-isopropyl ethyl amine (0.15 mL, 0.9 mmol, 1.5 equivalent). The reaction mixture was stirred over night at room temperature. After completion of reaction, it was diluted with DCM, washed with water followed by washing with 0.5 N HCL and finally with brine. Organic layer was dried over sodium sulfate and concentrated in vacuo. Silica gel column was run using DCM:methanol (9.6:0.4 v/v) solvent system as eluent to afford 56 (300 mg, 67 %) as brown dense liquid.

$^{1}$H NMR 400 mHz ($CDCl_3$) δ 0.67 (s, 3H), 0.85-0.87 (dd, 6H), 0.90-0.92 (d, 3H), 0.99-1.99 (46H), 2.49 (br, 1H), 3.14 (br, 2H), 3.34-3.48 (m, 5H), 4.06 (s, 4H), 5.32-5.33 (t, 1H)

$^{13}C$ NMR 100 mHz ($CDCl_3$) δ 11.88-42.34 (28C), 50.16, 50.61, 56.18, 56.76, 71.14, 71.22, 79.50, 121.38, 168.48

**4.17 6- azidohexanoic acid :**

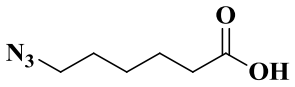


To a solution of bromohexanoic acid (6g, 31 mmol, 1 equivalent) in DMF (20 mL) was added sodium azide (4 g, 62 mmol, 2 equivalent). The solution was refluxed over night. After completion of reaction the solution was cooled and DMF was evaporated. The residue was dissolved in DCM. Organic layer was washed with 0.1 N HCL, dried over sodium sulfate and concentrated in vacuo to obtain 6-azidohexanoic acid (3.96 g, 81%) as yellow oil.

$^{1}H$ NMR 400 mHz ($CDCl_3$) δ 1.41-1.46 (m, 2H), 1.59-1.71 (m, 4H), 2.34-2.38 (t, 2H), 3.26-3.29 (t, 2H)

$^{13}C$ NMR 100 mHz ($CDCl_3$) δ 24.29, 26.21, 28.57, 36.65, 51.32, 178.03

**4.1.18 :**

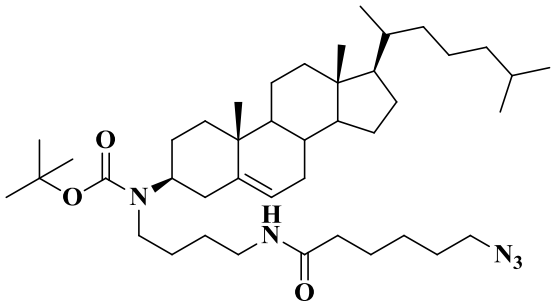


A solution of amine (12;p) (700mg, 1.26 mmol, 1 equivalent) in DCM (20 mL) was prepared. To this solution, 6-azidohexanoic acid (400 mg, 2.51 mmol, 2 equivalent), EDCI (362 mg, 1.89 mmol, 1.5 equivalent) and tri-ethylamine (0.1 mL, 0.63 mmol, 0.5 equivalent) were added. The reaction mixture was stirred for 24 h at room temperature. After completion of reaction as evidence by TLC, reaction mixture was diluted with 10 mL DCM and washed with water, 0.5 N HCL finally with brine. Organic layer was dried over sodium sulfater, filtered and concentrated in vacuo. Crude was purified by silica gel column using 4% methanol in DCM as eluent to afford 20 (600 mg, 68%) as colorless oil.

$^{1}$H NMR 400 mHz ($CDCl_3$) δ 0.68 (s, 3H), 0.85-0.87 (dd, 6H), 0.90-0.92 (d, 3H), 0.99-2.02 (52H), 2.17-2.20 (t, 2H), 2.5 (br, 1H), 3.10-3.12 (br, 2H), 3.24-3.29 (m, 3H), 5.32-5.33 (t, 1H)

$^{13}$C NMR 100 mHz ($CDCl_3$) δ 11.88-42.34 (28C), 50.16, 51.24, 53.42, 56.19, 56.77, 121.35, 177.53

**4.1.19 65', 66', 57'-66':**

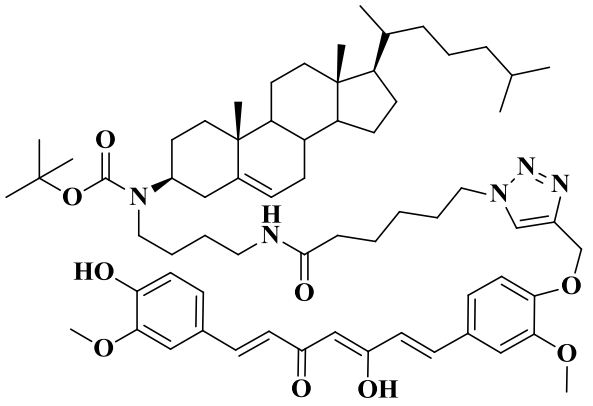

**65'**

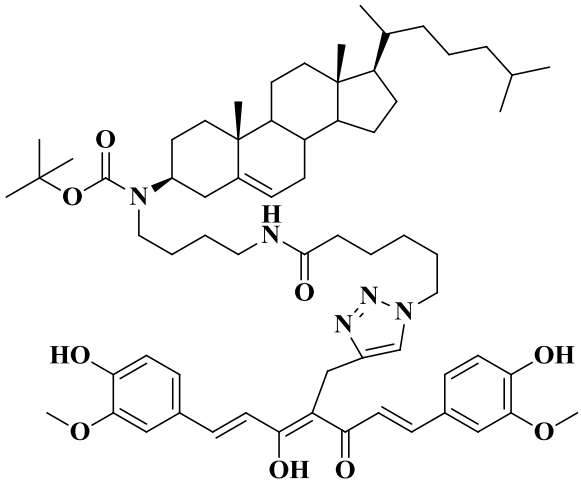

**66'**

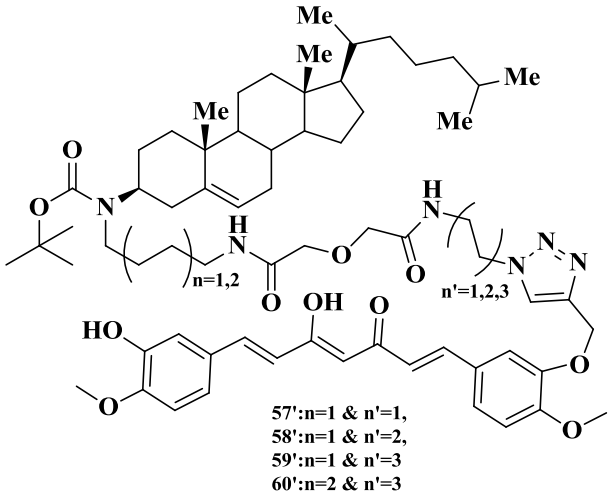


57':n=1 & n'=1,
58':n=1 & n'=2,
59':n=1 & n'=3
60':n=2 & n'=3

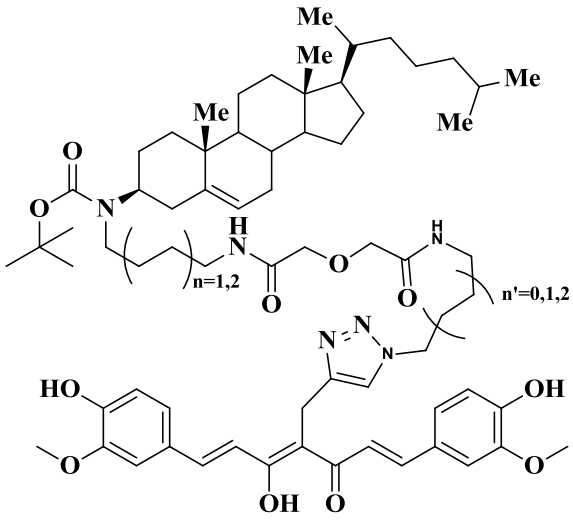


61':n=1,n'=0
62':n=1,n'=1
63':n=1,n'=2
64':n=2,n'=2

Alkyne (3/5) (2 equivalent) and azide (19/20/21/22/24) (1 equivalent) were dissolved in tetrahydrofuran:water (1:1). To that, sodium ascorbate (0.04 equivalent) and copper sulfate (0.02 equivalent) were added and reaction mixture was stirred for 24 h at 65$^{o}$C. After completion of reaction DCM was added to reaction mixture and organic layer was washed with water followed by brine. Organic layer was dried over sodium sulfate,

filtered and concentrated in vacuo. Silica gel column was run using DCM:methanol (9.6:0.4 v/v) solvent system as eluent to afford 25-34 (40-40 %) as orange solid.

**65':** $^{1}$H NMR 400 mHz ($CDCl_3$) δ 0.67 (s, 3H), 0.85-0.87 (dd, 6H), 0.90-0.92 (d, 3H), 0.99-2.02 (50H), 2.13-2.16 (t, 2H), 2.5 (br, 1H), 3.12 (br, 2H), 3.26 (m, 3H), 3.90 (s,3H), 3.93 (s, 3H), 4.31-4.34 (t, 2H), 5.31 (br, 3H), 6.45-6.50 (m, 2H), 6.92-6.94 (d, 1H), 7.05-7.12 (m, 6H), 7.56-7.63 (m, 3H)

$^{13}$C NMR 100 mHz ($CDCl_3$) δ 11.87-42.33 (31C), 50.13, 50.18, 55.97, 56.18, 56.74, 63.04, 101.25, 109.73-128.87 (13C), 140.12-149.69 (8C), 153.99, 182.91, 183.59

**66':** $^{1}$H NMR 400 mHz ($CDCl_3$) δ 0.67 (s, 3H), 0.85-0.87 (dd, 6H), 0.90-0.92 (d, 3H), 0.99-2.02 (50H), 2.5 (br, 1H), 3.12 (br, 2H), 3.25 (m, 3H), 3.89 (s,3H), 3.91 (s, 3H), 4.24-4.25 (t, 2H), 5.32 (br, 1H), 6.66-6.70 (m, 1H), 6.89-7.08 (m, 8H), 7.56-7.71 (m, 2H)

$^{13}$C NMR 100 mHz ($CDCl_3$) δ 11.87-42.33 (31C), 49.99, 50.13, 53.43, 56.03, 56.10, 56.18, 56.75, 109.73-127.73 (13C), 142.44-148.97 (8C), 183.59, 194.58

**57':** $^{1}$H NMR 400 mHz ($CDCl_3$) δ 0.66 (s, 3H), 0.85-0.87 (dd, 6H), 0.90-0.92 (d, 3H), 0.97-2.01 (44H), 2.5 (br, 1H), 3.12 (br, 2H), 3.35 (m, 2H), 3.80 (m, 3H), 3.90 (s, 3H), 3.92 (s, 3H), 3.99 (s, 2H), 4.01 (s, 2H), 4.51 (t, 2H), 5.29 (br, 3H), 6.46 (m, 1H), 6.92-6.94 (d, 1H), 7.05-7.12 (m, 7H), 7.57-7.59 (m, 2H),7.71 (s, 1H)

$^{13}$C NMR 100 mHz ($CDCl_3$) δ 11.87-42.32 (28C), 49.44, 50.13, 55.97, 56.17, 56.73, 62.82, 101.29 109.73-127.65 (12C), 140.75, 146.86, 147.97, 149.61

**58':** $^{1}$H NMR 400 mHz ($CDCl_3$) δ 0.67 (s, 3H), 0.85-0.87 (dd, 6H), 0.90-0.92 (d, 3H), 0.98-2.01 (48H), 2.5 (br, 1H), 3.13 (br, 2H), 3.31-3.34 (m, 4H), 3.90 (s, 3H), 3.94 (s,

3H), 4.03 (s, 4H), 4.36-4.39 (t, 2H), 5.30 (br, 3H), 6.45-6.50 (m, 2H), 6.92-6.94 (d, 1H), 7.05-7.12 (m, 6H), 7.56-7.60 (m, 2H), 7.67 (s, 1H)

$^{13}$C NMR 100 mHz ($CDCl_3$) δ 11.87-42.32 (30C), 49.83, 50.12, 55.97, 56.17, 56.73, 62.99, 71.20, 71. 24, 101.28, 109.73-128.93 (12C), 140.07-149-67 (8C), 182.86, 183.63

**59':** $^{1}$H NMR 400 mHz ($CDCl_3$) δ 0.67 (s, 3H), 0.85-0.87 (dd, 6H), 0.90-0.92 (d, 3H), 0.98-2.01 (52H), 2.5 (br, 1H), 3.13 (br, 2H), 3.23-3.33 (m, 4H), 3.91 (s, 3H), 3.94 (s, 3H), 4.03 (s, 4H), 4.33-4.36 (t, 2H), 5.33 (br, 3H), 6.46-6.51 (m, 2H), 6.92-6.94 (d, 1H), 7.05-7.12 (m, 6H), 7.56-7.63 (m, 3H)

$^{13}$C NMR 100 mHz ($CDCl_3$) δ 11.87-42.33 (32C), 50.13, 55.98, 56.18, 56.75, 63.06, 71.26, 101.26, 109.71-128.89 (12C), 140.11-149-69 (8C), 182.95, 183.56

**60':** $^{1}$H NMR 400 mHz ($CDCl_3$) δ 0.68 (s, 3H), 0.85-0.87 (dd, 6H), 0.90-0.92 (d, 3H), 0.99-2.04 (56H), 2.5 (br, 1H), 3.15 (br, 2H), 3.25-3.35 (m, 5H), 3.91 (s, 3H), 3.94 (s, 3H), 4.04 (s, 4H), 4.33-4.36 (t, 2H), 5.32 (br, 3H), 6.46-6.51 (m, 2H), 6.92-6.94 (d, 1H), 7.05-7.12 (m, 6H), 7.56-7.63 (m, 3H)

$^{13}$C NMR 100 mHz ($CDCl_3$) δ 11.87-42.33 (32C), 50.13, 55.98, 56.18, 56.75, 63.06, 71.26, 101.26, 109.71-128.89 (12C), 140.11-149-69 (8C), 182.95, 183.56

**61':** $^{1}$H NMR 400 mHz ($CDCl_3$) δ 0.67 (s, 3H), 0.85-0.87 (dd, 6H), 0.90-0.92 (d, 3H), 0.98-2.04 (44H), 2.5 (br, 1H), 3.12 (br, 2H), 3.34-3.35 (br, 3H), 3.90 (s,3H), 3.93 (s, 3H), 3.99 (s, 4H), 4.41-4.45 (m, 2H), 5.30 (br, 1H), 6.69-6.73 (d, 1H), 6.88-7.11 (m, 7H), 7.59-7.72 (m, 2H)

$^{13}$C NMR 100 mHz ($CDCl_3$) δ 11.87-42.33 (29C), 50.13, 56.05, 56.18, 56.74, 70.82, 114.94, 124.22, 146.96

**62':** $^{1}$H NMR 400 mHz ($CDCl_3$) δ 0.60 (s, 3H), 0.78-0.80 (dd, 6H), 0.85 (d, 3H), 0.91-1.95 (48H), 2.3 (br, 1H), 3.06-3.33 (m, 7H), 3.83 (s,3H), 3.85 (s, 3H), 3.95 (s, 4H), 4.20-4.23 (t, 2H), 5.25 (br, 1H), 6.60-6.64 (d, 1H), 6.80-7.02 (m, 7H), 7.50-7.64 (m, 2H)

$^{13}$C NMR 100 mHz ($CDCl_3$) δ 10.85-41.30 (31C), 48.66, 49.10, 55.02, 55.15, 55.73, 70.14, 108.87, 113.94, 120.41, 123.17, 144.24, 145.98

**63':** $^{1}$H NMR 400 mHz ($CDCl_3$) δ 0.67 (s, 3H), 0.85-0.87 (dd, 6H), 0.90-0.92 (d, 3H), 0.98-2.02 (52H), 2.5 (br, 1H), 3.13-3.40 (m, 8H), 3.89 (s,3H), 3.91 (s, 3H), 4.04 (s, 4H), 4.24-4.26 (m, 2H), 5.30 (br, 1H), 6.64-6.68 (d, 1H), 6.84-7.08 (m, 7H), 7.55-7.71 (m, 2H)

$^{13}$C NMR 100 mHz ($CDCl_3$) δ 11.87-42.33 (33C), 50.13, 53.42, 56.01, 56.17, 56.75, 71.17, 109.92, 115.03, 117.74, 123.24, 124.14, 126.0, 127.73, 145.15, 148.95, 183.14

**64':** $^{1}$H NMR 400 mHz ($CDCl_3$) δ 0.68 (s, 3H), 0.85-0.87 (dd, 6H), 0.90-0.92 (d, 3H), 0.99-2.04 (52H), 2.6 (br, 1H), 3.08-3.41 (m, 8H), 3.90 (s,3H), 3.91 (s, 3H), 4.04 (s, 4H), 4.23-4.26 (m, 2H), 5.31-5.32 (br, 1H), 6.66-6.69 (d, 1H), 6.86-7.08 (m, 8H), 7.56-7.60 (d, 1H), 7.67-7.71 (d, 1H)

$^{13}$C NMR 100 mHz ($CDCl_3$) δ 11.89-42.35 (35C), 50.18, 56.06, 56.11, 56.21, 71.19, 109.92-127.79 (14C), 142.36-148.94 (7C), 168.94, 183.14, 194.57

**4.1.20 57-66:**

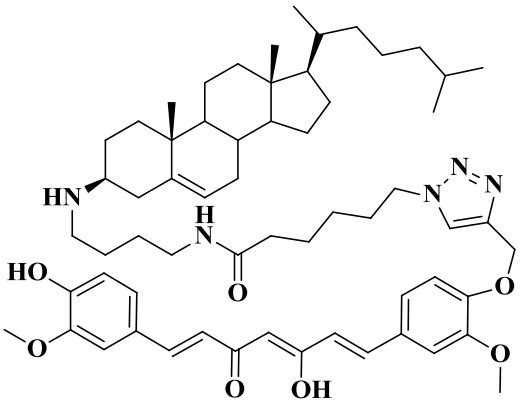


**65**

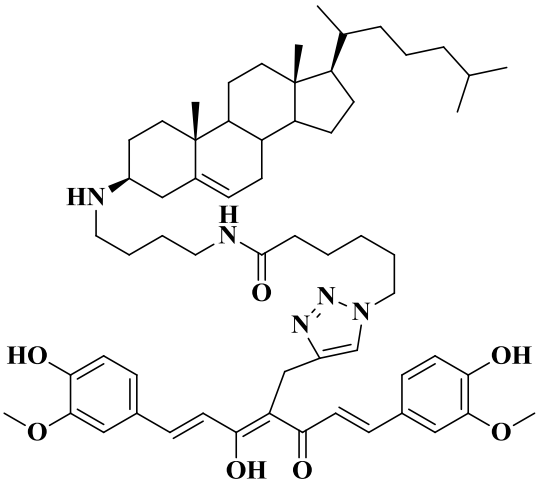


**66**

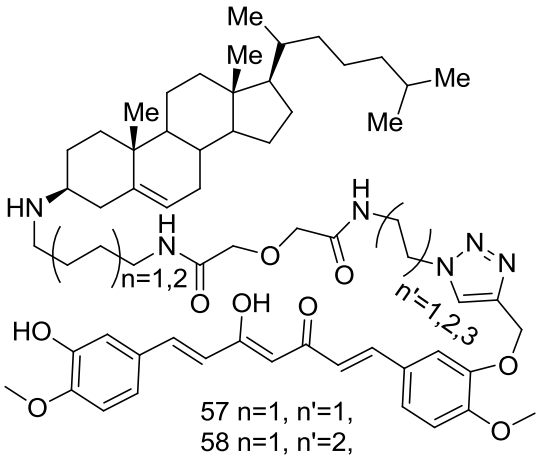


57 n=1, n'=1,
58 n=1, n'=2,
59 n=1, n'=3
60 n=2, n'=3

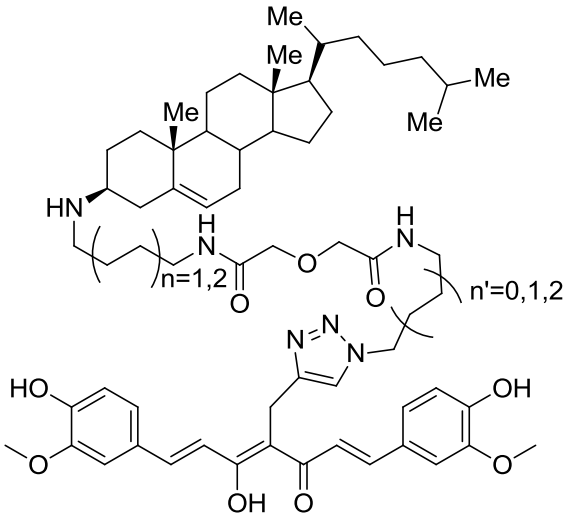


61 n=1,n'=0
62 n=1,n'=1
63:n=1,n'=2
64:n=2,n'=2

Per 4 mmol of compound (25-34), 4 mL of DCM was taken to make solution. To this solution, added 1-4 mL of TFA and stirred for 2-6 h at room temperature. After completion of reaction solution was rotavapored. Preparative TLC was run using

DCM:methanol (8.5:1.5 v/v) solvent system to afford pure final compound (35-44) (20-30 %) as orange solid.

**65:** $^{1}$H NMR 400 mHz ($CDCl_3$) δ 0.65 (s, 3H), 0.84-0.86 (dd, 6H), 0.87-0.90 (d, 3H), 0.96-2.04 (41H), 2.13-2.16 (t, 2H), 2.6 (br, 1H), 2.96 (br, 2H), 3.22 (m, 3H), 3.87 (s,3H), 3.92 (s, 3H), 4.33 (br, 2H), 5.35 (br, 3H), 6.49 (d, 2H), 6.92-6.94 (d, 1H), 7.04-7.19 (m, 6H), 7.55-7.63 (m, 3H)

$^{13}$C NMR 100 mHz ($CDCl_3$) δ 11.86-42.29 (28C), 44.53, 49.91, 50.32, 50.18, 55.93, 55.97, 56.17, 56.63, 58.44, 62.73, 101.34, 109.77-128.87 (12C), 138.13-149.64 (8C), 182.83, 183.64

**66:** $^{1}$H NMR 400 mHz ($CDCl_3$) δ 0.67 (s, 3H), 0.85-0.87 (dd, 6H), 0.90-0.92 (d, 3H), 0.99-2.28 (41H), 2.48 (br, 1H), 2.64 (br, 1H), 2.89-2.99 (m, 2H), 3.22-3.26 (m, 3H), 3.40 (br, 2H), 3.87 (s,3H), 3.90 (s, 3H), 4.24-4.28 (t, 2H), 5.39 (br, 1H), 6.69-6.74 (m, 1H), 6.88-7.13 (m, 8H), 7.59-7.71 (m, 2H)

$^{13}$C NMR 100 mHz ($CDCl_3$) δ 11.87-42.30 (28C), 49.94, 51.27, 56.03, 56.09, 56.15, 56.66, 110.00-127.72 (13C), 138.14-149.00 (8C), 174.07, 183.19, 194.69

**57:** $^{1}$H NMR 400 mHz ($CDCl_3$) δ 0.58 (s, 3H), 0.77-0.79 (dd, 6H), 0.83 (d, 3H), 0.90-2.00 (35H), 2.40 (br, 1H), 2.52-2.58 (t, 1H), 2.9 (br, 3H), 3.28 (br, 2H), 3.79 (s, 3H), 3.85 (s, 3H), 3.89 (s, 4H), 4.53 (t, 2H), 5.13 (s, 2H), 5.30 (br, 3H), 6.36-6.42 (m, 2H), 6.83-6.85 (d, 1H), 6.91-7.02 (m, 6H), 7.46-7.51 (m, 2H), 7.72 (s, 1H)

$^{13}$C NMR 100 mHz ($CDCl_3$) δ 10.85-41.27 (25C), 43.43, 48.34, 48.89, 54.90, 54.94, 55.15, 57.43, 61.57, 69.62, 100.36, 108.75-127.65 (12C), 137.12-148.59 (8C), 168.23, 168.50, 181.66, 182.72

**58:** $^{1}$H NMR 400 mHz ($CDCl_3$) δ 0.65 (s, 3H), 0.84-0.87 (dd, 6H), 0.89-0.90 (d, 3H), 0.94-2.03 (39H), 2.36 (br, 1H), 2.47 (t, 1H), 2.87-2.95 (br, 3H), 3.25-3.39 (m, 4H), 3.88 (s, 3H), 3.92 (s, 3H), 4.00 (s, 4H), 4.33-4.37 (t, 2H), 5.24 (s, 2H), 5.37 (br, 1H), 6.44-6.50 (m, 2H), 6.91-6.93 (d, 1H), 6.97-7.10 (m, 5H), 7.54-7.59 (m, 2H), 7.71 (s, 1H)

$^{13}$C NMR 100 mHz ($CDCl_3$) δ 11.87-42.29 (27C), 44.30, 49.90, 50.07, 55.91, 55.96, 56.17, 56.60, 58.33, 62.70, 70.75, 70.89, 101.35, 109.81-129.04 (12C), 138.03-149.44 (8C), 182.74, 183.71

**59:** $^{1}$H NMR 400 mHz ($CDCl_3$) δ 0.65 (s, 3H), 0.85-0.87 (dd, 6H), 0.90-0.92 (d, 3H), 0.95-2.01 (43H), 2.37 (br, 1H), 2.46 (br, 1H), 2.84-2.96 (br, 3H), 3.21-3.25 (m, 4H), 3.89 (s, 3H), 3.93 (s, 3H), 4.01 (s, 4H), 4.31-4.33 (m, 2H), 5.28 (s, 2H), 5.36 (br, 1H), 6.45-6.49 (m, 2H), 6.91-6.93 (d, 1H), 6.98-7.11 (m, 5H), 7.54-7.60 (m, 2H), 7.67 (s, 1H)

$^{13}$C NMR 100 mHz ($CDCl_3$) δ 11.85-42.30 (29C), 49.92, 50.26, 55.97, 56.07, 56.17, 56.63, 58.26, 62.87, 70.86, 71.02, 101.30, 109.20-128.97 (12C), 138.09-149-69 (8C), 169.03, 169.55, 182.86, 183.64

**60:** $^{1}$H NMR 400 mHz ($CDCl_3$) δ 0.66 (s, 3H), 0.85-0.87 (dd, 6H), 0.90-0.92 (d, 3H), 0.99-2.04 (56H), 2.36 (br, 1H), 2.47 (br, 1H), 2.84-2.96 (br, 3H), 3.21-3.25 (m, 4H), 3.90 (s, 3H), 3.94 (s, 3H), 4.03 (s, 4H), 4.31-4.34 (t, 2H), 5.28 (s, 2H), 5.36 (br, 1H), 6.46-6.51 (m, 2H), 6.71-673 (d, 1H), 6.89-6.92 (d, 1H), 6.99-7.19 (m, 5H), 7.56-7.69 (m, 3H)

$^{13}$C NMR 100 mHz ($CDCl_3$) δ 11.86-42.33 (29C), 53.41, 56.00, 56.20, 56.67, 71.16, 109.78, 114.79, 121.76, 123.59, 140.08

**61:** $^{1}$H NMR 400 mHz ($CDCl_3$) δ 0.64 (s, 3H), 0.85-0.87 (dd, 6H), 0.90-0.91 (d, 3H), 0.98-2.04 (35H), 2.34-2.48 (br, 2H), 2.93 (br, 3H), 3.34-3.35 (br, 3H), 3.90 (s,3H), 3.93

(s, 3H), 3.99 (s, 4H), 4.41-4.45 (m, 2H), 5.34 (br, 1H), 6.70-6.73 (br, 2H), 6.88-7.04 (m, 6H), 7.47-7.65 (m, 2H)

$^{13}$C NMR 100 mHz ($CDCl_3$) δ 11.87-42.33 (26C), 50.13, 56.05, 56.18, 56.74, 70.82, 114.94, 124.22, 146.96

**62:** $^{1}$H NMR 400 mHz ($CDCl_3$) δ 0.65 (s, 3H), 0.85-0.87 (dd, 6H), 0.90-0.91 (d, 3H), 0.94-2.01 (39H), 2.37 (br, 1H), 2.48 (br, 1H), 2.94-2.98 (br, 3H), 3.87 (s,3H), 3.88 (s, 3H), 3.97 (s, 4H), 4.26 (m, 2H), 5.35 (br, 1H), 6.68-6.72 (d, 1H), 6.86-7.07 (m, 6H), 7.57-7.69 (m, 2H)

$^{13}$C NMR 100 mHz ($CDCl_3$) δ 10.85-42.30 (28C), 49.92, 56.03, 56.16, 56.63, 58.38, 115.14, 147.18, 148.48, 149.22, 194.54

**63:** $^{1}$H NMR 400 mHz ($CDCl_3$) δ 0.59 (s, 3H), 0.76-0.80 (dd, 6H), 0.83-0.84 (d, 3H), 0.88-1.95 (43H), 2.32 (br, 1H), 2.47 (br, 1H), 2.83 (br, 3H), 2.98-3.15 (m, 4H), 3.79 (s,3H), 3.80 (s, 3H), 3.94 (s, 4H), 4.14-4.18 (m, 2H), 5.29 (br, 1H), 6.60-6.64 (d, 1H), 6.79-6.98 (m, 8H), 7.48-7.62 (m, 2H)

$^{13}$C NMR 100 mHz ($CDCl_3$) δ 10.84-41.29 (30C), 43.55, 48.93, 55.02, 55.16, 55.63, 57.13, 69.94, 109.18-126.71 (14C), 137.12-148.21 (7C), 168.04, 182.12, 193.68

**64:** $^{1}$H NMR 400 mHz ($CDCl_3$) δ 0.66 (s, 3H), 0.85-0.87 (dd, 6H), 0.90-0.92 (d, 3H), 0.95-2.02 (47H), 2.37 (br, 1H), 2.47 (br, 1H), 2.89 (br, 3H), 3.06-3.23 (m, 4H), 3.87 (s, 3H), 3.89 (s, 3H), 4.01 (s, 4H), 4.23-4.26 (m, 2H), 5.36 (br, 1H), 6.66-6.73 (d, 1H), 6.86-7.09 (m, 6H), 7.23 (m, 1H), 7.34 (m, 1H), 7.55-7.69 (m, 2H)

$^{13}C$ NMR 100 mHz ($CDCl_3$) δ 11.87-42.32 (32C), 44.64, 49.98, 53.42, 56.05, 56.19, 56.68, 58.14, 71.04, 110.20-130.43 (14C), 138.30-149.30 (7C), 168.92, 168.97, 183.15, 194.6

**4.2 Biology**

**4.2.1 Inhibition of Aβ42 Oligomerization: (A**β42+compound+lipid raft)

**1) 50uM of Aβ42 stock solution**: 40ug Aβ42 dissolved in 17uL of DMSO and diluted in 160uL of F-12 media.

**2) 2 mM of compounds stock solution:**

**3) Preparation of samples:** Compounds (1uL) are added to each eppendorf tube and then Aβ42 (5uL) was incubated with 44uL of rat brain lipid rafts ($5^{th}$ fraction) at 4 $^{0}$C for 30min/1h.

| Items | Volume/Final Conc | Control |
|---|---|---|
| Aβ42 (50uM) | 5uL/5uM | 5uL/5uM |
| Compounds | 1uL/40uM | F-12 medium 1uL |
| Lipid rafts | 44uL | 40uL |
| Total Volume | 50uL | 50uL |

4) After incubation, to the mixture (20uL) was added 20uL of tricine sample buffer (with reducing agents) and boiled for 5min.

5) The samples (20uL) were electrophored on a 10-20% tris/tricine gel. (100 V, 2h)

6) The proteins are transferred to PVDF membrane. (100 V, 1h)

7) The membranes are blocked with 5% non-fat milk.(1h)

8) The membranes are blotted with anti-Aβ42 antibody (6E10: 1/1000, 5% non-fat milk) (overnight)

9) Wash with TBS-T buffer. (3x15min)

10) Apply secondary antibody (anti-mouse: 1/2000, 5% non-fat milk)(1h)

11) Wash with TBS-T buffer (3x15min)

12) Develop X-ray films in dark room.

**4.2.2 Inhibition of Aβ42 Oligomerization: (Aβ42+compound)**

1) 50uM of Aβ42 stock solution: 40ug Aβ42 dissolved in 17uL of DMSO and diluted in 160uL of F-12 media.

2) 2mM of compounds stock solution:

3) Preparation of samples: Compounds (1uL) are added to 44uL Ham's F-12 media and then it was incubated with 5uL Aβ42 at 37 $^{0}$C for 4h.

| Items | Volume/Final Conc | Control |
|---|---|---|
| Aβ42 (50uM) | 5uL/5uM | 5uL/5uM |
| Compounds | 1uL/2mM | F-12 medium 1uL |

| | | |
|---|---|---|
| Ham's F-12 media | 44uL | 44uL |
| Total volume | 50uL | 50uL |

4) After incubation, the samples were spun down at 14000g for 15 min. The supernatant (20uL) was mixed with equal amount of tricine sample buffer (without reducing agent) and mixture (20uL) was electrophoresed on 10-20% tris/tricine gel. The control was stored at -80 $^{0}$C and mixed with equal amount of tricine sample buffer before electrophoresed.

5) The proteins are transferred to PVDF membrane. (100 V, 1h)

6) The membranes are blocked with 5% non-fat milk.(1h)

7) The membranes are blotted with anti-Aβ42 antibody (6E10: 1/1000, 5% non-fat milk) (overnight)

8) Wash with TBS-T buffer. (3x15min)

9) Apply secondary antibody (anti-mouse: 1/2000, 5% non-fat milk)(1h)

10) Wash with TBS-T buffer (3x15min)

11) Develop X-ray films in dark room.

**4.2.3 MC65 cells assays:**

**MC65 cells culture:**

**Stock solution**:

**10 mg/mL tetracycline**: Dissolve 10mg of TC into 1mL 70% ethanol and the stock solution is stored at -20 $^0$C.

**40 mg/mL G418**: Dissolve 40mg of G418 into 1mL DMEM medium and the stock solution is stored in 4 $^0$C.

**Growing medium**: DMEM is supplemented with 10% FBS, 100/100 P/S, 1 ug/mL TC and 0.2 mg/mL G418.

Thaw frozen cells quickly at 37 $^0$C water bath. Cells are suspended in 10mL DMEM (complete). Centrifuge at 2500 rpm for 3 min. Cells are re-suspended in 10mL DMEM (complete) and put into T25 flasks. Medium is changed every two days. After 70-90 confluence, split cells (1 to 2 ratio) into T75 flasks (remove medium, wash cells with PBS – 10 mL/twice, remove PBS, 1mL 0.25% trypsin-EDTA is added and incubate for 30 s, 9 mL DMEM is added, centrifuge for 3 min at 2500 rpm, the pellet is re-suspended in DMEM (complete) for splitting.). Change medium every 2 days.

**4.2.4 Western blot assay:**

MC65 cells were seeded in 6-well plates [0.5 * $10^6$/well, working volume 2 mL – DMEM growing media]. After incubation at 37 $^0$C, 5% $CO_2$ for 24 h or more (change media every two days. 70-80 confluence), the medium was removed and washed twice with

PBS. The medium was replaced with fresh Opti-MEM (Invitrogen)and compounds in Opti-MEM (with or without TC) wereadded. After 24 h incubation, cells were collected on ice andcentrifuged. Pellet was lysed by sonication in 1_ lysis buffer(62.5 mM Tris base, pH 6.8, 2% SDS, 50 mM DTT, 10%glycerol, 0.1% bromphenol blue, and 5 mg/mL each chymostatin,leupeptin, aprotinin, pepstatin, and soybean trypsin inhibitor)and protein level was determined using CoomassieProtein Assay Reagent (Pierce, Rockford, IL). Equal amountsof protein (10 μg) were separated by SDS-PAGE on 10-20%tris-tricine gel (Bio-Rad) and transferred onto a PVDF membrane(Bio-Rad). The blots were blocked with 5% milk in TBSTween20 (0.1%) at room temperature for 1 h and probed withprimary 6E10 (1:2000) antibody overnight at 4 _C. Theblots were then incubated with horseradish peroxidaseconjugatedsecondary antibody (1:2000. Kirkegaard & Perry, Gaithersburg, MD). The proteins were visualized by WesternBlot Chemiluminescence Reagent (NEN Life Science Products,Boston, MA).

**4.2.5Cell viability assay: (MTS)**

MC65 cells were seeded in 96-well plates [1 * $10^5$/well, working volume 100uL – DMEM growing media]. After incubation at 37 $^0$C, 5% $CO_2$ for 24 h (depends on the cells state) (70-80 Confluence) the medium was removed and washed 3 times with PBS. Opti-MEM (50uL) was added and incubated for 1h (need to set +TC control). 50uL drug solution (double the concentration of final concentration) in Opti-MEM was added. Incubated for 72 h. 20 uL MTS agents were added and incubated at 37 $^0$C, 5% $CO_2$ for 1h. Read the plate at 490nM in plate reader.

**4.2.6 Cell viability assay: (MTT)**

MC65 cells were seeded in 96-well plates [1 * $10^5$/well, working volume 100uL – DMEM growing media]. After incubation at 37 $^0$C, 5% $CO_2$ for 24 h (depends on the cells state) (70-80 Confluence) the medium was removed and washed 3 times with PBS. Opti-MEM (50uL) was added and incubated for 1h (need to set +TC control). 50uL drug solution (double the concentration of final concentration) in Opti-MEM was added. Incubated for 72 h. After incubating for 72 h media was replaced with fresh opti-MEM using centrifuge. 10uL of MTT (5mg/mL in PBS) was added and incubated for 4 hr. Removed 60 uL of opti-MEM solution from total of 110 uL and added 100 uL of DMSO to dissolve the crystals generated from the reaction of living cells and MTT reagent. Finally, plate was read at 490 on plate reader.

**4.2.7 DCFH-DA assay**: MC65 cells were seeded in 96-well plates [4 * $10^4$/well, working volume 100 uL DMEM media). After incubation at 37 $^0$C, 5% $CO_2$ for 24 h (depends on the cells state – 70-80 confluence), the medium is removed and washed 3 times with PBS. Control was set up (one side complete DMEM (+TC control), the other side use pure opti-MEM (-TC control), 100 uL medium is added. For drug treated wells, Opti-MEM (50 uL) is added and incubated for 1h. Then 50 uL drug solution (double the concentration needed) in opti-MEM was added. Incubated for 24 h. 10 mM stock DCFH-DA was diluted into opti-MEM to a final 50 uM concentration, then 100 uL was added to each well (final DCFH-DA concentration was 25 uM) and incubated at 37 $^0$C, 5% $CO_2$

for 30 min. Media was removed and washed with opti-MEM twice. Finally 100 uL opti-MEM was added and read for fluorescence at 485/520 nM.

**4.2.8 Immunocytochemistry Assay:**

**Reagents:**

- A11 oligomer Rabbit polyclonal antiboay (50 ug, AHB0052-Invitrogen)
- Alexa Fluor 568 donkey anti – rabbit IgG (0.5 mL, A10042-Invitrogen)
- Alexa 488 conjugated cholera toxin B (100 ug, C34775-Invitrogen)

**Solutions:**

- **4% paraformaldehyde (PFA) in PBS**

  o.4 g paraformaldehyde in 5mL PBS was added 100 uL 1N NaOH. Heat this mixture at 60 $^{0}$C until the PFA is dissolved. Dilute the solution to 10 mL with PBS.

- 20 mL 1% BSA in PBS
- Working solutions of all antibodies in 0.1% BSA in PBS

**Protocol:**

MC65 cells were plated onto Lab-Tec chamber slides 4-well at 2 * $10^5$ well in 500 uL working volume of DMEM supplemented with 10% FBS, 1 ug/mL TC and 0.2 mg/mL GG418. After 24 h incubation at 37 $^{0}$C and 5% $CO_2$, (50 % confluence) the medium was removed and rinsed twice in 500 uL (per chamber) PBS at room temperature. 500 uL opti-MEM was added to each chamber with or without TC. Cells were incubated for 2 h. Then test compounds in 500 uL opti-MEM were added and the cells were incubated for

24 h. Rinsed 3 times with warm (37 0C) PBS (500 uL/chamber) (5 min each). Incubated the cells with Alexa 488-conjugated CTX (10ug/ml in 0.1% BSA in PBS) for 15 min on ice. Rinsed once with ice-cold PBS (1mL/well). Fixed the cells for 30 min at RT with 500 uL/chamber 4% paraformaldehyde. Washed 3 times with RT PBS (500 uL/chamber). Permeabilized cells for 30 min at RT with 0.1% Trition × 100 and 0.1% BSA in PBS. Washed 3 times with RT PBS. Incubated the cells in 1% BSA (0.5 mL) for 1h. Washed 3 times with RT PBS. Incubated cells in 250 uL of the working concentration of A11 rabbit antibody diluted in 0.1% BSA in PBS (1:500 v/v) for 2 h. Washed 3 times with RT PBS. Secondary antibody in the dark: anti-rabbit Alex 568 (1:500) (diluted into 0.1% BSA in PBS). Washed 3 times with RT PBS. DAPI Hoechst 33342 (5 ug/mL in PBS) treated for 5 min. Washed 3 times with RT PBS. Drained excess liquid and allowed the slide to dry and removed the plastic chamber piece and sealer holding it in place completely. Place one drop of Vectashield Mounting Media on each sheet of cells (1 for each chamber) and cover with No. 1.5 thickness cover slip. Gently push out any air bubbles and seal the edges with clear nail polish. Stored slides at 4 $^{0}$C in the dark before and in between viewing under fluorescence.

**References:**


1) http://www.alz.org

*2)* Graeber, M. B.; Mehraein, P. Reanalysis of the first case of Alzheimer's disease. *Eur Arch Psychiatry. Clin. Neurosci.* **1999**, *249*, 10-13

3) Lott, I. T.; Head, E. Down syndrome and Alzheimer's disease: a link between development and aging. *Ment. Retard. Dev. Disabil. Res. Rev.* **2001**, *7*, 172-178.

**4)** Ferri, C. P.; Prince, M.; Brayne, C. Global prevalence of dementia: a Delphi consensus study. *Lancet* **2005**, *366*, 2112-2117

5) Hebert, L. E.; Scherr, P. A.; Bienias, J. L.; Bennett, D. A; Evans, D. A. Alzheimer disease in the US population: prevalence estimates using the 2000 census. *Arch. Neurol.* **2003**, *60*, 1119-1122.

6) Perneczky, R.; Wagenpfeil, S.; Komossa, K.; Grimmer, T.; Diehl, J.; Kurz, A. Mapping scores onto stages: mini-mental state examination and clinical dementia rating. *Am. J. Geriatr. Psychiatry* **2006**, *14*, 139-144.

7) Petersen, R. C. Mild cognitive impairment as a diagnostic entity. *y*

*8)* Petersen, R. C.; Doody, R.; Kurz, A. Current concepts in mild cognitive impairment. *Arch. Neurol.* **2001**, *58*, 1985-1992.

9) Akiyama, H.; Barger, S.; Barnum, S. Inflammation and Alzheimer's disease. *Neurobiol. Aging* **2000**, *21*, 383-421.

10) Kosik, K. S. Tau protein and Alzheimer's disease. *Curr. Opin. Cell. Biol.* **1990**, *2*, 101-104.

11) Lee, V. M.; Balin, B. J.; Otvos, L., Jr; Trojanowski, J. Q. A68: a major subunit of paired helical filaments and derivatized forms of normal Tau. *Science* **1991**, *251*, 675-678.

*12)* Braak, H; and Braak, E. Neuropathological stageing of Alzheimer-related changes. *Acta. Neuropathol.* **1991**, *82*, 239-259.

13) Christie, R. H.; Bacskai, B. J.; Zipfel, W. R.; Williams, R. M.; Kajdasz, S. T.; Webb, W. W.; Hyman, B. T. Growth arrest of individual senile plaques in a model of Alzheimer's disease observed by in vivo multiphoton microscopy. *J. Neurosci.* **2001**, *21*, 858-864.

14) Atwood, C. S.; Martins, R. N.; Smith, M. A.; Perry, G. Senile plaque composition and posttranslational modification of amyloid-beta peptide and associated proteins. *Peptides* **2002**, 23, 1343-1350.

15) Armstrong, R. A. Beta-amyloid plaques: stages in life history or independent origin? *Dement. Geriatr. Cogn. Disord.* **1998**, *9*, 227-238.

16) Blennow, K.; de Leon, M. J.; Zetterberg, H. Alzheimer's disease. *Lancet* **2006**, *368*, 387-403.

17) Wiltfang, J.; Esselmann, H.; Bibl, M. Highly conserved and disease-specific patterns of carboxyterminally truncated Abeta peptides 1-37/38/39 in addition to 1-40/42 in Alzheimer's disease and in patients with chronic neuroinflammation. *J. Neurochem.* **2002**, *81*, 481-496.

18) Dickson, D. W. Neuropathological diagnosis of Alzheimer's disease: a perspective from longitudinal clinicopathological studies. *Neurobiol. Aging.* **1997**, *18*, S21-26.

19) Gotz, J.; Ittner, L. M.; Schonrock, N.; Cappai, R. An update on the toxicity of A-beta in Alzheimer's disease. *Neuropsychiatr. Dis. Treat.* **2008**, *4*, 1033-1042.

*20)* Eckman, C. B.; Eckman, E. A. An update on the amyloid hypothesis. *Neurol. Clin.* **2007**, *25*, 669-682.

*21)* Cacabelos, R. Pharmacogenomics and therapeutic prospects in dementia. *Eur. Arch.Psychiatry Clin. Neurosci.* **2008**, *258*, 28-47.

22) Zheng, H.; Jiang, M.; Trumbauer, M. E. Beta-Amyloid precursor protein-deficient mice show reactive gliosis and decreased locomotor activity. *Cell* **1995**, *81*, 525-531.

23) Fiore, F.; Zambrano, N.; Minopoli, G.; Donini, V.; Duilio, A.; Russo, T. The regions of the Fe65 protein homologous to the phosphotyrosine interaction/phosphotyrosine binding domain of Shc bind the intracellular domain of the Alzheimer's amyloid precursor protein. *J. Biol.Chem.* **1995**, *270*, 30853-30856.

24) Maynard, C. J.; Cappai, R.; Volitakis, I.; Cherny, R. A.; White, A. R.; Beyreuther, K.; Masters, C. L.; Bush, A. I.; Li, Q. X. Overexpression of Alzheimer's disease amyloid-beta opposes the age-dependent elevations of brain copper and iron. *J. Biol. Chem.* **2002**, *277*, 44670-44676.

25) Yankner, B. A.; Duffy, L. K.; Kirschner, D. A. Neurotrophic and neurotoxic effects of amyloid beta protein: reversal by tachykinin neuropeptides. *Science* **1990**, *250*, 279-282.

26) Pike, C. J.; Burdick, D.; Walencewicz, A. J.; Glabe, C. G.; Cotman, C. W. Neurodegeneration induced by beta-amyloid peptides in vitro: the role of peptide assembly state. *J. Neurosci.* **1993**, *13***,** 1676-1687.

27) Pike, C. J.; Walencewicz, A. J.; Glabe, C. G.; Cotman, C. W. In vitro aging of beta-amyloid protein causes peptide aggregation and neurotoxicity. *Brain Res.* **1991**, *563***,** 311-314.

28) Colton, C. A.; Wilcock, D. M.; Wink, D. A.; Davis, J.; Van Nostrand, W. E.; Vitek, M. P.The effects of NOS2 gene deletion on mice expressing mutated human AbetaPP. *J. Alzheimers. Dis.* **2008**, *15***,** 571-587.

29) Wilcock, D. M.; Lewis, M. R.; Van Nostrand, W. E.; Davis, J.; Previti, M. L.; Gharkholonarehe,N.; Vitek, M. P.; Colton, C. A. Progression of amyloid pathology to Alzheimer'sdisease pathology in an amyloid precursor protein transgenic mouse model by removal of nitric oxide synthase 2. *J. Neurosci.* **2008**, *28***,** 1537-1545.

30) McGowan, E., Pickford, F., Kim, J. et al. Abeta42 is essential for parenchymal and vascular amyloid deposition in mice. *Neuron* **2005**, *47***,** 191-199.

31) Klein, W. L.; Stine, W. B.; Teplow, D. B. Small assemblies of unmodified amyloid beta-protein are the proximate neurotoxin in Alzheimer's disease. *Neurobiol. Aging* **2004**, *25***,** 569-580.

32) Mucke, L.; Masliah, E.; Yu, G. Q. High-level neuronal expression of abeta 1-42 in wild-type human amyloid protein precursor transgenic mice: synaptotoxicity without plaque formation. *J. Neurosci.* **2000**, *20***,** 4050-4058.

33) Walsh, D. M.; Klyubin, I.; Fadeeva, J. V.; Rowan, M. J.; Selkoe, D. J. Amyloid-beta oligomers: their production, toxicity and therapeutic inhibition. *Biochem. Soc. Trans.* **2002**, *30*, 552-557.

34) Lambert, M. P.; Barlow, A. K.; Chromy, B. A.(1998) Diffusible, nonfibrillar ligands derived from Abeta1-42 are potent central nervous system neurotoxins. *Proc. Natl. Acad. Sci. USA* **1998**, *95*, 6448-6453.

35) Gong, Y.; Chang, L.; Viola, K. L.; Lacor, P. N.; Lambert, M. P.; Finch, C. E.; Krafft, G. A.;Klein, W. L. Alzheimer's disease-affected brain: presence of oligomeric A beta ligands (ADDLs) suggests a molecular basis for reversible memory loss. *Proc. Natl. Acad. Sci. USA* **2003**,*100*, 10417-10422.

36) Rich, J. B.; Rasmusson, D. X.; Folstein, M. F.; Carson, K. A.; Kawas, C.; Brandt, J. Nonsteroidal anti-inflammatory drugs in Alzheimer's disease. *Neurology* **1995**, *45*, 51-55.

37) Stewart, W. F.; Kawas, C.; Corrada, M.; Metter, E. J. Risk of Alzheimer's disease and duration of NSAID use. *Neurology* **1997**, *48*, 626-632.

38) Mackenzie, I. R; Munoz, D. G. Nonsteroidal anti-inflammatory drug use and Alzheimer-type pathology in aging. *Neurology* **1998**, *50*, 986-990.

39) In t' Veld, B. A.; Ruitenberg, A.; Hofman, A.; Launer, L. J.; van Duijn, C. M.; Stijnen, T.;Breteler, M. M.; Stricker, B. H. Nonsteroidal antiinflammatory drugs and the risk of Alzheimer's disease. *N. Engl. J. Med.* **2001**, *345*, 1515-1521.

40) Bonifati, D. M.; Kishore, U. Role of complement in neurodegeneration and neuroinflammation. *Mol. Immunol.* **2007**, *44*, 999-1010.

41) Butterfield, D. A.; Griffin, S.; Munch, G.; Pasinetti, G. M. Amyloid beta-peptide and amyloid pathology are central to the oxidative stress and inflammatory cascades under which Alzheimer's disease brain exists. *J. Alzheimers. Dis.* **2002**, *4,* 193-201.

42) Watson, D.; Castano, E.; Kokjohn, T. A. Physicochemical characteristics of soluble oligomeric Abeta and their pathologic role in Alzheimer's disease. *Neurol. Res.* **2005**, *27,* 869-881.

43) Shie, F. S.; Woltjer, R. L. Manipulation of microglial activation as a therapeutic strategy in Alzheimer's disease. *Curr Med Chem* **2007**, *14,* 2865-2871. Cacabelos, R. Pharmacogenomics and therapeutic prospects in dementia. *Eur. Arch. Psychiatry Clin. Neurosci.* **2008**, *258,* 28-47.

44) Pratico, D. Oxidative stress hypothesis in Alzheimer's disease: areappraisal. *Trends Pharmacol. Sci.* **2008**, 29, 609–615.

45) Petersen, R. B.; Nunomura, A.; Lee, H. G.; Casadesus, G.; Perry,G.; Smith, M. A.; Zhu, X. Signal transduction cascades associated with oxidative stress in Alzheimer's disease. *J. Alzheimer's Dis*. **2007**, *11*, 143–152.

46) Reddy, P. H.; Beal, M. F. Amyloid β, mitochondrial dysfunctionand synaptic damage: implications for cognitive decline in aging and Alzheimer's disease. *Trends Mol. Med.* **2008**, *14*, 45–53.

47) Fukui, H.; Moraes, C. T. The mitochondrial impairment, oxidative stress and neurodegeneration connection: reality or just an attractivehypothesis? *Trends Neurosci.* **2008**, *31*, 251–256.

48) Cacabelos, R. Pharmacogenomics and therapeutic prospects in dementia. *Eur. Arch. Psychiatry Clin. Neurosci.* **2008**, *258*, 28-47.

*49)* Roses, A. D. Apolipoprotein E alleles as risk factors in Alzheimer's disease. *Annu. Rev. Med.* **1996**, *47*, 387-400.

50) Tanzi, R. E.; Bertram, L. Twenty years of the Alzheimer's disease amyloid hypothesis: a genetic perspective. *Cell* **2005**, *120*, 545-555.

51) Bird, T. D. Genetic aspects of Alzheimer disease. *Genet. Med.* **2008**, *10*, 231-239.

52) Zhong, N.; Weisgraber, K. H. Understanding the association of apolipoprotein E4 with Alzheimer disease: clues from its structure. *J. Biol. Chem.* **2009**, *284*, 6027-6031.

*53)* Bu, G.; Cam, J.; Zerbinatti, C. LRP in amyloid-beta production and metabolism. *Ann. NY Acad. Sci.* **2006**, *1086*, 35-53.

54) Selkoe, D. J. Alzheimer's disease: genes, proteins, and therapy. *Physiol. Rev.* **2001**, *81*, 741-766.

55) DeMattos, R. B.; Cirrito, J. R.; Parsadanian, M. ApoE and clusterin cooperatively suppress Abeta levels and deposition: evidence that ApoE regulates extracellular Abeta metabolism in vivo. *Neuron* **2004**, *41*, 193-202.

56) Jiang, Q.; Lee, C. Y.; Mandrekar, S. ApoE promotes the proteolytic degradation of A beta. *Neuron* **2008**, *58*, 681-693.

57) Swerdlow, R. H.; Khan, S. M. A "mitochondrial cascade hypothesis" for sporadic Alzheimer's disease. *Med. Hypotheses* **2004**, *63*, 8-20.

58) Miners, J. S.; Baig, S.; Palmer, J.; Palmer, L. E. Kehoe, P. G.; Love, S. Abeta-

degrading enzymes in Alzheimer's disease. *Brain Pathol.* **2008**, *18*, 240-252.

*59)* Geldmacher, D. S. Differential diagnosis of dementia syndromes. *Clin. Geriatr. Med.* **2004,** *20*, 27-43.

60) Gil-Bea, F. J.; Garcia-Alloza, M.; Dominguez, J.; Marcos, B.; Ramirez, M. J. Evaluation of cholinergic markers in Alzheimer's disease and in a model of cholinergic deficit. *Neurosci. Lett.* **2005**, *375*, 37-41.

61) Pakaski, M.; Kalman, J. Interactions between the amyloid and cholinergic mechanisms in Alzheimer's disease. *Neurochem. Int.* **2008**, *53*, 103-111.

62) Whitehouse, P. J.; Price, D. L.; Struble, R. G.; Clark, A. W.; Coyle, J. T.; Delon, M. R. Alzheimer's disease and senile dementia: loss of neurons in the basal forebrain. *Science* **1982**, *215*, 1237-1239.

63) Allain, H.; Bentue-Ferrer, D.; Tribut, O.; Gauthier, S.; Michel, B. F.; Drieu-La Rochelle, C. Alzheimer's disease: the pharmacological pathway. *Fundam. Clin. Pharmacol.* **2003**, *17*, 419-428.

64) Mayeux, R.; Sano, M. Treatment of Alzheimer's disease. *N. Engl. J. Med.* **1999**, *341*, 1670-1679.

65) Shah, R. S., Lee, H. G., Xiongwei, Z., Perry, G., Smith, M. A. and Castellani, R. J. Current approaches in the treatment of Alzheimer's disease. *Biomed. Pharmacother.* **2008**, *62*, 199-207.

66) Kornhuber, J.; Bormann, J.; Retz, W.; Hubers, M.; Riederer, P. Memantine displaces [3H] MK-801 at therapeutic concentrations in postmortem human frontal cortex. *Eur. J. Pharmacol.* **1989**, *166*, 589-590.

67) Misztal, M.; Frankiewicz, T.; Parsons, C. G.; Danysz, W. Learning deficits induced by chronic intraventricular infusion of quinolinic acid--protection by MK-801 and memantine. *Eur. J. Pharmacol.* **1996**, *296*, 1-8.

68) Zajaczkowski, W.; Quack, G.; Danysz, W. Infusion of (+) -MK-801 and memantine – contrasting effects on radial maze learning in rats with entorhinal cortex lesion. *Eur. J. Pharmacol.* **1996**, *296*, 239-246.

69) Reisberg, B.; Doody, R.; Stoffler, A.; Schmitt, F.; Ferris, S.; Mobius, H. J. Memantine in moderate-to-severe Alzheimer's disease. *N. Engl. J. Med.* **2003**, *348*, 1333-1341.

70) Tariot, P. N.; Farlow, M. R.; Grossberg, G. T.; Graham, S. M.; McDonald, S.; Gergel, I. Memantine treatment in patients with moderate to severe Alzheimer disease already receiving donepezil: a randomized controlled trial. *JAMA* **2004**, *291*, 317-324.

71) Imbimbo, B. P. Therapeutic potential of gamma-secretase inhibitors and modulators. *Curr. Top. Med. Chem.* **2008**, *8*, 54-61.

*72)* Sadowski, M.; Wisniewski, T. Disease modifying approaches for Alzheimer's pathology. *Curr. Pharm. Des.* **2007**, *13*, 1943-1954.

73) Schenk, D.; Barbour, R.; Dunn, W. Immunization with amyloid-beta attenuates Alzheimer-disease-like pathology in the PDAPP mouse. *Nature* **1999**, *400*, 173-177.

74) Roberds, S. L.; Anderson, J.; Basi, G. BACE knockout mice are healthy despite

lacking the primary beta-secretase activity in brain: implications for Alzheimer's disease therapeutics. *Hum. Mol. Genet.* **2001**, *10*, 1317-1324.

75) Ghosh, A. K.; Kumaragurubaran, N.; Hong, L.; Koelsh, G.; Tang, J. Memapsin 2 (beta-secretase) inhibitors: drug development. *Curr. Alzheimer. Res.* **2008**, *5*, 121-131.

76) Wong, G. T.; Manfra, D.; Poulet, F. M. Chronic treatment with the gamma-secretase inhibitor LY-411,575 inhibits beta-amyloid peptide production and alters lymphopoiesis and intestinal cell differentiation. *J. Biol. Chem.* **2004**, *279*, 12876-12882.

77) Radke, A. L.; Reynolds, L. E.; Melo, R. C.; Dvorak, A. M.; Weller, P. F.; Spencer, L. A. Mature human eosinophils express functional Notch ligands mediating eosinophil autocrine regulation. *Blood* **2009**, *113*, 3092-3101.

78) van Es, J. H.; van Gijn, M. E.; Riccio, O. Notch/gamma-secretase inhibition turns proliferative cells in intestinal crypts and adenomas into goblet cells. *Nature* **2005**, *435*, 959-963.

79) Milano, J.; McKay, J.; Dagenais, C. Modulation of notch processing by gamma-secretase inhibitors causes intestinal goblet cell metaplasia and induction of genes known to specify gut secretory lineage differentiation. *Toxicol. Sci.* **2004**, *82*, 341-358.

80) Barten, D. M.; Meredith, J. E.; Zaczek, R.; Houston, J. G.; Albright, C. F. Gamma-secretase inhibitors for Alzheimer's disease: balancing efficacy and toxicity. *Drugs R. D.* **2006**, *7*, 87-97.

81) Morihara, T.; Chu, T.; Ubeda, O.; Beech, W.; Cole, G. M. Selective inhibition of Abeta42 production by NSAID R-enantiomers. *J. Neurochem.* **2002**, *83*, 1009-1012.

82) Weggen, S.; Eriksen, J. L.; Das, P. A subset of NSAIDs lower amyloidogenic Abeta42 independently of cyclooxygenase activity. *Nature* **2001**, *414*, 212-216.

83) Kukar, T.; Prescott, S.; Eriksen, J. L.; Holloway, V.; Murphy, M. P.; Koo, E. H.; Golde, T. E;Nicolle, M. M. Chronic administration of R-flurbiprofen attenuates learning impairments in transgenic amyloid precursor protein mice. *BMC Neurosci.* **2007**, *8*, 54.

84) Gasparini, L.; Rusconi, L.; Xu, H.; Del Soldato, P.; Ongini, E. Modulation of beta amyloid metabolism by non-steroidal anti-inflammatory drugs in neuronal cell cultures. *J. Neurochem.* **2004**, *88*, 337-348.

*85)* Kukar, T. L.; Ladd, T. B.; Bann, M. A. Substrate-targeting gamma-secretase modulators. *Nature* **2008**, *453*, 925-929.

86) Stock, N.; Munoz, B.; Wrigley, J. D. The geminal dimethyl analogue of Flurbiprofen as a novel Abeta42 inhibitor and potential Alzheimer's disease modifying agent. *Bioorg. Med. Chem. Lett.* **2006**, *16*, 2219-2223.

87) Zandi, P. P.; Anthony, J. C.; Hayden, K. M.; Mehta, K.; Mayer, L.; Breitner, J. C. Reduced incidence of AD with NSAID but not H2 receptor antagonists: the Cache County Study. *Neurology* **2002**, *59*, 880-886.

88) Jankowsky, J. L.; Slunt, H. H.; Gonzales, V. Persistent amyloidosis following suppression of Abeta production in a transgenic model of Alzheimer disease. *PLoS. Med.* **2005**, *2*, 355.

89) Refolo, L. M.; Fillit, H. M. New directions in neuroprotection: basic mechanisms, molecular targets and treatment strategies. *J. Alzheimers. Dis.* **2004**, *6*, S1-2.

90) Brookmeyer, R.; Gray, S.; Kawas, C. Projections of Alzheimer's disease in the United States and the public health impact of delaying disease onset. *Am. J. Public Health* **1998**, *88*, 1337-1342.

91) Hardy, J.; Selkoe, D. J. The amyloid hypothesis of Alzheimer'sdisease: progress and problems on the road to therapeutics. *Science* **2002**, *297*, 353–356.

92) Patrico, D. Oxidative stress hypothesis in Alzheimer's disease: a reappraisal. *Trends Pharmacolo. Sci* **2008**, *29*, 609-615.

93) Selkoe, D. J. Soluble oligomers of the amyloid beta-protein impairsynaptic plasticity and behavior. *Behav. Brain Res.* **2008**, *192*, 106–113.

94) Lue, L. F.; Kuo, Y. M.; Roher, A. E.; Brachova, L.; Shen, Y.;Sue, L.; Beach, T.; Kurth, J. H.; Rydel, R. E.; Rogers, J. Solubleamyloid beta peptide concentration as a predictor of synaptic change in Alzheimer's disease. *Am. J. Pathol.* ***1999***, *155*,853–862.

95) McLean, C. A.; Cherny, R. A.; Fraser, F. W.; Fuller, S. J.; Smith,M. J.; Beyreuther, K.; Bush,A. I.; Masters, C. L. Soluble pool of Abeta amyloid as a determinant of severity of neurodegeneration inAlzheimer's disease. *Ann. Neurol.* **1999**, *46*, 860–866.

96) King, M. E.; Kan, H. M.; Baas, P. W.; Erisir, A.; Glabe, C. G.;Bloom, G. S. Tau-dependent microtubule disassembly initiated byprefibrillar beta-amyloid. *J. Cell Biol.* **2006**, *175*, 541–546.

97) Zhang, Y.; McLaughlin, R.; Goodyer, C.; LeBlanc, A. Selectivecytotoxicity of intracellular amyloid beta peptide 1-42 throughp53 and Bax in cultured primary human neurons. *J. Cell Biol.* **2002**, *156*, 519–529.

98) Lal, R.; Lin, H.; Quist, A. P. Amyloid beta ion channel: 3D structure and relevance to amyloid channel paradigm. *Biochim.Biophys. Acta* **2007**, *1768*, 1966–1975.

99) Green, K. N.; LaFerla, F. M. Linking calcium to Abeta and Alzheimer's disease. *Neuron* **2008**, *59*, 190–194.

100) Gasparini, L.; Dityatev, A. Beta-amyloid and glutamate receptors. *Exp. Neurol.* **2008**, *212*, 1–4.

101) Chafekar, S. M.; Baas, F.; Scheper, W. Oligomer-specific Abeta toxicity in cell models is mediated by selective uptake. *Biochim.Biophys. Acta* **2008**, *1782*, 523–531.

102) Peterson, R. B; Nunomura, A.; Lee, H. G.; Casadesus, G.; Perry, G.; Smith, M. A.; Zhu, X. Signal transduction cascades associated with oxidative stress in Alzheimer's disease. *J. Alzheimer's Dis.* **2007**, *11*, 143-152.

103) Reddy, P. H.; Beal, M. F. Amyloid β, mitochondrial dysfunction and synaptic damage: implications for cognitive decline in aging and Alzheimer's disease. *Trends Mol. Med.* **2008**, *14*, 45-53

104) Fukui, H.; Moraes, C. T. The mitochondrial impairment, oxidative stress and neurodegenaration connection: reality or just an attractive hypothesis? *Trends Neurosci.* **2008**, *31*, 251-256.

105) Cordy, J. M.; Hooper, N. M.; Turner, A. J. The involvement oflipid rafts in Alzheimer's disease. *Mol. Membr. Biol.* **2006**, *23*, 111–122.

106) Kim, S. I.; Yi, J. S.; Ko, Y. G. Amyloid beta oligomerizationis induced by brain lipid rafts. *J. Cell. Biochem.* **2006**, *99*, 878–889.

107) Choo-Smith, L. P.; Garzon-Rodriguez, W.; Glabe, C. G.; Surewicz,W. K. Acceleration of amyloid fibril formation by specific binding of Abeta-(1-40) peptide to ganglioside-containing membrane vesicles. *J. Biol. Chem.* **1997**, *272*, 22987–22990.

108) Atwood, C. S.; Moir, R. D.; Huang, X.; Scarpa, R. C.; Bacarra,N. M.; Romano, D. M.; Hartshorn,M. A.; Tanzi, R. E.; Bush, A. I. Dramatic aggregation of Alzheimer abeta by Cu(II) is induced by conditions representing physiological acidosis. *J. Biol. Chem.* **1998**, *273*, 12817–12826.

109) Wakabayashi, M.; Okada, T.; Kozutsumi, Y.; Matsuzaki, K.GM1ganglioside-mediated accumulation of amyloid β-protein on cell membrane. *Biochem. Biophys. Res. Commun.* **2005**, *328*, 1019–1023.

110) Wang, S. S.; Rymer, D. L.; Good, T. A. Reduction in cholesteroland sialic acid content protects cells from the toxic effects of betaamyloid peptides. *J. Biol. Chem.* **2001**, *276*, 42027–42034.

111) Ariga, T.; McDonald, M. P.; Yu, R. K. Role of ganglioside metabolism in the pathogenesis of Alzheimer's disease--a review. *J. Lipid Res.* **2008**, *49*, 1157–1175.

112) Oda, A.; Tamaoka, A.; Araki, W. Oxidative stress up-regulatespresenilin 1 in lipid rafts in neuronal cells. *J. Neurosci. Res.* **2010**, *88*, 1137–1145.

113) Panza, F.; Solfrizzi, V.; Frisardi, V; Imbimbo, B. P.; Capurso, C.;D'Introno, A.; Colacicco, A. M.; Seripa, D.; Vendemiale, G.;Capurso, A.; Pilotto, A. Beyond the neurotransmitter-focused approach in treating Alzheimer's disease: drugs targeting betaamyloidand tau protein. *Aging Clin. Exp. Res.* **2009**, *21*, 386–406.

114) Sabbagh, M. N. Drug development for Alzheimer's disease: whereare we now and where are we headed? *Am. J. Geriatr. Pharmacother.* **2009**, *7*, 167–185.

115) Cavalli, A.; Bolognesi, M. L.; Minarini, A.; Rosini, M.; Tumiatti,V.; Recanatini, M.; Melchiorre, C. Multi-target-directed ligands tocombat neurodegenerative diseases. *J. Med. Chem.* **2008**, *51*, 347–372.

116) Amit, T.; Avramovich-Tirosh, Y.; Youdium, M. B.; Mandel, S.Targeting multiple Alzheimer's disease etiologies with multimodal neuroprotective and neurorestorative iron chelators. *FASEB J.* **2008**, *22*, 1296–1305.

117) Kim, Y. S.; Lee, J. H.; Ryu, J.; Kim, D. J. Multivalent & multifunctionalligands to β-amyloid. *Curr. Pharm. Des.* **2009**, *15*, 637–658.

118) Portoghese, P. S. From models to molecules: opioid receptor dimers, bivalent ligands, and selective opioid receptor probes. *J. Med. Chem.* **2001**, *44*, 2259–2269.

119) Yang, F.; Lim, G. P.; Begum, A. N.; Ubeda, O. J.; Simmons, M. R.; Ambegaokar, S. S.;Chen, P. P.; Kayed, R.;Glabe,C.G.; Frautschy,S. A.; Cole, G. M. Curcumin inhibits formation of amyloid beta oligomers and fibrils, binds plaques, and reduces amyloid in vivo. *J. Biol. Chem.* **2005**, *280*, 5892–5901.

120) Ray, B.; Lahiri, D. K. Neuroinflammation in Alzheimer's disease:different molecular targets and potential therapeutic agents including curcumin. *Curr. Opin. Pharmacol.* **2009**, *9*, 434–444.

121) Frautschy, S. A.; Cole, G. M. Why pleiotropic interventions are needed for Alzheimer's disease. *Mol. Neurobiol.* **2010**, *41*, 392–409.

122) Kim, J.; Lee, H. J.; Lee, K. W. Naturally occuring phytochemicals for the prevention of Alzheimer's disease. *J. Neurochem.* **2010**, *112*, 1415–1430.

123) Rajendran, L.; Schneider, A.; Schlechtingen, G.; Weidlich, S.; Ries, J.; Braxmeier, T.; Schwille, P.; Schulz, J. B.; Schroeder, C.; Simons, M.; Jennings, G.; Knolker, H. J.; Simons, K. Efficient inhibition ofthe Alzheimer's disease beta-secretase by membrane targeting. *Science* **2008**, *320*, 520–523.

124) Hussey, S. L.; He, E.; Peterson, B. R. Synthesis of chimeric 7alphasubstituted estradiol derivatives linked to cholesterol and cholesterylamine. *Org. Lett.* **2002**, *4*, 415–418.

125) Kolb, H. C.; Sharpless, K. B. The growing impact of click chemistry on drug discovery. *Drug Discovery Today* **2003**, *8*, 1128–1137.

126) Ouberai, M.; Dumy, P.; Chierici, S.; Garcia, J. Synthesis and biological evaluation of clicked curcumin and clicked KLVFFA conjugates as inhibitors of β-amyloid fibril formation. *Bioconjugate Chem.* **2009**, *20*, 2123–2132.

127) Pabon, H. J. J. Synthesis of curcumin and related compounds. *Rec.Trav. Chim.* **1964**, *83*, 379–386.

128) Sopher, B. L.; Fukuchi, K.; Smith, A. C.; Leppig, K. A.; Furlong, C. E.; Martin, G. M. Cytotoxicity mediated by conditional expression of a carboxyl-terminal derivative of the beta-amyloid precursor protein. *Brain Res. Mol. Brain Res.* **1994**, *26*, 207–217.

129) Maezawa, I.; Hong, H. S.; Wu, H. C.; Battina, S. K.; Rana, S.; Iwamoto, T.; Radke, G. A.; Petterson, E.; Martin, G. M.; Hua, D. H.; Jin, L. W. A novel tricyclic pyrone compound ameliorates cell death associated with intracellular amyloid-β oligomeric complexes. *J. Neurochem.* **2006**, *98*, 57–67.

130) Sopher, B. L.; Fukuchi, K. I.; Kavanagh, T. J.; Furlong, C. E.; Martin, G. M. Neurodegenerative mechanisms in Alzheimer's disease. *Mol. Chem. Neuropathol.* **1996**, *29*, 153–167.

131) Xia, W.; Zhang, J.; Kholodenko, D.; Citron, M.; Podlisny, M. B.; Teplow, D. B.; Haass, C.; Seubert, P.; Koo, E. H.; Selkoe, D. J. Enhanced production and oligomerization of the 42-residue amyloid beta-protein by Chinese hamster ovary cells stably expressing mutant presenilins. *J. Biol. Chem.* **1997**, *272*, 7977–7982.

132) Walsh, D. M.; Tseng, B. P.; Rydel, R. E.; Podlisny, M. B.; Selkoe, D. J. The oligomerization of amyloid beta-protein begins intracellularly in cells derived from human brain. *Biochemistry* **2000**, *39*, 10831–10839.

133) Kayed, R.; Head, E.; Thompson, J. L.; McIntire, T. M.; Milton, S. C.; Cotman, C. W.; Glade, C. G. Common structure of soluble amyloid oligomers implies common mechanism of pathogenesis. *Science* **2003**, *18*, 486–489.

134) Lantto, T. A.; Colucci, M.; Zavadova, V.; Hiltunen, R.; Raasmaja,A. Cytotoxicity of curcumin, resveratrol and plant extracts from basil, juniper, laurel and parsley in SH-SY5Y and CV1-P cells. *Food Chem.* **2009**, *117*, 405–411.

135) Oyama, Y.; Hayashi, A.; Ueha, T.; Maekawa, K. Characterization of 20,70-dichlorofluorescin fluorescence in dissociated mammalian brain neurons: estimation on intracellular content of hydrogen peroxide. *Brain Res.* **1994**, *635*, 113–117.

136) Forrest, V. J.; Kang, Y. H.; McClain, D. E.; Robinson, D. H.; Ramakrishnan, N. Oxidative stress-induced apoptosis prevented by Trolox. *Free Radical Biol. Med.* **1994**, *16*, 675–684.

137) Woltjer, R. L.; Nghiem, W.; Maezawa, I.; Milatovic, D.; Vaisar, T.; Montine, K. S.; Montine, T. J. Role of glutathione in intracellular amyloid-β precursor protein/carboxy-terminal fragment aggregation and associated cytotoxicity. *J. Neurochem.* **2005**, *93*, 1047–1056.

138) Adachi, Y.; Suzuki, H; Sugiyama, Y. Comparative studies on in vitro methods for evaluating in vivo function of MDR1 P-glycoprotein. *Pharm. Res.* **2001**, *18*, 1660–1668.

139) Mensch, J.; Melis, A.; Mackie, C.; Verreck, G.; Brewster, M. E.; Augustijns, P. Evaluation of various PAMPA models to identify the most discriminating method for the prediction of BBB permeability. *Eur. J. Pharm. Biopharm.* **2010**, *74*, 495–502.

140) Garberg, P.; Ball, M.; Borg, N.; Cecchelli, R.; Fenart, L.; Hurst, R. D.; Lindmark, T.; Mabondzo, A.; Nilsson, J. E.; Raub, T. J.; Stanimirovic, D.; Terasaki, T.; Oberg, J. O.; Osterberg, T. In vitromodels for the blood-brain barrier. *Toxicol. In Vitro* **2005**, *19*, 299–334.

141) Poller, B.; Gutmann, H.; Krahenbuhl, S.; Weksler, B.; Romero, I.;Couraud, P. O.; Tuffin, G.; Drewe, J.; Huwyler, J. The human brain endothelial cell line hCMEC/D3 as a human blood-brain barrier model for drug transport studies. *J. Neurochem.* **2008**, *107*, 1358–1368.

142) Lohmann, C.; Huwel, S.; Galla, H. J. Predicting blood-brain barrier permeability of drugs: evaluation of different in vitro assays. *J. Drug Target* **2002**, *10*, 263–276.

143) Usta, M.; Wortelboer, H. M.; Vervoort, J.; Boersma, M. G.; Rietjens, I. M.; van Bladeren, P. J.; Cnubben, N. H. Human glutathione S-transferase-mediated glutathione conjugation of curcumin and efflux of these conjugates in Caco-2 cells. *Chem. Res. Toxicol.* **2007**, *20*, 1895–1902.

144) Giacomini, K. M.; Huang, S. M.; Tweedie, D. J.; Benet, L. Z.; Brouwer, K. L.; Chu, X.; Dahlin, A.; Evers, R.; Fischer, V.; Hillgren, K. M.; Hoffmaster, K. A.;

Ishikawa, T.; Keppler, D.; Kim, R. B.; Lee, C. A.; Niemi, M.; Polli, J. W.; Sugiyama, Y.; Swaan, P. W.; Ware, J. A.; Wright, S. H.; Wah Yee, S.; Zamek-Gliszczynski, M. J.; Zhang, L. Membrane transporters in drug development. Nat. Rev. *Drug Discovery* **2010**, *9*, 215–236.

145) Wang, Y. J.; Thomas, P.; Zhong, J. H.; Bi, F. F.; Kosaraju, S.; Pollard, A.; Fenech, M.; Zhou, X. F. Consumption of grape seed extract prevents amyloid-beta deposition and attenuates inflammation in brain of an Alzheimer's disease mouse. *Neurotoxic. Res.* **2009**, *15*, 3–14.

146) Garcia-Alloza, M.; Borrelli, L. A.; Rozkalne, A.; Hyman, B. T.;Bacskai, B. J. Curcumin labels amyloid pathology in vivo, disrupts existing plaques, and partially restores distorted neuritis in anAlzheimer's mouse model. *J. Neurochem.* **2007**, *102*, 1095–1104.

147) Ryu, E. K.; Choe, Y. S.; Lee, K. H.; Choi, Y.; Kim, B. T. Curcumin and dehydrozingerone derivatives: synthesis, radiolabeling, and evaluation for beta-amyloid plaque imaging. *J. Med. Chem.* **2006**, *49*, 6111–6119.

148) Baum, L.; Ng, A. Curcumin interaction with copper and iron suggests one possible mechanism of action in Alzheimer's disease animal models. *J. Alzheimer's Dis.* **2004**, *6*, 367-377